Surface Modified Cross-linked Poly(vinyl alcohol)/poly(vinyl pivalate) Suspension Particles

by

Donna-Leigh D'Aguiar

Thesis presented in partial fulfilment of the requirements for the degree of

Master of Science (Polymer Science)

at the

University of Stellenbosch

Promoter: Prof Ronald D. Sanderson

Co-promoter: Prof Harald Pasch

Faculty of Science

Department of Chemistry and Polymer Science

December 2010

Declaration

I, the undersigned, hereby declare that the work contained in this thesis (submitted electronically) is entirely my own, and that I have not previously in its entirety or in parts thereof submitted it to any other university or for any other qualification.

Donna-Leigh D'Aguiar

December 2010

To God, the One who gives me reason and strength. May He bless also all those I love and cherish so dearly, my Mother, Father and Christopher.

Abstract

In papermaking, fillers and additives are used to enhance paper properties. In this study spherical modified poly(vinyl alcohol) (PVA) particles were prepared for use as fillers. In order to determine the mechanism of adhesion of additives to cellulose (paper) fibres, these particles were modified to have surface functionality, with cationic and anionic surface charges, similar to charged polyelectrolyte additives.

Typically, retention aids used to improve the fibre–fibre and fibre–filler bonding are able to conform to the surface of the fibres and fillers. Oppositely charged components show strong affinity for each other, e.g. cationic polyelectrolyte groups adhere to anionic surface charges on the fibres.

The spherical PVA particles were prepared by the saponification of spherical poly(vinyl pivalate) (PVPi) precursor particles. These PVPi particles, prepared via suspension polymerisation, were cross-linked with a divinyl ether comonomer. The vinyl pivalate (VPi) suspension polymerisation was successfully carried out and afforded relatively uniformly distributed PVPi particles, with diameters of 0.5–10 μm.

The cross-linked PVPi particles were then saponified in tetrahydrofuran (THF) as swelling solvent, to afford PVA with various degrees of saponification (DS). The spherical shape was lost and fibrous material was obtained when uncross-linked PVPi particles were saponified. Cross-linking the spherical PVPi particles (PVA precursor) proved innovative, and essential in maintaining the spherical form during saponification to PVA/PVPi. By varying the saponification time periods, various DS were obtained, as characterised by solid state NMR spectroscopy.

Surface modification of the PVA/PVPi particles was carried out with cationic and anionic groups via the Williamson ether synthesis. Ionic modification of these rigid spherical PVA/PVPi particles was carried out in order to study their adherence to cellulose fibres, compared to the adherence of similarly modified starches with cellulose fibres. Fluorescent labelling of the different modified particles was carried out using two complimentary coloured fluorescent markers. Fluorescence imaging and scanning electron microscopy (SEM) enabled the observation of particle–fibre and particle–particle interaction. Results indicated that the negative groups are sparse on the cellulose fibres, and therefore particles with low functionality but which are able change shape and conform and adhere to the surface of the cellulose fibres are required for effective adhesion.

These modified spherical PVA/PVPi particles are unique as they mirror the chemistry of functionalised starch and cellulose particles, yet maintain their shape and have a fixed size, measurable by SEM and transmission electron microscopy (TEM). Field-flow fractionation was also used to characterise and measure these relatively large cross-linked and fixed diameter particles.

Opsomming

In papierproduksie word vulstowwe en bymiddels gebruik om die eienskappe van papier te verbeter. In hierdie studie is sferiese poli(vinielalkohol) (PVA) partikels berei vir gebruik as vulstowwe. Om ten einde die meganisme van die bymiddelklewing aan die sellulose vesels (papier) te bepaal, is die oppervlakke van hierdie partikels gewysig met kationiese of anioniese groepe, om 'n oppervlak soortgelyk aan dié van funksionele poliëlektrolietbymiddels te verskaf.

Die retensiemiddels wat gebruik word om die vesel–vesel en vesel–vulstof binding te verbeter is tipies in staat om te konformeer aan die oppervlak van die vesels en vulstowwe. Teenoorgesteld-gelaaide komponente toon 'n sterk affiniteit vir mekaar, bv. kationiese poliëlektrolietgroepe is vasklewend aan die anioniesgelaaide oppervlakke van die vesel.

Die sferiese PVA partikels is berei deur die verseping van sferiese poli(vinielpivalaat) (PVPi) partikels. Hierdie voorloper PVPi partikels, berei deur suspensiepolimerisasie, is gekruisbind met 'n divinieleter ko-monomeer. Die vinielpivalaat (VPi) suspensiepolimerisasie is suksesvol uitgevoer en relatief eenvormig verspreide sferiese PVPi partikels is berei, met deursnitte tussen 0.5–10 μm.

Die gekruisbinde PVPi partikels is daarna gesaponifiseer in tetrahidrofuraan (THF) as oplosmiddel, om PVA met verskillende grade van verseping (DS) te berei. Die sferiese vorm raak verlore en veselagtige materiaal is verkry wanneer PVPi partikels met geen kruisbinding verseep is. Kruisbinding van die sferiese PVPi partikels (PVA voorloper) is voordelig en noodsaaklik om die sferiese vorm tydens die verseping tot PVA/PVPi te behou. Deur die tydsduur van verseping te verander, is verskeie grade van verseping verkry en bevestig deur vaste toestand KMR spektroskopie.

Oppervlakwysiging van die PVA/PVPi partikels, om kationiese en anioniese groepe aan te heg, is uitgevoer via die Williamson etersintese. Ioniese wysiging van hierdie stram, sferiese PVA/PVPi partikels is uitgevoer om ten einde hul klewing met sellulose vesels te bestudeer en te vergelyk met die klewing van soortgelyk gewysigde stysels. Fluoressensie merking van die verskillende gewysigde partikels is uitgevoer met behulp van twee komplimentêre gekleurde fluoressensie merkers. Fluoressensie beeldvorming en SEM verskaf die waarneming van partikel–vesel en partikel–partikel interaksie. Die resultate dui daarop dat die negatiewe groepe van die sellulose vesels skaars is, en daarom is partikels met ‘n lae funksionaliteit, maar wat in staat is om van vorm te verander, aan te pas en te konformeer aan die oppervlak van die sellulose vesels, nodig vir effektiewe adhesie.

Hierdie gewysigde sferiese PVA/PVPi partikels is uniek aangesien hulle die chemie van gewysigde stysel en sellulose partikels naboots, maar steeds hul vorm behou met 'n vaste grootte; meetbaar deur SEM en TEM. Veld-vloei-fraksionering is ook gebruik vir die karakterisering van hierdie relatief groot, stram, gekruisbinde partikels met bepaalde deursneë.

Acknowledgements

Firstly, I would like to thank the Lord God for being with me every step of the way.

My supervisor, Prof R.D. Sanderson: Thank you for your guidance, your immense wisdom which you are always willing to share, as well as all the academic and financial support you have offered me. Thanks also to my co-supervisor Prof H. Pasch.

I would like to thank the following people and organisations for their motivation, encouragement and contributions to this project:

The staff members at the Polymer Science department: Mrs E. Cooper, Mrs A. Fourie, Mr D. Koen, Mr J. Motshweni, Mr C. Maart and Mr H. Groenewald. A special thanks to Dr M. Hurndall for all the help, understanding and encouragement.

The analysis team: Solid state NMR (Jaco and Heidi, Central Analytical Facility (CAF), Stellenbosch University) and a very special thanks to Ben Loos for fluorescence imaging, (CAF), Stellenbosch University; as well as to Elsabe for XRD (CAF), Stellenbosch University.

Mondi Business Paper, the NRF as well as the University of Stellenbosch for funding of this study.

All Mondi Business Paper group members, including Dr M. Zou, Dr H. Matahwa, C. Terblanche, H. Chirowodza and A. Makan.

I would also like to thank Prof. B. Klumperman and Prof P. Mallon for their help. Thank you, to all the Free Radical Lab members, for all your help and support.

My friends, for always being there, sticking with me through the good times, along with the bad.

I am forever thankful to my parents and family for their love, encouragement and support; especially my mother, for showing me love that only a mother can. My fiancé, Chris, thank you so much for believing in me. I am so very blessed to have you in my life and I love you all, so very much.

I am thankful to you all. May the Lord forever bless you.

Table of Contents

List of Figures

List of Schemes

List of Tables

List of Abbreviations

AIBN	2,2′-azobis(isobutyronitrile)
AsFl-FFF	Asymmetric flow field-flow fractionation (or AF4)
ATR-FTIR	Attenuated total reflectance-Fourier transform infrared spectroscopy
CHPTMAC	3-Chloro-2-hydroxy-propyltrimethylammonium chloride
CP/MAS	Cross-polarization magic-angle-spinning
DBTL	Dibutyltin dilaurate
DDI	Distilled deionized
DMSO	Dimethylsulphoxide
D_n	Number-average particle diameter
DP	Degree of polymerisation
dRI	Differential refractive index
DS	Degree of saponification
DSC	Differential scanning calorimetry
DTGA	Differential TGA
D_{vad}	Volume-average particle diameter
D_w	Weight-average particle diameter
EDX	Energy-dispersive X-ray analysis
EtOH	Ethanol
FFF	Field-flow fractionation
FITC	Fluorescein isothiocyanate
FTIR	Fourier transform infrared spectroscopy
HLB	Hydrophile lipophile balance
IPA	Isopropanol
IR	Infrared
LDS	laser diffraction spectrometry
MALS	Multi-angle light scattering
MAS	Magic angle spinning
MeOH	Methanol
NMR	Nuclear magnetic resonance spectroscopy
PAS-FTIR	Photoacoustic Fourier transform infrared spectroscopy
PCC	Precipitated calcium carbonate

PD	Polydispersity index
PVA	Poly(vinyl alcohol)
PVAc	Poly(vinyl acetate)
PVAc/PVPi	Poly(vinyl acetate)/poly(vinyl pivalate)[†] [see also P(VPi/VAc), below]
PVA/PVPi	Poly(vinyl alcohol)/poly(vinyl pivalate)[‡]
PVAs	Poly(vinyl alcohol)s
PVPi	Poly(vinyl pivalate)
P(VPi/VAc)	Poly(vinyl pivalate/vinyl acetate)[§]
RBITC	Rhodamine B isothiocyanate
SEC	Size exclusion chromatography
SEM	Scanning electron microscopy
SMCA	Sodium monochloroacetate
SPE/MAS	Single-pulse-excitation magic-angle-spinning
SS NMR	Solid state nuclear magnetic resonance spectroscopy
TEGDE	Tri(ethylene glycol) divinyl ether (a cross-linking comonomer)
TEM	Transmission electron microscopy
T_g	Glass transition temperature
TGA	Thermogravimetric analysis
THF	Tetrahydrofuran
T_m	Crystalline melting temperature (T_m^*)[**]
T_{onset}	Onset temperature of thermal decomposition
UV	Ultraviolet
VAc	Vinyl acetate
VPi	Vinyl pivalate
XRD	X-ray diffraction (or X-ray powder diffraction, XRPD)

[†] PVAc/PVPi used when referring to this in the present study

[‡] The particle, after hydrolysis, remains cross-linked and is therefore one molecule, with a shell of almost pure PVA, a core of pure PVPi, and an intermediate zone of partially hydrolysed PVPi, hence the nomenclature used here.

[§] P(VPi/VAc) used in literature sources

[**] For the purpose of this study, T_m^* represents the melting temperature of the crystalline segments within the cross-links of the material, observed in DSC endotherms.

Chapter 1: Introduction and Objectives

1.1 Introduction

Polymeric materials can be classified either as synthetic or natural, based on their origin. Natural polymers, as the name suggests, constitute all naturally occurring macromolecules like DNA and proteins, natural rubbers, polysaccharides, starch and cellulose. As a result of the increasing need for raw materials and the depletion of natural products, the demand for synthetically produced and enhanced materials has increased. Thus, synthetic polymers have gained importance, particularly as they are easily tailored to suit specific needs and meet property or behavioural requirements. Synthetic polymers are considered to be man-made polymers or plastics like the commonly used polypropylene, polyethylene, polyurethane, polystyrene, poly(vinyl chloride) and poly(vinyl alcohol). One of the greatest disadvantages and milestones to overcome in most synthetic polymers is their lack of biocompatibility, biodegradability and toxicity. It is therefore important to carry out research into fields such as: the modification of natural polymers, the incorporation of natural materials into synthetic polymers, and the synthesis of polymers with properties similar to natural materials, to provide materials with improved properties, especially with regards to biodegradability and non-toxicity.

Poly(vinyl alcohol) (PVA), synthesised from poly(vinyl acetate) (PVAc) as precursor, is a widely used polymer with extraordinary properties such as water solubility, oxygen barrier properties, solvent and oil resistance, excellent thermal and mechanical properties, non-toxicity, biodegradability and biocompatibility.[1-3] PVA therefore has a wide range of industrial application and uses, for example in the paper and packaging,[3-5] fibre and film,[2,6-8] and medical[9-13] fields. By modification of the PVA material, using either pre- or post-polymerisation techniques, the properties of PVA can be improved and tailored to suit various needs and advanced applications. Pre-polymerisation modification entails copolymerisation of a vinyl ester precursor monomer with a comonomer of desired functionality, and subsequent saponification,[14-16] while post-polymerisation modification involves either grafting[17,18] or secondary reactions of the hydroxyl groups[19,20] of the PVA.

PVA is widely used in the paper industry, together with cellulose fibres,[21,22] starches[23,24] and precipitated calcium carbonate (PCC)[25] filler. The starch used in the paper industry is able to mould (i.e. change shape) and cover the surface of the cellulose fibre. It was therefore considered to be of interest to study the interaction of spherical, shape-maintaining particles, which have similar surface functional chemistry to that of modified starch, with cellulose fibres. There is very little information

on PVA particles prepared using poly(vinyl pivalate) (PVPi) as precursor polymer, as saponification of the latter would lead to highly syndiotactic fibrous material.[26-29] It would thus be interesting to study tailored, cross-linked PVPi particles. These cross-linked particles would then maintain their shape when hydrolysed and ionically modified. The interaction of these modified spherical particles with cellulose fibres could provide a better understanding of how well-defined particles improve paper properties, such as strength and stiffness, in comparison to the similar but 'floppy' starches. (Here, the term 'floppy' means that the starch material is able to swell/dissolve in water, become lax and change shape or conform onto the surface of cellulose fibres.) Fluorescent labelling, by attaching a fluorescent marker on the surface of the modified spherical particles, could be used for visually imaging the different modified particles and their interaction with cellulose fibres. It was considered that this fluorescence imaging technique would provide an innovative and unique method for analysing the interactions between the various paper components and the cellulose fibres.

At the start of this study, there were no reports on the preparation of cross-linked spherical PVA particles in which PVPi was used as precursor. However, as the study progressed, a patent[30] was published covering the preparation of cross-linked polymer particles for use as inkjet recording materials. This however, related to only a small section of the current study. Therefore, this work is still mostly unique and novel.

Modified starches are used to reinforce and improve paper properties, but there is little information on the adhesive properties of shape-maintaining particles with surface chemical makeup similar to the modified starches. Therefore, the focus of this study was to prepare core-shell particles that maintained their shape (having a modified and charged surface 'shell'), to investigate their adhesive properties with cellulose fibres, and then compare them with the modified floppy starches. This will allow for a better understanding of the principles of wet-end chemistry in paper production, where the starches (that can 'mould' to fit the fibre surface) are used as reinforcing additives.

1.2 Aim and objectives

The main aim of this study was to prepare modified core-shell particles (PVPi core and PVA shell) with a fixed shape (compared to the 'floppy' shape/swollen nature of common starch), to be used as fillers in cellulose (used in papermaking), and to compare the interaction between these new defined particles and cellulose fibre with the interactions achieved with currently used starch fillers and cellulose fibre.

The specific objectives were therefore the following.

1. Prepare spherical PVA precursor particles, PVPi, with controlled particle size and particle size distributions. This specifically included to:
   - Prepare PVPi microspheres within the size range 0.5–10 μm, after investigating and designing a simple method of preparation
   - Prepare cross-linked PVPi particles, to protect the shape of the PVPi particles, as PVA precursors
2. Prepare core-shell PVA/PVPi particles with different shell thicknesses (or degrees of hydrolysis) by surface saponification. Here it is important to:
   - Determine and control the extent of saponification
   - Study the effects of saponification on the thermal properties and particle morphology (and to ensure that spherical morphology was maintained after cross-linking).
3. Surface modify the prepared spherical PVA/PVPi particles to possess cationic and anionic functionalities; thus achieving shape-maintaining ionic charged particles that mimic the surface chemistry of the starch material used in the paper industry.
4. Label the modified PVA/PVPi particles with fluorescent dyes of complimentary colours to:
   - Investigate the particle–particle, particle–cellulose fibre and particle–filler interactions, and
   - Compare the adhesive nature of the shape-maintaining (rigid) surface modified particles with that of the ‘floppy’ modified starch material.
5. Attempt to separate the prepared and modified PVA/PVPi particles according to their size using the asymmetric flow field-flow fractionation (AsFl-FFF) technique (chemical composition was not to be compared, as for that, thermal or electrical techniques are required).

1.3 Layout of thesis

This document comprises five chapters.

Chapter 1: Introduction and objectives. The first chapter presents a very brief introduction to the topic of this study, and lists the aim and objectives.

Chapter 2: Historical and theoretical background. This chapter presents a literature review of several topics relevant to this study, including a basic overview into the chemistry of PVA. Where applicable, mention is made of how the information presented is related to the experimental work carried out in this study.

Chapter 3: Experimental. Detailed descriptions of synthetic routes and experimental procedures used in the study are given. The analytical techniques used in this study are discussed briefly.

Chapter 4: Results and discussion. The fourth chapter comprises the bulk of the thesis, where all results are presented and discussed. This chapter includes five main sections of work, with relevant subsections: the suspension polymerisation of vinyl pivalate to produce the spherical PVPi as PVA precursor; preparation of spherical semi-crystalline PVA particles; preparation of surface active PVA particles by modification, to obtain cationic and anionic functionalities; fluorescent labelling of these particles with complimentary coloured probes: a cellulose fibre study; and the separation of the prepared spherical PVPi and PVA/PVPi particles by FFF.

Chapter 5: Summary, conclusions and recommendations. The final chapter presents a summary of the work done (including the challenges encountered), the conclusions, and recommendations for future work.

1.4 References

1. S.-Y. Zheng, Z.-C. Chen, D.-S. Lu, Q. Wu, and X.-F. Lin, *J. Appl. Polym. Sci.*, **2005**, 97(6), 2186-2191.
2. J. Su, Q. Wang, R. Su, K. Wang, Q. Zhang, and Q. Fu, *J. Appl. Polym. Sci.*, **2008**, 107(6), 4070-4075.
3. C.A. Finch ed. *Polyvinyl Alcohol: Developments*, John Wiley & Sons Ltd: Chichester, 1992.
4. C.A. Finch ed. *Polyvinyl Alcohol: Properties and Applications*, John Wiley & Sons Ltd.: London, 1973.
5. G.G. Xu, C.Q. Yang, and Y. Deng, *J. Appl. Polym. Sci.*, **2004**, 93(4), 1673-1680.
6. Y. Nagara, T. Nakano, Y. Okamoto, Y. Gotoh, and M. Nagura, *Polymer*, **2001**, 42(24), 9679-9686.
7. W.S. Lyoo and W.S. Ha, *Polymer*, **1999**, 40(2), 497-505.
8. T. Subbiah, G.S. Bhat, R.W. Tock, S. Parameswaran, and S.S. Ramkumar, *J. Appl. Polym. Sci.*, **2005**, 96(2), 557-569.
9. S.G. Lee, J.P. Kim, W.S. Lyoo, J.W. Kwak, S.K. Noh, C.S. Park, and J.H. Kim, *J. Appl. Polym. Sci.*, **2005**, 95(6), 1539-1548.
10. T.L. Uyen Nguyen, B. Farrugia, T.P. Davis, C. Barner-Kowollik, and M.H. Stenzel, *J. Polym. Sci., Part A: Polym. Chem.*, **2007**, 45(15), 3256-3272.
11. C.J. Lee, W.S. Lyoo, I.C. Kwon, S.G. Lee, J.P. Kim, and M.H. Han. Microsphere Embolic Materials Having a Dual Structure of Poly(Vinyl Acetate) Core and Poly(Vinyl Alcohol) Shell and Method for Preparing the Same. United States Patent: US006191193B1, 2001.
12. N.A. Peppas and D. Tennenhouse, *J. Drug Del. Sci. Tech*, **2004**, 14(4), 291-297.
13. G.F. Liversidge, K.C. Cundy, J.F. Bishop, and D.A. Czekai. Surface Modified Drug Nanoparticles. United States Patent: US005145684A, 1992.
14. T. Moritani and J. Yamauchi, *Polymer*, **1998**, 39(3), 559-572.
15. T. Moritani and K. Kajitani, *Polymer*, **1997**, 38(12), 2933-2945.
16. T. Moritani and J. Yamauchi, *Polymer*, **1998**, 39(3), 553-557.
17. M.K. Beliakova, A.A. Aly, and F.A. Abdel-Mohdy, *Starch-Stärke*, **2004**, 56(9), 407-412.
18. Z.-F. Zhou, W.-b. Xu, D. He, J.-x. Fan, F. Yu, and F.-M. Ren, *J. Appl. Polym. Sci.*, **2007**, 103(2), 848-852.
19. G.S. Mukherjee, N. Shukla, R.K. Singh, and G.N. Mathur, *J. Sci. Ind. Res.*, **2004**, 63(7), 596-602.
20. S.Y. Nam, H.J. Chun, and Y.M. Lee, *J. Appl. Polym. Sci.*, **1999**, 72(2), 241-249.

21. H. Holik ed. *Handbook of Paper and Board*, Wiley-VCH: Weinheim, 2006.
22. B.P.a.B.M. Association, *Paper Making: A General Account of Its History, Processes, and Applications*, William Clowes and Sons Limited: Great Britain, 1950.
23. S. Bratskaya, S. Schwarz, G. Petzold, T. Liebert, and T. Heinze, *Ind. Eng. Chem. Res.*, **2006**, 45(22), 7374-7379.
24. K. Kubota, Z. Meiwa, H. Takahshi, and Y. Hasebe. Method of Improving Paper Stiffness. European Patent: EP1550770B1, 2003.
25. E. Antunes, F.A.P. Garcia, P. Ferreira, and M.G. Rasteiro, *Chem. Eng. Res. Des.*, **2008**, 86(10), 1155-1160.
26. W.S. Lyoo, C.S. Park, J.H. Yeum, B.C. Ji, C.J. Lee, S.S. Lee, and J.Y. Lee, *Colloid Polym. Sci.*, **2002**, 280(12), 1075-1083.
27. W.S. Lyoo and W.S. Ha, *Polymer*, **1996**, 37(14), 3121-3129.
28. W.S. Lyoo, J.H. Kim, and H.D. Ghim, *Polymer*, **2001**, 42(14), 6317-6321.
29. W.S. Lyoo, S.S. Han, J.H. Kim, W.S. Yoon, C.J. Lee, I.C. Kwon, J. Lee, B.C. Ji, and M.H. Han, *Angew. Makromol. Chem.*, **1999**, 271(1), 46-52.
30. T. Chen and E.L. Burch. Use and Preparation of Crosslinked Polymer Particles for Inkjet Recording Materials. United States Patent: US007507439B2, 2009.

Chapter 2: Historical and Theoretical Background

2.1 Introduction

There are many areas where uses of new forms of poly(vinyl alcohol) (PVA) are yet to be discovered, leaving a wide window for research. One of the windows open for such research is to prepare round surface functional PVA particles that functionally mimic modified starch particles, yet maintain a round shape. The differences in shape of the rigid PVA microspheres and the 'floppy' starch particles, ought to shed light on the differences that are found between the respective interaction with cellulose fibres. Colleagues who have been active in the field of papermaking, and paper additives and fillers, for the past few years, recently patented a new way of making paper,[1,2] with major improvements achieved when using 'floppy' modified starch particles.

This study involved making spherical PVA particles for use in studying their interaction and adherence to cellulose fibres compared to the soft formable (floppy) starch material, currently in use in papermaking.

In this chapter, an historical and theoretical background to several topics relevant to this study are introduced and discussed. In addition, mention will be made of how this information related directly to, or was directly applied to, the experimental work carried out in this study (e.g. Sections 2.3.4, 2.5, 2.5.1.2, 2.5.2.3, 2.6, 2.7.3 and 2.8).

2.2 Poly(vinyl alcohol) (PVA)

Primarily prepared by the hydrolysis or saponification of a vinyl ester, poly(vinyl alcohol) (PVA) is believed to be the first totally synthetic colloid. It was originally synthesised by Herrmann and Haehnel in the early 1920s.[3] Today PVA, which is still synthesised via a conversion from a poly(vinyl ester) precursor, is a widely used polymer and available in a range of different grades. Vinyl acetate (VAc) is typically used as monomer precursor for the preparation of PVA. The different grades of PVA vary in the degree of polymerisation as well as the degree of hydrolysis, thus supporting a range of applications and uses. The various grades, with their specific degrees of polymerisation and hydrolysis, among other factors, offer a variety of properties and characteristics, which can provide favourable qualities in specific applications.

2.2.1 History

Haehnel and Herrmann first discovered PVA in 1924, when they combined an alkali (caustic soda) with poly(vinyl acetate) (PVAc) in an alcohol based solution and obtained ivory-coloured PVA.[3-6] At about the same time, a similar discovery was made by Staudinger,[4-6] who studied the reversible transformation between PVA and PVAc via esterification and saponification. Scientific reports on the PVA macromolecule were simultaneously published by both research groups in 1927.

PVA found its first major application in warp-sizing of synthetic fibres, like rayon.[5] It was also used as a colloid stabiliser or emulsifier in emulsion polymerisations and as a thickening agent in aqueous dispersions – applications that have been extensively researched and expanded, and are still used today. These and other important uses were suggested by Herrmann and Haehnel[3,5] in their first major publications (ca. 1931). Meanwhile, Staudinger was also reporting similar findings and proposing similar end uses. The preparation of water soluble PVA films was mainly for medical uses, such as surgical sutures: 'synthofil' is one such PVA fibre, produced by F.B. Braun ca. 1935.[5]

2.2.2 Properties, applications and synthesis

PVA has a variety of properties. Its behavioural characteristics are indicative of a vinyl polymer, including the complexities brought about by grafted structures and stereoregular diversity. PVA also has distinct properties, characteristic of polyhydroxyl compounds. The properties of PVA are dependent on the degree of hydrolysis (i.e. partial or full), the percentage residual poly(vinyl ester) precursor present, and its respective contribution to the overall material properties. Partially hydrolysed poly(vinyl alcohol)s (PVAs) are essentially considered to be copolymers of the vinyl ester precursor monomer (typically VAc) and the hypothetical vinyl alcohol monomer, and hence will have unique properties according to their compositions. The type of vinyl ester precursor polymer used in the preparation of PVA, therefore, greatly influences its properties.

Commercially, PVA is synthesised by the saponification (or hydrolysis) of the PVAc precursor polymer, in alcohol, with sodium hydroxide as saponifying agent.[4,7] Depending on the degree of hydrolysis of commercial grades of PVA, and thus the respective PVAc contents, the PVA consequently portrays a combination of both the copolymer properties, affording a variety of different PVA grades.

PVA, synthesised from PVAc precursor, is a widely used polymer, with extraordinary properties, such as water solubility, oxygen barrier properties, solvent and oil resistance, excellent thermal and mechanical properties, non-toxicity, biodegradability and biocompatibility.[4,8,9] PVA therefore has a wide range of industrial application and uses, for example in the paper and

packaging,[3,4,10] fibre and film,[9,11-13] and medical[14-18] fields. The saponification of poly(vinyl ester) precursors like PVAc or poly(vinyl pivalate) (PVPi) yields a linear, semicrystalline PVA polymer. These linear polymers are extensively used as films, fibres in clothing, membranes and medicines. These PVA fibres and films are potentially high-performance materials because, in addition to their excellent oxygen barrier properties and alkali resistance, their high abrasion resistance, high tensile moduli and high impact and tensile strengths are properties often superior to those of other known polymers.[14,19] By increasing the degree of saponification (DS), the syndiotacticity, and especially the molecular weight, these physical properties can be maximised.

2.2.2.1 Water solubility

The structure of any polymer, unquestionably, affects its properties and therefore has a great influence on the final polymer application(s). PVA is essentially a polyhydroxyl with a 1,3-glycol repeating structure.[5] The hydroxyl groups are capable of undergoing both inter- and intramolecular hydrogen bonding, which influences water solubility and also crystallinity. Water thus has a great influence on the crystal structure of PVA, which is by nature hydrophilic.[5]

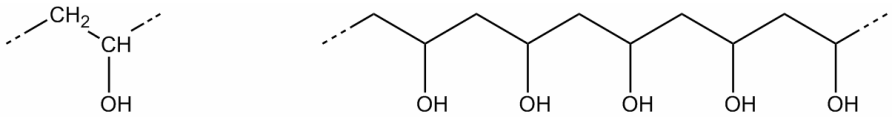

Figure 2.1 PVA structure, showing the repeat glycol unit and the polymer chain.

PVA is mainly used in aqueous solution, and its solubility in water is greatly dependent on the degree of polymerisation (DP) and degree of hydrolysis (or DS). Depending on the DP and hydrolysis, a certain percentage of residual acetate groups will still be present in the final PVA product. PVA has a high affinity towards water as a result of the large number of hydroxyl groups, but solubility is hindered by the strong hydrogen bonds (both intra- and intermolecular) that lead to crystallisation. This is overcome by the hydrophobic nature of the residual acetate (or ester precursor) groups in partially hydrolysed PVA. The intra- and intermolecular bonds between neighbouring hydroxyl groups are essentially weakened by the added hydrophobicity. Therefore, the solubility of the PVA will be influenced by the content of residual acetate groups, so that when sufficient acetate (or ester) groups are present, the degree of water solubility increases. However, if the residual acetate content is too high, the polymer will effectively become less water soluble, and rather more soluble in aliphatic esters and aromatic hydrocarbons.[4,7] Nevertheless, because of the influences of the residual acetate groups (and the number thereof) on the evolution of heat, high temperature solubility and critical phase separation temperature, the solubility behaviour of PVA in water remains complex.[4]

2.2.2.2 Crystallinity and thermal properties

The strong hydrogen bonds and the small size of the hydroxyl groups, allow for chain orientation and regular crystal lattice formation, resulting in the partial crystallinity of PVA. Consequently, PVA has very good mechanical and thermal properties. The degree of crystallinity is greatly dependent on the degree of hydrolysis, which ultimately influences the solubility. If there is only partial hydrolysis in the PVA, the resulting disorder greatly hinders and prevents crystallinity.[20] Heat treatment results in a more ordered packing, hence causing crystallisation of the PVA. Therefore the degree of crystallinity is affected by the thermal history that the polymer has been subjected to.[4,5] It has been reported that heat treatment at a high temperature and for a long period results in a higher degree of crystallinity.[5] By applying a suitable heat treatment procedure, it is possible to make hydrophilic polymers that are resistant to water. This is an important quality, as this allows for the production of PVA material (generally fibres) with unique properties, such as resistance to hot water and softening or shrinking in boiling water.

PVA has a wide glass transition temperature (T_g) range, or range of softening points. Literature reports values from approximately 75–90 °C,[5,21-23] but it is generally accepted that 100% amorphous PVA has a T_g of 85 °C. Altering the thermal history of the material influences the T_g: the higher the temperature of annealing the higher the T_g value. For example, it has been shown that for PVA fibre or film samples that were only subjected to temperatures below 130 °C, the T_g values were in the lower temperature range of about 75 °C. Samples treated at temperatures of about 230 °C, however, had T_g values between 85 °C and 90 °C. The shifts in the T_g values of the different samples are expected as the thermal properties (softening and melting) are related to each other. Hence the thermal history will affect both crystallinity and glass transition temperature.[4] When subjected to longer and/or higher temperature treatments, a higher crystallinity is obtained, as chains are allowed to orientate into a highly ordered crystalline structure. The strong hydrogen bonds and thus highly ordered packing ultimately hinders or reduces chain rotation and mobility, consequently affecting glass transitions.[20] The highly ordered chains now require more energy (i.e. heat) for molecular movement, and therefore higher temperatures to reach or surpass the T_g (or softening point). Thus, the T_g will also be affected by the DP, DS and water content.

2.2.2.3 Structure and stereoregularity

Stereoregularity refers to the stereochemical arrangement of adjacent repeating units in a polymer chain. The stereoregularity of PVA plays a key role in determining its applications. The three stereoregularities are isotactic, syndiotactic and atactic (or heterotactic),[4,24] each with unique chemical

and physical characteristics. The significance of the stereoregularities thus lies in the difference in chemical and physical properties of the different PVAs. Figure 2.2 (a–c) shows the different tacticities, where all the substituents are orientated regularly on the same side of the polymer chain (isotactic), regularly alternating on opposite sides of the chain (syndiotactic), or randomly orientated on either side along the polymer backbone (atactic).[4,25]

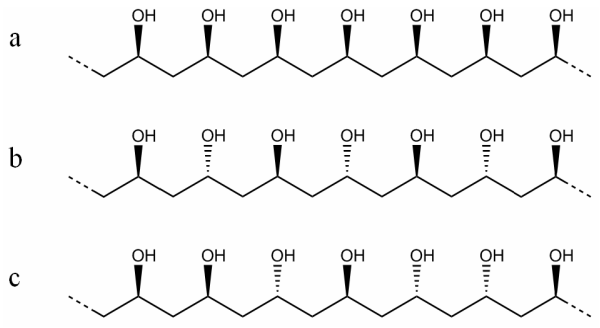

Figure 2.2 Stereochemical arrangements for fully hydrolysed PVA: (a) isotactic, (b) syndiotactic and (c) atactic.

PVA is prepared via the hydrolysis or saponification of a poly(vinyl ester) precursor, as discussed in Section 2.3, and a different stereoregularity is obtained depending on the type of vinyl ester precursor monomer used. In the past, PVA was predominantly prepared by the polymerisation of VAc, and subsequently hydrolysed or saponified PVAc yielded a PVA with a randomly distributed, atactic configuration.[4,24,26] Nowadays, as a result of the various vinyl monomer precursors available, a variety of stereoregularities can be obtained. Table 2.1 shows a few isotactic- and syndiotactic-specific monomers, as well as the atactic VAc monomer. Copolymerisation of VAc with different vinyl monomers has also been used to vary the final stereoregularity and subsequent properties of the resultant PVA.[4,14,19,24,26-28]

It is interesting to note that the vinyl ether monomers generally yield isotactic-rich precursor polymers, while the vinyl esters yield syndiotactic-rich polymer precursors. Bulky vinyl ester monomers, like diphenylacetate or vinyl pivalate (VPi), yield polymers rich in syndiotacticity when polymerised.[19]

Of all the radically polymerised PVAs, PVA produced from PVPi as precursor polyester has the highest sydiotacticity. The PVA obtained, when prepared via low-temperature polymerisation of VPi, has an s-dyad content > 60%.[14] It is therefore possible to prepare PVAs with various degrees of tacticity by copolymerisation of VAc and VPi, for example. Consequently, the relationship between the tacticity and physical properties of the PVA can be investigated.[19,27,28]

Table 2.1 Precursor monomers used for stereospecific PVA synthesis[3-5,26]

Isotactic	Syndiotactic	Atactic
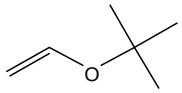 *t*-butylvinylether	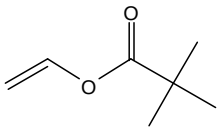 vinyl pivalate	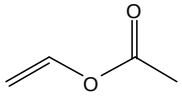 vinyl acetate
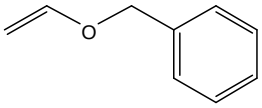 benzylvinylether	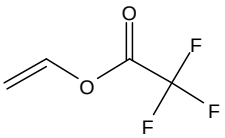 vinyl trifluoroacetate	
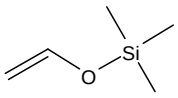 vinyltrimethylsilylether	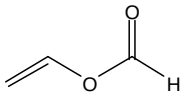 vinyl formate	

2.2.2.4 Applications and other general properties

The degree of polymerisation and degree of hydrolysis, as well as the distribution of the hydroxyl groups, are key factors that influence the basic properties of PVA. Various grades of PVA are commercially produced, generally depending on the degree of hydrolysis. The principal PVA grades are classified into two main groups, namely fully and partially hydrolysed PVA, with 97.5–99.5% and 87–89% hydrolysis, respectively.[4] Subgroups of the partially hydrolysed groups/grades include 80% hydrolysis and an 'intermediate' group of 88–98%.

The molecular weight and especially the stereoregularity (Section 2.2.2.3) play a substantial role in the end use and applications of PVA. The molecular weight of PVA can be controlled, to some extent, by varying certain conditions during the precursor polymerisation. For example, a lower polymerisation temperature and initiator concentration will yield a higher molecular weight polymer.

Millions of tons of synthetic polymer material are being produced each year, making biodegradability and non-toxicity valuable qualities for any polymer, especially as the amount of plastic waste is increasing by several tons each year.[4,7] PVA is the only synthetic vinyl polymer confirmed to be biodegradable[8] and together with its water solubility, this feature makes PVA very advantageous in terms of easier degradation and elimination. Besides being both biodegradable and non-toxic, PVA has many other favourable characteristics, making it a very versatile and widely used polymer. Such characteristics include water solubility (and non-solubility, depending the sample

preparation and heat treatment), crystallisability and inter- and intramolecular hydrogen bonding, and subsequently excellent mechanical and thermal properties. PVA can withstand IR and UV radiations and relatively high temperatures. Additional PVA characteristics include its excellent barrier properties and resistance to oxygen, scents, flavours, fats, grease, oils and organic solvents. In paper applications, PVA is used as a polymeric additive to enhance oxygen, oil and moisture resistance.

2.3 PVA synthesis and synthetic routes

PVA is synthesised via the polymerisation and hydrolysis of a vinyl monomer precursor, generally a vinyl ester. The vinyl alcohol monomer is unstable, and tautomerises into the more stable acetaldehyde form.[3,6,29] Consequently, the vinyl alcohol monomer is not available in sufficient quantities or purities for PVA polymerisation or synthesis.[3-5] Hence, PVA is generally produced via a two-step synthetic process, wherein vinyl monomers are used for the synthesis of precursor polymers, which are subsequently modified to PVA.

The PVA precursor polymers can be prepared by the free radical synthesis of the vinyl ester monomers via one of three principal methods: suspension or emulsion, bulk or mass, or solution polymerisation[3] (see Section 2.4.1 on suspension polymerisation). PVA is industrially prepared via the radical polymerisation of VAc in all these processes.[3-5] The subsequent modification to PVA is commonly hydrolysis (especially for the industrial used VAc), however, alternative techniques such as saponification and aminolysis may also be used (Section 2.3.2).

Of the many different living polymerisation techniques, such as cationic or anionic polymerisation, ring opening or free radical polymerisation, etc., and the various modification techniques, only those applicable to the contents of this study are discussed further.

2.3.1 Free radical vinyl polymerisation and vinyl monomer precursors

Addition polymerisation is understood as the reaction of a large number of small molecules which permanently combined together as a large molecule of repeat units. The polymer composition is therefore identical to that of the monomers, except for possible variations associated with end-groups. Free radical addition polymerisation is particularly applicable to carbon compounds containing one or more double bonds.[30]

For the preparation of PVA precursors, the vinyl monomers (especially vinyl esters) are commonly polymerised via free radical polymerisations. This includes the typical free radical steps of: initiator decomposition, monomer initiation, chain propagation, possible chain transfer and reinitiation, and finally termination, either by disproportionation or combination.[4,20,31] This type of

polymerisation mechanism, its respective steps, and the kinetics thereof, has been extensively described by Finch,[4] Hamielec and Tobita,[32] Sakurada and Okaya,[5] Matyjaszewski and Davis,[33] Odian[34] and Chirowodza.[35] This will not be reviewed here.

Initially, PVA was prepared exclusively using VAc as precursor monomer, yielding only atactic PVA, but recent discoveries indicate that a highly syndiotactic PVAc is obtained when VAc is polymerised in fluoroalcohols.[5] Various vinyl monomers have been used for the synthesis of PVA, each resulting in unique properties, and hence respective end uses and applications. In addition to those monomers mentioned in Table 2.1, monomers that may be used for the preparation of a vinyl polymer precursor include vinyl acetate derivatives like vinyl chloroacetate, vinyl bromoacetate, vinyl benzoate, and vinyl ethers, divinyl compounds and acetaldehydes.[3] For the purpose of this study, focus remains on the vinyl ester precursors, particularly VPi and (where necessary) VAc.

2.3.2 Conversion of poly(vinyl ester) to PVA

Depending on the poly(vinyl ester) precursor used and the desired end product properties, the method used for PVA preparation will vary: hydrolysis, saponification (also known as transesterifaction) or aminolysis.[4] Scheme 2.1 provides a general illustration of the different modification methods.

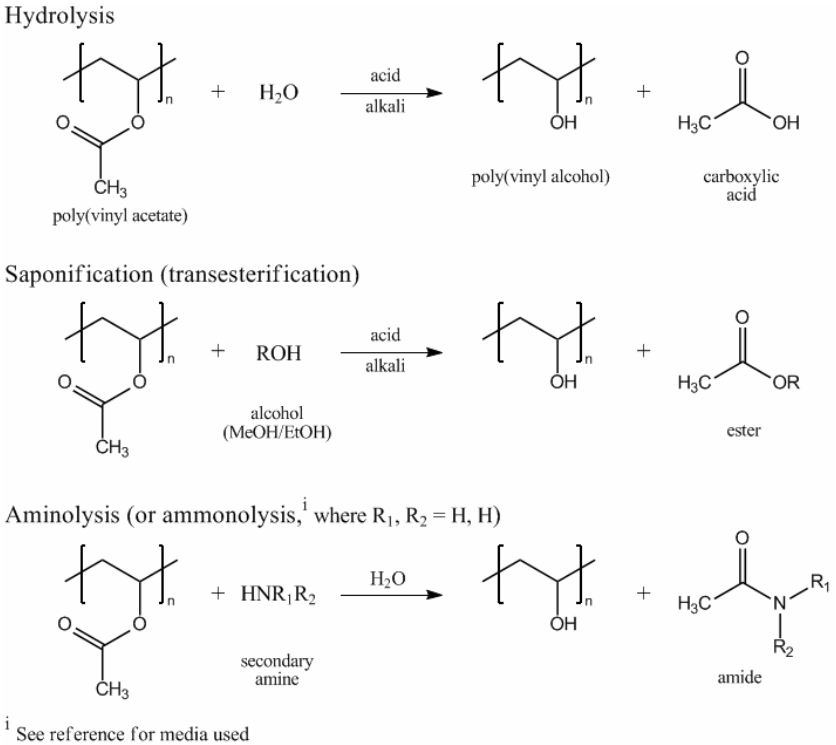

[i] See reference for media used

Scheme 2.1 Various modification techniques used for the preparation of PVA from PVAc;[4] where R, R_1 and R_2 are alkyl groups.

In both hydrolysis and saponification reactions, small (catalytic) amounts of either acid or base are used to promote the ester to alcohol conversion (Scheme 2.1 above). There are a variety of catalysts that may be used for the modification (hydrolysis or saponification). A few common base (or alkaline) catalysts include potassium hydroxide, sodium hydroxide, sodium carbonate and sodium methoxide (or ethoxide). Commonly used acid catalysts include sulphuric acid, mineral acids and hydrochloric acid.[3] When ammonia is used as catalyst for PVAc hydrolysis (i.e. aminolysis), it provides favourable whitening properties, although it has lower catalytic activity compared to sodium hydroxide (for example).[3]

Saponification, formally known as transesterification or alcoholysis, is the most important industrially used method for the production of PVA.[4] In terms of the degree of hydrolysis (or saponification), the extent thereof depends on reaction conditions such as the type and concentration of the active hydrolysing/saponifying agent and/or catalyst present, and the temperature and duration of the process. Therefore, by regulating these conditions, the various industrial PVA grades, with different degrees of hydrolysis are easily obtained.

Saponification is the main technique used in this study, although hydrolysis (using small volumes of water) was also used in the modification step. The main difference between saponification and hydrolysis is the different solvents used in the reaction: either alcohol or water. The terms saponification and hydrolysis (and derivatives thereof) are often used interchangeably, but for all practical purposes, they describe the same process.

2.3.3 Poly(vinyl pivalate) (PVPi) or poly(vinyl ester) as precursors to PVA

A variety of vinyl monomers can be used as precursor monomers for the synthesis of PVA, as mentioned in Section 2.3.1. With regards to the present study, the focus remains on the monomer selected for use, namely VPi.

VPi as a precursor to PVA is unique, in that it is a previously not fully investigated monomer,[36] and very little information on this is available in literature. With the exception of the alkyl carbon pendant groups (red, Figure 2.3), the VAc and VPi monomers are structurally quite similar. As illustrated in Figure 2.3, and as the names suggest, the differences in the alkyl group/carbon(s) of the ester functional groups are obvious – a methyl group in the vinyl acetate (i.e. acetyl group), while vinyl pivalate hosts a *t*-butyl group (i.e pivaloyl group). Due to these differences, the properties of these monomers, and their respective polymers, are very different.

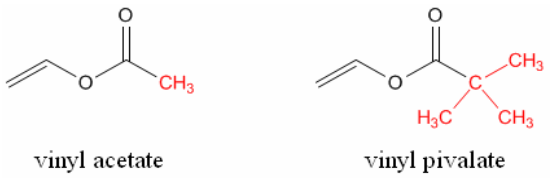

Figure 2.3 Chemical structures of the VAc and VPi monomers.

Thus, although PVPi also has ester functional groups, it does not mimic PVAc. The polymerisation mechanisms are different, with monomer addition and insertion affected by the nature of the pendant groups. Hence, PVAc is atactic, whereas PVPi is syndiotactic. The tacticity is a direct result of the nature of the ester group, namely its bulkiness or the spatial restrictions. The bulky pivaloyl groups result in an alternating sequence of the hydrolysed form, hence resulting in a higher degree of syndiotacticity. The increased syndiotacticity consequently results in an increase in the crystallinity. For use as an additive in the paper industry, syndiotacticity-rich PVA is more desirable than atactic PVA because its high crystallinity provides enhanced mechanical and thermal properties.[27,37] Thus, for this study, and with later cellulose fibre studies in mind, the more syndiotactic VPi was chosen as precursor monomer for PVA preparation.

With regards to pendant groups, VPi (and the corresponding PVPi) has pivaloyl group(s) [$(CH_3)_3CO$] instead of the acetyl group(s) of the VAc (and the corresponding PVAc). Thus, in contrast to VAc, VPi has no labile hydrogens present in the acyl group and is therefore unable to undergo chain transfer via hydrogen abstraction.[36] Hence, VPi cannot form branches like the VAc monomer, because it does not have the conjugated methyl pendant group necessary for branching to occur. Thus linear polymer chains are produced with VPi to afford PVPi.

When considering the free radical polymerisation of VAc (and assuming VPi acts in the same way), taking into account that recombination may become a factor at lower temperatures,[4] termination predominantly takes place via disproportionation. This type of termination mechanism, whereby two reactive chains come together and exchange radicals and/or protons, yields two separate chains, one of which has a double bond end group (see Scheme 2.2).

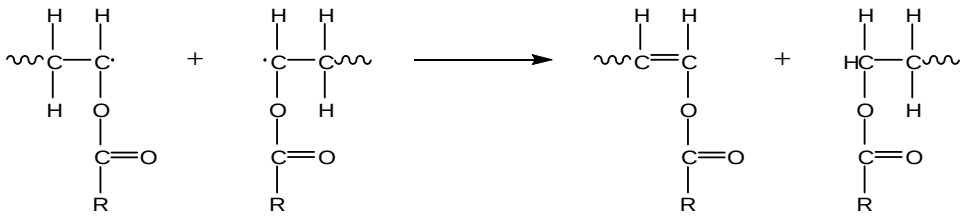

Scheme 2.2 **Radical termination of the propagating chain species by disproportionation, illustrated for vinyl ester polymers, where R represents the alkyl group of the respective ester. (For example, R represents a methyl group in the case of VAc, or a *t*-butyl group in the case of VPi.)**

On conversion of the poly(vinyl ester) to PVA by means of hydrolysis or saponification, these double bonds yield aldehyde end groups, which decrease the overall PVA thermal stability. This is due to an increase in the ability to form conjugated double bonds, and thus a lower initial activation energy for water splitting. This explains why an increasing colour change accompanies hydrolysis.

2.3.4 Saponification of PVPi

For many years, PVPi was not easily hydrolysed, owing to the steric hindrances of the substituents. Later, it was found that it could be fully hydrolysed using tetrahydrofuran (THF) as solvent, under a nitrogen atmosphere.[5] Of all the vinyl ester monomers, VPi has the slowest rate of hydrolysis.[3] Generally, a relatively high degree of polymerisation is attained for PVA when PVPi is used as precursor polymer. Futhermore, in comparison to PVA derived from PVAc, PVPi derived PVA has a 20 °C higher melting point and is more difficult to dissolve in water.[5] The syndiotactic and crystalline nature and the non-branched linear chains of PVPi, as well as most of its other characteristics, ensure that VPi is a suitable monomer precursor.

Extensive research has been carried out into the preparation and production of PVA. Won Lyoo and his many coworkers studied the preparation of PVA via the saponification of PVAc[29,38,39] or PVPi[12,37,40-43] homopolymers, or the PVAc/PVPi copolymer.[14,19,27,28,44,45] Two very distinct saponification methods were utilised for the conversion of the respective poly(vinyl esters) to PVA. One method involved the dissolution of the poly(vinyl ester) precursor in THF, while the other was in an alcohol as solvent, typically methanol (MeOH). Potassium hydroxide would typically be the catalyst used with THF, while sodium hydroxide would typically be used with MeOH, but neither catalyst is restricted to either solvent system. The preferred industrial process for the preparation of PVA from PVAc is transesterification in MeOH with catalytic amounts of sodium methoxide.[6]

With regards to the saponification of the PVAc/PVPi copolymer, both the THF[27,28] and alcohol[19] solution based techniques have been investigated. The THF method worked well, resulting in the hydrolysis of both the acetate and pivalate components, but also resulting in a fibrous PVA product. According to Lyoo et al.[19] (who studied PVAc/PVPi copolymers and the saponification thereof with MeOH as solvent), PVPi is more effectively saponified using KOH as catalyst, and a higher DS is obtained when higher saponification temperatures and higher alkali concentrations are used. On the other hand, Lee et al.[14] describe the heterogeneous saponification of the P(VPi/VAc) copolymer microspheres, and show core-shells with surface modification. The core-shell PVA particles were saponified from P(VPi/VAc) using an aqueous based saponification solution with an alkali solution (sodium hydroxide, sodium sulphate and methanol/ethanol) as saponification agent.

In the present study, for the preparation of PVA from PVPi, both the heterogeneous saponification[14] and the traditional THF saponification (with KOH catalyst)[27,28] methods were used. The latter method (THF based method) proved to be successful for the preparation of PVA but the former (aqueous based method) was less successful, contrary to what was reported by Lee et al.[14] for surface hydrolysed core-shells. When THF is used in the saponification of PVAc and/or PVPi, the resulting PVA material is very fibrous in nature. Information on studies of the preparation of PVA by the hydrolysis or saponification of PVPi particles, where the particles maintain their spherical shape during saponification, is not readily available in literature, if at all. This leads to the next topic to be considered, i.e. the preparation of spherical PVA particles from PVPi particles, and their cross-linking.

2.4 Spherical particles

Spherical polymer particles can be synthesised via a variety of different polymerisation techniques, each yielding particles of various sizes. These procedures include dispersion, precipitation, suspension, seeded and emulsion polymerisation, and soap-free, micro- or mini-emulsion polymerisation techniques.[46] These processes were compared and discussed in a detailed review by Guang Ma[47] and a survey by Arshady.[48]

Each of the above-mentioned techniques offers various advantages and different particle size ranges and size distributions. For example, there are clear differences between emulsion and suspension polymerisation, which are also known as ‘bead’ or ‘pearl’ polymerisation. Emulsion polymerisation yields particles that are usually smaller than 1–2.5 μm in diameter, while suspension polymerisation yields larger particles from about 1 μm up to 100 μm, or larger.[20,46,48-50] For the purpose of the present study, suspension polymerisation was used for the preparation of particles mostly within the size range 1–10 μm.

2.4.1 Suspension polymerisation

In the case of VAc and VPi (PVA precursor monomers), suspension and emulsion polymerisation are often used to prepare PVAc or PVPi (or PVAc/PVPi copolymer) particles. The suspension polymerisation process was selected in the present study, because it offers the required particle size range.

2.4.1.1 General reaction conditions

Suspension polymerisation can be described as the process of dispersing the (relatively) water insoluble monomer(s) as liquid droplets in aqueous medium, stabilised by steric stabilisers and dispersed by continuous vigorous stirring. Monomer soluble initiators are used and stirring/agitation is maintained throughout polymerisation, to produce the dispersed solid phase polymer particles. As polymerisation takes place, the monomer droplets polymerise into sticky, viscous monomer-swollen particles, and eventually fully polymerise into rigid particles. The main aim is to prepare an 'as uniform as possible' monomer droplet dispersion in the aqueous phase and maintain controlled coalescence during the polymerisation process.[50]

The main practical problem associated with suspension polymerisation is particle coalescence or coagulation, and the prevention thereof. In the three stages of polymerisation and particle growth (early, intermediate and later), particle coalescence is of major concern in the intermediate stage. In the intermediate phase the particles are very sticky and tacky, and are essentially 'monomer-plasticised' polymer particles.[30] The semi-solid, tacky particles therefore coalesce readily, but redispersion of these intermediate-phase sticky particles becomes increasingly difficult. Coalescence is not as significant in the beginning stages, as the droplets are sufficiently fluid to continuously separate as they coalesce. In the final stages, coalescence is restricted because the particles are too hard and robust to coalesce. Adequate agitation (stirring) is therefore required and important.

In the present study, it was important to minimise the intermediate period, so as to reduce the amount of coalescence, and hence to obtain a narrower particle size distribution. In addition to controlling the agitation speed, the polymerisation conditions such as temperature and the various components' concentrations were altered in attempts to achieve rapid polymerisation of the particles and to restrict the intermediate stage coalescence.

2.4.1.2 Advantages

The advantages that suspension polymerisation offers are that a fluid system will be maintained throughout the reaction and heat dissipation is not a significant problem, because excess heat

(generated by strongly exothermic reactions) is absorbed and expelled by the dispersion medium.[14,30] For a suspension prepared polymer, the molecular weight is controlled by the amount and type of initiator and suspension agent used, the monomer-to-water ratio, the polymerisation temperature and agitation speed.[14] High agitation speeds result in higher conversion and molecular weight. There are few studies on VPi suspension polymerisation, but many on the suspension polymerisation of VAc. Higher conversions are reached (for VAc) when using suspension methods compared to other polymerisation methods.[14] The polymer material obtained from suspension polymerisation is less contaminated than emulsion polymerisation material. Polymer isolation is relatively simple (typically achieved simply by filtration or centrifugation), and problems like toxicity, flammability and the overall expense of the polymerisation are minimised when water is used as a dispersion medium.

2.4.2 Spherical PVA particles

Spherical PVA particles are ideal for use in medical applications, due to their good biocompatibility, efficient binding properties and thus blocking efficiency, and few 'foreign-body reactions *in vivo*'.[14] Commercially, such embolic PVA particles are produced by pulverising PVA sponges, but irregularities of the particle size and shape cause inflammation and other complications. Regularly shaped and sized particles are therefore a more appropriate solution. Uniform poly(vinyl ester) microspheres, like PVPi or the P(VPi/VAc) copolymer, are possible promising precursors for the production of PVA embolic materials. These may have a specific tacticity, according to the intended application and depending on the monomer/polymer precursor tacticity and content. Specifically for medical applications, the shape of the material is important, as are the stability, durability and biocompatibility. PVPi would satisfy the latter; however, maintaining (uniform) shape on saponification still requires investigation.

Lee et al.,[14,51] Lyoo et al.[29,39-41,52] and Song and Lyoo[42] have produced spherical monodispersed PVPi, PVAc or P(VPi/VAc) copolymer particles as PVA precursors, by either suspension or emulsion techniques. In producing spherical PVA particles, Lee et al.[14] propose the idea of carrying out a heterogeneous surface saponification of the P(VPi/VAc) copolymer using an aqueous-alcohol medium with an alkali sodium hydroxide solution as saponifying agent. As discussed in Section 2.3.4, and in the paper itself, the saponification of PVPi is very difficult to achieve in any medium other than THF.

There is limited reported research on the preparation of spherical PVA microspheres or even core-shell PVA particles that are uniform in size and shape. The PVA precursor material often results in fibrous material when hydrolysed or saponified. Hence it is difficult to prepare such particles, and,

once prepared (if at all), their spherical shape is difficult to maintain. The introduction of cross-linking is therefore suggested in an effort to maintain the spherical shape during saponification, and subsequent sieving of the formed particles provides a possible means for obtaining particles with monodisperse particle sizes.

2.5 Chemical modification of PVA

PVA is a highly sought after polymer due to a range of excellent properties, as previously mentioned. For use in certain fields, PVA is modified to suit specific applications and needs. In the medical industry, for example, PVA is cross-linked to insolubilise the material. In fields such as biotechnology, medical drug delivery, clothing and construction, fibres and films, and solid phase organic synthesis, the importance of (and need for) polymer supports has led to extensive developments of 'spherical support materials'.[53] These spherical support materials, prepared either by emulsion or suspension polymerisation reactions, are typically cross-linked, but other modification or polymer functionalisation methods also exist, including grafting and ionic modification.

Cross-linking affords a polymeric material with unique characteristics that the polymer would otherwise not have, such as insolubilisation or gelation, and swelling capacity. Increasing water resistance and insolubilisation of PVA is necessary for applications that require the use of fibres and films, and coatings, adhesives, sizing, etc.[54,55]

The properties of PVA can be improved, and even tailored to suit various advanced applications, by modifying the PVA. PVA modification may be carried out either during polymerisation, such as in the case of copolymerisation,[54,56-58] or by post-polymerisation modification. Pre-polymerisation methods entail modification of the PVA precursor polymer and can be achieved by copolymerising the vinyl ester (typically VAc) precursor monomer with a comonomer of desired functionality, and subsequent saponification thereof.[56-58] Post-polymerisation modification of PVA can be achieved by grafting[59,60] or by specific reactions of the hydroxyl groups.[61,62] The PVA hydroxyl groups are subject to undergo all reactions typical of that of ordinary secondary alcohols, and can therefore be modified by secondary reactions of these hydroxyl groups post-polymerisation.

These methods of modification were used in the present study. Pre-polymerisation modification included cross-linking the PVA precursor using a difunctional cross-linking agent as a comonomer with the VPi. This provided the PVPi particles with the desired stability to resist deformation and fibrillation during saponification. Post-polymerisation modification resulted in the attachment of chemically active functional groups to the surface of the PVA particles. Following the principle that opposites attract, attaching cationic groups onto the PVA imparts ionic bonding with the

naturally anionic cellulose fibres,[35,57] providing a stronger interaction than hydrogen bonding alone. By chemical modification of PVA using ionic groups, particles that mimic the functional chemistry of modified starches are prepared. This allows for a comparison between the interactions of the modified PVA particles with cellulose fibres and the interaction of the modified starch with fibres. This will ultimately lead to a better understanding of the principles of wet end chemistry in paper production.

2.5.1 Cross-linked PVA

There are many methods available for cross-linking PVA, especially in terms of chemical cross-linking, where a wide variety of cross-linking agents have been suggested.[54,55,63,64] Cross-linking procedures include intermolecular cross-linking via acetalisation,[55] esterification and subsequent cross-linking through double bonds,[65] and self-cross-linkable PVA materials have also been reported.[54] As alternatives to chemical cross-linking, physical methods, including irradiation[66-68] and heat treatment[55,69] have also been used as cross-linking techniques. Grafting copolymerisations, using a hydrophobic monomer are commonly used to prepare entirely insoluble PVA.[70] The cross-linking density has a great influence on the final properties of the cross-linked materials.[71,72] Factors that may be influenced by cross-linking include viscoelasticity,[63] mechanical and thermal properties,[53,65,71] permeability and swelling characteristics.[64,70,72]

2.5.1.1 Copolymerisation

Copolymerisation is achieved when two different monomers take part in the polymerisation process, producing a polymer chain that incorporates both monomers. In general, copolymerisation of monomers may take place by one of four methods, according to the arrangement of the monomeric groups relative to each other within the copolymer chain, and the sequence in which they are polymerised or inserted together. These four commonly known copolymer sequences are alternating, random, block or graft,[73,74] as illustrated in Figure 2.4.

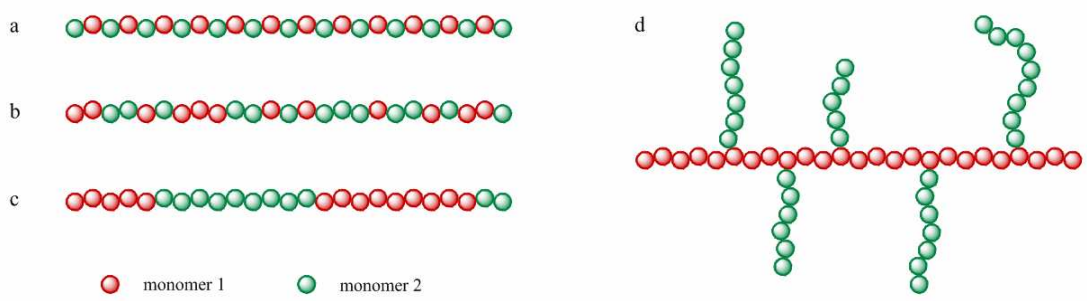

Figure 2.4 **Illustration of the different copolymer types: (a) alternating, (b) random, (c) block and (d) graft copolymers.**

2.5.1.2 Cross-linking by copolymerisation

Cross-linking of the PVA precursor via copolymerisation constitutes the incorporation of a second comonomer, having specific (cross-linking) functionalities, with the vinyl ester monomer in the initial polymerisation. The cross-linked polymer is subsequently saponified to cross-linked PVA, where the cross-linking comonomer should not be susceptible to hydrolysis.[56,57,75] The degree of cross-linking is directly related to the percentage comonomer (cross-linking agent) incorporated in the copolymerisation.

Cross-linking by free radical copolymerisation of a vinyl and divinyl monomer[32] was the technique selected for use in this study. The proposed network structure of this type of cross-linked polymer is illustrated in Figure 2.5, showing the active radical centres, cross-links and live pendant double bonds (of the divinyl monomer) still active for propagation. A divinyl ether [tri(ethylene glycol) divinyl ether, (TEGDE)] was used as the cross-linking comonomer, and cross-linking was achieved through the double bonds on either end of TEGDE. This comonomer was selected to be used in the copolymerisation with VPi because, being an ether, it is supposedly resistant to hydrolysis. It was assumed that a random copolymer configuration was obtained.

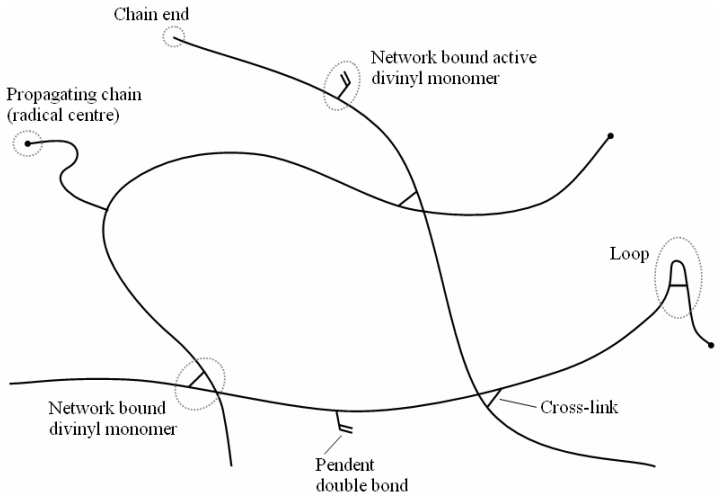

Figure 2.5 Schematic illustration of a cross-linked polymer network prepared by the free radical copolymerisation of a vinyl and divinyl monomer.[32]

The molecular weight, in particular, is a fundamental factor affecting the physical properties of a material.[14] Cross-linking increases the molecular weight by joining adjacent molecules, and may offer certain material improvements. An alternative method of cross-linking is post-polymerisation modification, whereby the PVA is first prepared and then cross-linked.[70,76] This allows for unique surface cross-linking and depending on reaction conditions and desired properties, ultimately permits the preparation of materials such as shell cross-linked micelles.[76]

2.5.1.3 Recent research pertaining to PVA particles

In a recent patent of Chen and Burch,[75] published during the course of this study (2009), methods of producing cross-linked organic particles or pigments, with porous and/or swellable properties, for use as an inkjet print medium, are described. Many methods for producing porous, hydrolysed, cross-linked and/or spherical organic particles required for this application are described. Various polymerisation techniques (suspension, emulsion, mini-emulsion) for the preparation of spherical poly(vinyl ester) particles, and their respective properties or characteristics, are also described. Different modification techniques and modification agents (saponification agents) for the production of PVA, e.g. hydrolysis, saponification, alcoholysis, etc., are mentioned. The different cross-linking methods and various cross-linking agents which may be employed (including TEGDE, relevant to this work) were mentioned in the text, but not all in the examples. This patent opens another door for possible research in, that functional cross-linked particles can adsorb specific inks with specific charges by electrostatic attraction.

2.5.2 Functionalisation of PVA (via the reaction of hydroxyl groups)

Modification or functionalisation of conventional organic polymers can be carried out to create new materials with specific functionality, often with improved properties and for specific applications. Techniques used for post-polymerisation modification, where PVA is first synthesised and then modified, include either grafting or functionalisation of the hydroxyl groups by secondary reactions.

Grafting reactions using copolymers of specific functionalities, or functional groups, allow for the preparation of PVA with desired functionality. There are typically three very distinct grafting methods used to prepare graft copolymers: *grafting onto*,[34] *from*[33,34] and *through*.[34] Briefly, *grafting onto* entails the reaction of the complimentary functional groups of the respective polymer counterparts, while *grafting from* comprises the growth of a polymer chain from, for instance, a polymeric macroradical species (or other polymer initiating species), and the copolymerisation of vinyl or acrylic (amongst others) macromonomers describes the *grafting through* process. The different grafting techniques with the various monomers (or their mixtures) used, have been described in literature[8,33,34,59,60,77-81] and reported by fellow students.[35,82]

In this study, it is the modification of PVA via chemical reactions specific to the functionalisation of the hydroxyl group that is of importance. PVA can be modified to possess a positive or negative charge, by chemical modification/reaction of the hydroxyl groups with monomers of specific functionalities, having the appropriate cationic or anionic charge. These cationic or anionic monomers may be incorporated onto the PVA by esterification or etherification reactions of the hydroxyl groups of PVA.

2.5.2.1 Etherification

Etherification of PVA affords single functionality at a single hydroxyl group. It is easier to ensure a consistent product with a chemical reaction modification, rather than grafting of monomers. This is achieved here by the process known as the "Williamson ether synthesis".[25] This two-step process (S_N2 reaction) can be used in the synthesis and preparation of cationic and anionic PVA, starch and cellulose.[83] The first step in the Williamson ether synthesis entails the formation of an alkoxide via the alkalisation of the hydroxyl groups, using a relatively strong base, such as sodium hydroxide. Subsequent reaction of the alkoxide with an alkyl halide is the second step in ether synthesis. Scheme 2.3 summarizes the basic steps of the Williamson etherification of PVA. In this study, etherification using an alkyl halide with specific functionality was used to functionalise the PVA particles. By using anionic or cationic functional alkyl halides, anionic and cationic functional PVAs were synthesised.

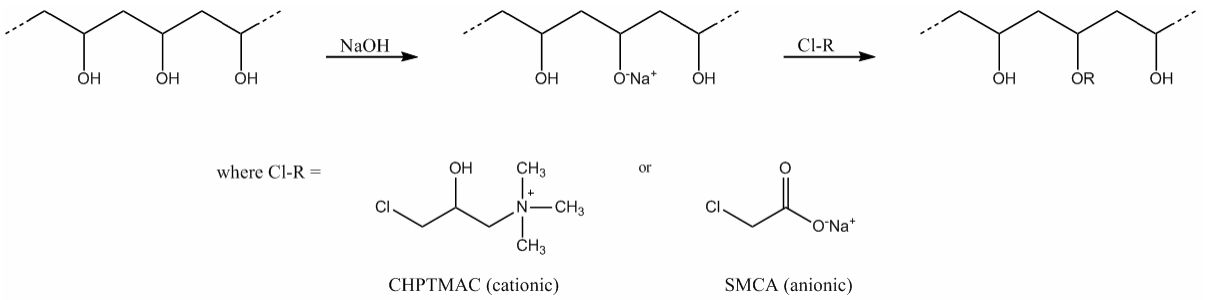

Scheme 2.3 Williamson etherification of PVA.

Cationic modification of starch was achieved by Haack et al.,[84] who employed the Williamson ether synthesis method, using 3-chloro-2-hydroxylpropyltrimethylammonium chloride (CHPTMAC) or 2,3-epoxypropyltrimethylammonium chloride as etherifying reagents. The cationic starch derivatives were prepared by reaction of the starch with cationisation agents under alkaline conditions in either aqueous or aqueous alcoholic media.

Anionic modification of starch was achieved by Volkert et al.[85] by the carboxymethylation of starch derived from the Williamson ether synthesis. Under basic conditions, the etherification agent (chloroacetic acid or sodium monochloroacetate (SMCA)) reacts with the hydroxyl functional groups on the starch in a nucleophilic substitution reaction. Similar work on the carboxymethylation of cellulose or PVA (using monochloroacetic acid or its sodium salt) has been reported by Aguir and M'Henni[86] and Mukherjee et al.,[61,87] respectively.

In this study, the techniques used to prepare surface functionalised spherical PVA particles were similar to the above two processes. The adhesive properties that these newly functionalised (cationic or anionic) PVA particles offered to their interactions with cellulose fibre surfaces were studied.

2.5.2.2 Esterification and alternative modification methods

In an esterification reaction, a carbohydrate reacts with an acid chloride or acid anhydride, under basic conditions.[83] In this way, PVA can be modified by esterification, using carboxylic acids or anhydrides. Giménez et al[88] prepared anionic PVA by the esterification with anhydrides, such as phthalic anhydride and succinic anhydride, thereby producing copolymers containing carboxylic acid groups. Others have used esterification reactions to prepare starch and cellulose derivatives.[89-91]

2.5.2.3 Cationic and anionic modified PVA

Cationic modification is well known, and has been used on an industrial scale, for functionalising unmodified non-ionic water-soluble materials,[57] including starch and PVA. In typical applications,

where non-ionic properties do not suffice, ionic modification is used to improve the material's properties, for example, the interaction with another substance. For instance, in papermaking, a typical application of cationic functionality is as internal reinforcing agent, where the cationically modified products adsorb effectively onto the fibrous water-dispersed cellulose pulp; binding through the carboxylic functionality on the surface of the fibres via ionic (acid base) interactions.[57]

In this study, PVA microspheres were modified by etherification to possess either cationic trimethylammonium chloride or anionic carboxylic acid surface functionalities. By incorporating these ionic species, a new functionality is created in the surface layer of the microspheres. It is expected that the various microspheres (neutral PVPi or PVA and charged cationic or anionic PVA) would exhibit properties and characteristics relative to the corresponding surface functionality. For example, functionalisation would afford a polyelectrolyte type complex to form between anionic water soluble cellulose fibres and the cationic PVA.[4] The charges of the microspheres were determined using zeta potential measurements, and the interaction between the various microspheres and cellulose fibres were observed using fluorescence imaging techniques.

2.6 Fluorescence and fluorescent labelling

Fluorescent labelling (fluorescent tagging) provides scientists with the ability to study organisms and biological matter. Fluorescence techniques are also being used in macromolecular and polymer fields, in applications such as polymer doping or impregnation,[92,93] fluorescent labelling to study bioconjugation,[94] polysaccharide properties[95] or surfactant-polymer interactions.[96] Studies using fluorescent markers are used to provide unique information on the polymer material and the interaction with surrounding material or matter in the application environment. Spectrophotometric and photoluminescence studies provide information regarding the specific characteristics of fluorescently labelled compounds, such as the excitation/emission wavelengths of cationic or anionic species. Fluorescence imaging offers unique visual illustrations of coagulation, flocculation, complex formation or general interaction of a labelled compound with its environment.

A detailed review by Winnik and Regismond[96] describes various methods and materials used in polymer–surfactant systems and the fluorescence techniques used to study these systems, and applications thereof. Industrially, the most important labelling techniques for polymers are those that introduce fluorophores by chemical modification of the polymer. However, alternative methods include copolymerisation with a dye-substituted monomer or the preparation of a polymer with specific reactive functional groups, and secondary reactions thereof with the appropriate dye.[96]

Using a procedure commonly employed for labelling polysaccharides such as starches, and starch or glucose derivatives, de Belder and Granath[97] labelled dextrans with fluorescein tags. The fluorescent groups are attached by reaction of the hydroxyl groups of the dextrose with the isothiocyanate group of the fluorescein tag.

Similar labelling techniques were successfully used in this study to prepare complementary coloured PVA microspheres. The interaction between the modified (cationic and anionic) PVA particles, and their interaction with cellulose fibres were investigated. The interaction of these modified PVA particles with cellulose fibres were then also compared with previous work on the interaction of similarly labelled starch derivatives (cationic and anionic) with cellulose fibres. These fluorescence studies were carried out by the author, in previous unpublished (preliminary) research in 2007, and by the author's co-workers.[82]

2.7 Paper chemistry

There are many useful and in-depth reviews,[98] books[99-101] and theses[82,102] about paper, papermaking, processing and production. The following brief discussion focuses on the aspects relevant to this work.

2.7.1 Cellulose fibres

Wood fibre is chemically composed of large carbohydrates and lignin, but extractives (like waxes, tannins and fats) may also be present. The high molecular weight carbohydrates are further subdivided into cellulose and hemicellulose. Cellulose is the most abundant polysaccharide and biopolymer, and is the main component used in the paper and packaging industry. Typical of carbohydrates, cellulose consists of only carbon, hydrogen and oxygen. Cellulose is a very organised fibrous structure; it is composed of thousands of D-glucose (glucan) units linked in a linear 1,4′-β-glycoside bond arrangement, as illustrated in Figure 2.6.[102-104]

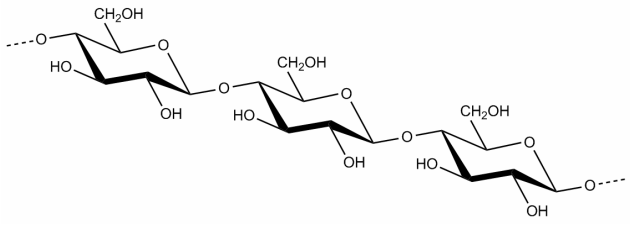

Figure 2.6 Primary cellulose structure, made up of thousands of D-glucose residues.

Each anhydroglucose unit houses three free hydroxyl groups. These account for the hydrogen bonding in the fibrous material, and also function as reactive sites for chemical modification (as described earlier, Section 2.5.2). Fibre bonding results primarily through intra- and intermolecular hydrogen bonding between the anhydroglucose units. Hemicellulose is an important internal binder as it assists in internal fibrillation, adding strength to the network structure that constitutes a cell wall.

A generally accepted fact is that there are carboxyl groups along the fibrous sequence, brought about during the processing of the fibre in papermaking, and resulting in an overall negative charge. The carboxyl groups improve fibre swelling in water and specific bond strength, and the carboxyl content of the pulp is therefore important in the papermaking process. These groups can also interact with wet-end chemicals like sizing or retention aids (e.g. cationic starch) and improve filler retention in paper sheets.

2.7.2 Polymeric additives and fillers in paper

The inter-fibre bond strength directly contributes to tensile failure, and hence improving these interactions is crucial to improving the properties of paper. The inter-fibre bond strength of fibres can be improved by fibre refining, but extreme refining can result in the loss of strength in individual fibres and overall paper bulkiness. Polysaccharide based polymeric additives are typically used to improve the inter-fibre bonding. Cationic starch is an important and widely used industrial additive for the improvement of paper dry strength.[105]

Other additives used to improve the bond strength include polyelectrolytes based on starch, guar gum and carboxymethylcellulose,[106,107] and cationic and anionic polyelectrolyte derivatives. These additives are large molecules that can conform or 'mould' onto the fibre surface by charge attraction. The charge density of the polyelectrolyte and its interaction and orientation with the fibre surface are important to ensure optimum final dry paper strength. The cationic polymers have a strong affinity towards the negatively charged refined fibre surface. A good medium between a high and low charge density is essential to optimise the orientation and amount of polyelectrolyte adsorbed onto the fibre surface. If the cationic charge density is in excess, charge attraction will result in the polyelectrolyte being flattened, becoming extended over the surface, and effectively enveloping the fibre. This limits the amount of polyelectrolyte adsorbed and reduces the desired interpenetrating effect of the polyelectrolyte. This may also result in overcharging of the fibre surface,[107] which poses the problems of reduced flocculation ability and fibre-fibre repulsions, causing a decrease in the inter-fibre bonding strength ability.

Fillers have been added to paper to improve its performance and properties. Depending on the nature of the filler, various properties, including chemical, mechanical and physical (appearance, printability), may be improved. A wide range of fillers are available for selected applications. Common types of fillers include, among others: glass fibre and beads, silica, carbon fibre, carbon black, molydemun disulphide, calcium carbonate and calcium phosphate, etc. Paper fillers were originally used to reduce furnishing costs, but now also impart a variety of very specific qualities and improvements to paper, which may include optical, physical and aesthetic enhancements. The inorganic filler materials used in the paper industry today are considered essential components, dependent on the different grades of paper.

2.7.3 Modified PVA particles as fillers

There are three types of non-hydrodynamic forces affecting particle behaviour, i.e. van der Waals, steric and electrostatic. Whether particles remain dispersed or flocculated depends on an equilibrium between these forces. The electrostatic charge surrounding the filler particle is important in terms of maintaining proper dispersion during processing and filler retention in paper. Zeta potential is an effective means of measuring the electrostatic charge of colloidal particles. This potential, arising from the interaction between the particle surface and solution environment, is affected by the chemical nature of the particle surface, solution environment, specific ion concentrations and ionic strength, which also affect the electrostatic contribution to the overall colloidal behaviour.

In this study, zeta potential measurements were used in order to determine the electrostatic charge of the different modified particles. This study looks at how spherical PVA particles, with various modifications, interact with the cellulose fibres. A brief study was made using cationic starch as an additional component in particle-fibre retention interaction, and another with the precipitated calcium carbonate (PCC) filler, based on the general assumption that PCC[108-110] is normally the preferred filler of choice for cost and whiteness in papermaking industry.

2.8 Field-flow fractionation

Material separation and characterisation are important in terms of scientific research, product analysis, identification, and practical requirements, etc. A wide range of analytical and separation techniques exist, each providing specific product information and advantages, but also having certain limitations. Field-flow fractionation (FFF) is an open channel separation tool which has the ability to overcome many of the challenges and limitations of traditional chromatographic techniques, including column blocking. FFF has immense potential and versatility in terms of its ability to analyse the larger scale

synthetic material and biological matter, and is thus gaining worldwide recognition for its usefulness. FFF, its different modes of operation, the various types of FFF techniques and the various coupled detector systems, have been described by Messaud et al.[111] and Giddings.[112]

FFF is fundamentally a group of elution techniques, where differential retention is a result of an external field or gradient, rather than in-phase partitioning as in the case of chromatographic techniques. FFF is a family of separation and characterisation techniques specific for analysis on colloids, particles, polymers, polymer–colloid complexes,[112] supramolecular assemblies and macromolecules. It has the ability to separate over a wide size range from about 1 nm to 100 μm.[111,113] There are many different types of FFF techniques; these include flow[114] (asymmetric[115,116] and symmetric), thermal,[113] electrical and dielectrophoretic.[117-119] Each interact with a different physico-chemical property of the analyte and have specific criteria regarding separation. For the present study, the asymmetric flow FFF (AsFl-FFF) coupled with a particle size detector was used.

FFF separates on the basis of diffusive transport and operates with both aqueous and organic solvent systems. It operates on the principle of influencing the flow rate of the analyte (particles) through an empty, narrow channel by applying an external field perpendicular to the sample flow direction, as shown in Figure 2.7 A. The high aspect ratio of the channel creates a parabolic flow profile. The flow velocity is at a maximum (v_{max}) in the centre of the channel and at a minimum (v_{min}) closest to the channel walls, Figure 2.7 B. The applied perpendicular force (i.e. asymmetric cross flow) drives the particles towards the accumulation wall, but a counteracting diffusive force drives the particles back. When these forces reach equilibrium, the particles are characteristically positioned in the parabolic velocity profile of the eluent flow stream. Separation thus occurs because the different particles reside in different flow velocity zones.[111,117,120] The particles with different characteristics (size, shape, charge, etc.) are carried at different velocities in relation to their position or localised laminas in the stream. The different particle types therefore are fractioned and emerge at different rates, and are then detected with the appropriate coupled detector, either on- or off-line.

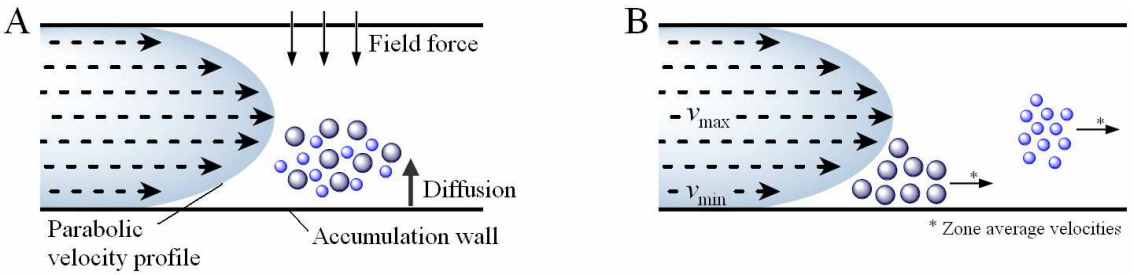

Figure 2.7 **Schematic representation of the normal mode FFF separation mechanism of two components. The analytes located at higher elevation and in the faster stream flow velocity elute faster than the analytes located lower and in the slower flow velocity.**

In FFF, the analytes can be separated by different modes of operation (separation mechanisms), which arise from different opposing forces. The elution order of the analyte is determined by the mode of operation. There are three main modes of operation: normal, steric and hyperlayer, see Figure 2.8. The normal mode separates the analytes based on diffusive transport and Brownian motion within the channel. Normal mode separation is typically used to fractionate particles/analytes smaller than about 1 μm: the smaller particles accumulate in the faster flow regions and elute before the larger particles. Normal mode elution order is from smallest to largest. Steric mode separation is applicable for analytes/particles larger than about 1 μm. Here diffusion becomes negligible and the particle retention depends on the distance from the accumulation wall. The smaller particles will approach the wall more closely than the larger particles; the latter's centre of mass is in the faster flow path and would therefore be swept out faster than the smaller particles in the slower flow regions. Steric mode operation therefore separates particles from largest to smallest. In hyperlayer mode operation, particles are separated based on hydrodynamic lift forces that drive the analytes to higher flow regions. This occurs when high flow velocities are used in separation. In hyperlayer mode separation, the larger particles elute before smaller particles.

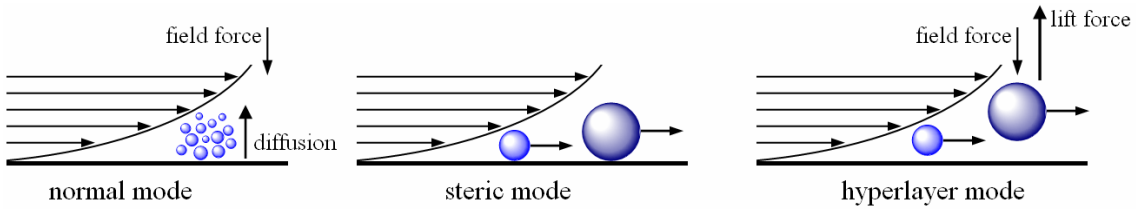

Figure 2.8 FFF operation modes: normal, steric and hyperlayer.

There are many different factors that influence the operation and results obtained from FFF analysis. The field strength is a particularly important experimental condition in FFF separation as it has a large influence on the separation times and resolution.

It would be interesting to study the various PVA particles prepared using different FFF techniques. The particles prepared in this study have a unique modified and hydrolysed surface, and fixed particle size (cross-linked). If studied with the correct FFF technique (i.e. thermal or electrical), these particles could serve as proposed standards for biological macromolecules, as they mimic the surface chemistry of cellulose, starch and polysaccharides. This would allow for standards of set sizes and accurate size readings, in comparison to the typical hydrodynamic volume. The various modified PVA microspheres therefore have the potential to be used as standards in size, chemical composition and charge separations.

2.9 References

1. A. Kornherr, F. Eder, B. Janse, R. Sanderson, J. Terblanche, and M. Zou. Process for Preparing Polysaccharide Gel Particles and Pulp Furnish for Use in Paper Making. European Patent Application: 09450061.8 – 2115, 2009.
2. A. Kornherr, F. Eder, B. Janse, R. Sanderson, J. Terblanche, and M. Zou. Process and Device for Preparing Starch Microgel Particles for the Paper Industry. European Patent Application: 09450062.6 – 2115, 2009.
3. C.A. Finch ed. *Polyvinyl Alcohol: Properties and Applications*, John Wiley & Sons Ltd.: London, 1973.
4. C.A. Finch ed. *Polyvinyl Alcohol: Developments*, John Wiley & Sons Ltd: Chichester, 1992.
5. I. Sakurada and T. Okaya, *Vinyl Fibres*, in *Handbook of Fibre Chemistry*, ed. M. Lewin, 3rd edn., CCR Press: New York, 2007, pp. 261-329.
6. M.L. Hallensleben, *Polyvinyl Compounds, Others*, in *Ullmann's Encyclopedia of Industrial Chemistry*, Wiley-VCH: Weinheim, 2005.
7. B.L. López, A.I. Mejía, and L. Sierra, *Polym. Eng. Sci.*, **1999**, 39(8), 1346-1352.
8. S.-Y. Zheng, Z.-C. Chen, D.-S. Lu, Q. Wu, and X.-F. Lin, *J. Appl. Polym. Sci.*, **2005**, 97(6), 2186-2191.
9. J. Su, Q. Wang, R. Su, K. Wang, Q. Zhang, and Q. Fu, *J. Appl. Polym. Sci.*, **2008**, 107(6), 4070-4075.
10. G.G. Xu, C.Q. Yang, and Y. Deng, *J. Appl. Polym. Sci.*, **2004**, 93(4), 1673-1680.
11. Y. Nagara, T. Nakano, Y. Okamoto, Y. Gotoh, and M. Nagura, *Polymer*, **2001**, 42(24), 9679-9686.
12. W.S. Lyoo and W.S. Ha, *Polymer*, **1999**, 40(2), 497-505.
13. T. Subbiah, G.S. Bhat, R.W. Tock, S. Parameswaran, and S.S. Ramkumar, *J. Appl. Polym. Sci.*, **2005**, 96(2), 557-569.
14. S.G. Lee, J.P. Kim, W.S. Lyoo, J.W. Kwak, S.K. Noh, C.S. Park, and J.H. Kim, *J. Appl. Polym. Sci.*, **2005**, 95(6), 1539-1548.
15. T.L. Uyen Nguyen, B. Farrugia, T.P. Davis, C. Barner-Kowollik, and M.H. Stenzel, *J. Polym. Sci., Part A: Polym. Chem.*, **2007**, 45(15), 3256-3272.
16. C.J. Lee, W.S. Lyoo, I.C. Kwon, S.G. Lee, J.P. Kim, and M.H. Han. Microsphere Embolic Materials Having a Dual Structure of Poly(Vinyl Acetate) Core and Poly(Vinyl Alcohol) Shell and Method for Preparing the Same. United States Patent: US006191193B1, 2001.
17. N.A. Peppas and D. Tennenhouse, *J. Drug Del. Sci. Tech*, **2004**, 14(4), 291-297.

18. G.F. Liversidge, K.C. Cundy, J.F. Bishop, and D.A. Czekai. Surface Modified Drug Nanoparticles. United States Patent: US005145684A, 1992.
19. W.S. Lyoo, J.H. Yeum, B.C. Ji, H.D. Ghim, S.S. Kim, J.H. Kim, J.Y. Lee, and J. Lee, *J. Appl. Polym. Sci.*, **2003**, 88(6), 1482-1487.
20. H. Warson and C.A. Finch, *Fundamentals of Polymer Chemistry*, in *Fundamental Chemistry of Latices and Applications in Adhesives*, ed. H. Warson, Vol. 1, John Wiley & Sons: Chichester, 2001.
21. J. Brandrup, E.H. Immergut, E.A. Grulke, A. Abe, and D.R. Bloch eds., *Polymer Handbook*, 4th edn., Wiley-Interscience: New Jersey, 1999.
22. H.F. Mark, *Encyclopedia of Polymer Science and Technology*, ed. J.I. Kroschwitz, 3rd edn., Vol. 12, John Wiley & Sons, Inc.: Hoboken, 2003, pp. 168-169.
23. T.R. Crompton ed. *Polymer Reference Book*, Rapra Technology Limited: Shawbury, 2006.
24. H.D. Ghim, J.P. Kim, and W.S. Lyoo, *Polymer*, **2003**, 44, 895-900.
25. J. McMurry, *Organic Chemistry*, 6th edn., Brooks/Cole: Belmont, 2004.
26. K. Yamada, T. Nakano, and Y. Okamoto, *J. Polym. Sci., Part A: Polym. Chem.*, **1999**, 37(14), 2677-2683.
27. W.S. Lyoo, J. Blackwell, and H.D. Ghim, *Macromolecules*, **1998**, 31(13), 4253-4259.
28. J.H. Yeum, B.C. Ji, S.K. Noh, H.Y. Jeon, J.W. Kwak, and W.S. Lyoo, *Polymer*, **2004**, 45(12), 4037-4043.
29. W.S. Lyoo and H.W. Lee, *Colloid Polym. Sci.*, **2002**, 280, 835-840.
30. D.C. Blackley, *Emulsion Polymerisation*, Applied Science Publishers Ltd: London, 1975.
31. G.E. Ham ed. *Kinetics and Mechanisms of Polymerization: Vinyl Polymerization (Part I)*, Vol. 1, Marcel Dekker, Inc: New York, 1967.
32. A.E. Hamielec and H. Tobita, *Polymerization Processes*, in *Ullmann's Encyclopedia of Industrial Chemistry*, Wiley-VCH: Weinheim, 2000.
33. K. Matyjaszewski and T.P. Davis eds., *Handbook of Radical Polymerization*, John Wiley & Sons, Inc, 2002.
34. G. Odian, *Principles of Polymerization*, 4th edn., John Wiley & Sons, Inc, 2004.
35. H. Chirowodza, *Synthesis and Characterization of Cationically and Anionically Modified Poly(Vinyl Alcohol) Microfibrils*, MSc Thesis, Stellenbosch University, 2009.
36. N. Kubota, A. Kajiwara, P.B. Zetterlund, M. Kamachi, J. Treurnicht, M.P. Tonge, R.G. Gilbert, and B. Yamada, *Macromol. Chem. Phys.*, **2007**, 208(22), 2403-2411.
37. W.S. Lyoo, S.S. Han, J.H. Kim, W.S. Yoon, C.J. Lee, I.C. Kwon, J. Lee, B.C. Ji, and M.H. Han, *Angew. Makromol. Chem.*, **1999**, 271(1), 46-52.

38. W.S. Lyoo, S.S. Han, J.H. Choi, H.D. Ghim, S.W. Yoo, J. Lee, S.I. Hong, and W.S. Ha, *J. Appl. Polym. Sci.*, **2001**, 80(7), 1003-1012.
39. W.S. Lyoo, S.G. Lee, J.P. Kim, S.S. Han, and C.J. Lee, *Colloid Polym. Sci.*, **1998**, 276(11), 951-959.
40. W.S. Lyoo, J.W. Kwak, J.H. Yeum, B.C. Ji, C.J. Lee, and S.K. Noh, *J. Polym. Sci., Part A: Polym. Chem.*, **2005**, 43(4), 789-800.
41. W.S. Lyoo, C.S. Park, J.H. Yeum, B.C. Ji, C.J. Lee, S.S. Lee, and J.Y. Lee, *Colloid Polym. Sci.*, **2002**, 280(12), 1075-1083.
42. D.H. Song and W.S. Lyoo, *J. Appl. Polym. Sci.*, **2007**, 104(1), 410-414.
43. W.S. Lyoo, H.D. Ghim, J.H. Kim, S.K. Noh, J.H. Yeum, B.C. Ji, H.T. Jung, and J. Blackwell, *Macromolecules*, **2003**, 36(14), 5428-5431.
44. S.S. Kim, I.S. Seo, J.H. Yeum, B.C. Ji, J.H. Kim, J.W. Kwak, W.S. Yoon, S.K. Noh, and W.S. Lyoo, *J. Appl. Polym. Sci.*, **2004**, 92(3), 1426-1431.
45. W.S. Lyoo, J.H. Yeum, O.W. Kwon, D.S. Shin, S.S. Han, B.C. Kim, H.Y. Jeon, and S.K. Noh, *J. Appl. Polym. Sci.*, **2006**, 102(4), 3934-3939.
46. K. Esumi ed. *Polymer Interfaces and Emulsions*, Marcel Dekker, Inc.: New York, 1999.
47. G.H. Ma, *Advances in Preparations and Applications of Polymeric Microspheres*, in *Polymer Interfaces and Emulsions*, ed. K. Esumi, Marcel Dekker, Inc.: New York, 1999.
48. R. Arshady, *Colloid Polym. Sci.*, **1992**, 270(8), 717-732.
49. L.H. Sperling, *Introduction to Physical Polymer Science*, 4th edn., John Wiley & Sons, Inc.: New Jersey, 2006.
50. E. Vivaldo-Lima, P.E. Wood, A.E. Hamielec, and A. Penlidis, *Ind. Eng. Chem. Res.*, **1997**, 36(4), 939-965.
51. S.G. Lee, J.P. Kim, I.C. Kwon, D.S. Shin, S.S. Han, and W.S. Lyoo, *J. Appl. Polym. Sci.*, **2006**, 101(6), 4064-4070.
52. W.S. Lyoo, C.S. Park, K.H. Choi, J.W. Kwak, W.S. Yoon, and S.K. Noh, *Polym. Plast. Technol. Eng.*, **2005**, 44(3), 475-487.
53. M.A. Gauthier, J. Luo, D. Calvet, C. Ni, X.X. Zhu, M. Garon, and M.D. Buschmann, *Polymer*, **2004**, 45(24), 8201-8210.
54. T. Moritani and T. Okaya, *Polymer*, **1998**, 39(4), 923-931.
55. K. Kumeta, I. Nagashima, S. Matsui, and K. Mizoguchi, *J. Appl. Polym. Sci.*, **2003**, 90(9), 2420-2427.
56. T. Moritani and J. Yamauchi, *Polymer*, **1998**, 39(3), 553-557.
57. T. Moritani and J. Yamauchi, *Polymer*, **1998**, 39(3), 559-572.

58. T. Moritani and K. Kajitani, *Polymer*, **1997**, 38(12), 2933-2945.
59. M.K. Beliakova, A.A. Aly, and F.A. Abdel-Mohdy, *Starch-Stärke*, **2004**, 56(9), 407-412.
60. Z.-F. Zhou, W.-b. Xu, D. He, J.-x. Fan, F. Yu, and F.-M. Ren, *J. Appl. Polym. Sci.*, **2007**, 103(2), 848-852.
61. G.S. Mukherjee, N. Shukla, R.K. Singh, and G.N. Mathur, *J. Sci. Ind. Res.*, **2004**, 63(7), 596-602.
62. S.Y. Nam, H.J. Chun, and Y.M. Lee, *J. Appl. Polym. Sci.*, **1999**, 72(2), 241-249.
63. J.-S. Park, J.-W. Park, and E. Ruckenstein, *J. Appl. Polym. Sci.*, **2001**, 82(7), 1816-1823.
64. A. Atta, N. Maysour, and K. Arndt, *J. Polym. Res.*, **2006**, 13(1), 53-63.
65. V. Giménez, J.A. Reina, A. Mantecón, and V. Cádiz, *Acta Polym.*, **1999**, 50(5-6), 187-195.
66. K.M. El Salmawi, *J. Macromol. Sci., Pure Appl. Chem.*, **2007**, 44(5), 541-545.
67. T.M.R. Miranda, A.R. Gonçalves, and M.T.P. Amorim, *Polym. Int.*, **2001**, 50(10), 1068-1072.
68. S. Mishra, R. Bajpai, R. Katare, and A.K. Bajpai, *Express Polym. Lett.*, **2007**, 1(7), 407-415.
69. F.J. Liou and Y.J. Wang, *J. Appl. Polym. Sci.*, **1996**, 59(9), 1395-1403.
70. A.M. Atta and R.A.M. El-Ghazawy, *Int. J. Polym. Mater.*, **2003**, 52(7), 623-636.
71. M. Krumova, D. López, R. Benavente, C. Mijangos, and J.M. Pereña, *Polymer*, **2000**, 41(26), 9265-9272.
72. J. Gohil, A. Bhattacharya, and P. Ray, *J. Polym. Res.*, **2006**, 13(2), 161-169.
73. B. Vollmert and E.H. Immergut, *Polymer Chemistry*, Springer-Verlag: New York, 1973.
74. F.W. Billmeyer, *Textbook of Polymer Science*, 2nd edn., Wiley-Interscience: New York, 1962.
75. T. Chen and E.L. Burch. Use and Preparation of Crosslinked Polymer Particles for Inkjet Recording Materials. United States Patent: US007507439B2, 2009.
76. S. Fujii, Y. Cai, J.V.M. Weaver, and S.P. Armes, *J. Am. Chem. Soc.*, **2005**, 127(20), 7304-7305.
77. R. Mehnert, K.W. Bögl, N. Helle, and G.A. Schreiber, *Radiation Chemistry*, in *Ullmann's Encyclopedia of Industrial Chemistry*, Wiley-VCH: Weinheim, 2000.
78. W.-Y. Chiang and Y.-H. Lin, *J. Appl. Polym. Sci.*, **2002**, 86(11), 2854-2859.
79. P. Chowdhury and C.M. Pal, *Eur. Polym. J.*, **1999**, 35(12), 2207-2213.
80. S. Shukla, A.K. Bajpai, and R.A. Kulkarni, *J. Appl. Polym. Sci.*, **2005**, 95(5), 1129-1142.
81. S. Mishra, A. Panda, and B.C. Singh, *J. Appl. Polym. Sci.*, **1999**, 73(5), 677-683.
82. H. Matahwa, *Chemical Modification of Polysaccharides with Hydrophilic Polymers for $CaCO_3$ Crystal Growth Modification and Filler Retention, for Paper Applications*, PhD Thesis, Stellenbosch University, 2008.

83. H.F. Mark, J.I. Kroschwitz ed. *Encyclopedia of Polymer Science and Technology*, 3rd edn., John Wiley & Sons, Inc.: Hoboken, 2003.
84. V. Haack, T. Heinze, G. Oelmeyer, and W.-M. Kulicke, *Macromol. Mater. Eng.*, **2002**, 287(8), 495-502.
85. B. Volkert, F. Loth, W. Lazik, and J. Engelhardt, *Starch-Stärke*, **2004**, 56(7), 307-314.
86. C. Aguir and M.F. M'Henni, *J. Appl. Polym. Sci.*, **2006**, 99(4), 1808-1816.
87. G.S. Mukherjee, *J. Mater. Sci.*, **2005**, 40(11), 3017-3019.
88. V. Giménez, A. Mantecón, J.C. Ronda, and V. Cádiz, *J. Appl. Polym. Sci.*, **1997**, 65(8), 1643-1651.
89. R. Auzély-Velty and M. Rinaudo, *Int. J. Biol. Macromol.*, **2003**, 31(4-5), 123-129.
90. C. Satgé, B. Verneuil, P. Branland, R. Granet, P. Krausz, J. Rozier, and C. Petit, *Carbohydr. Polym.*, **2002**, 49(3), 373-376.
91. J. Wu, J. Zhang, H. Zhang, J. He, Q. Ren, and M. Guo, *Biomacromolecules*, **2004**, 5(2), 266-268.
92. D. Zhang and D. Ma, *Appl. Optics*, **2007**, 46(15), 2996-3000.
93. C. Wu, Y. Zheng, C. Szymanski, and J. McNeill, *J. Phys. Chem. C*, **2008**, 112(6), 1772-1781.
94. A.W. York, C.W. Scales, F. Huang, and C.L. McCormick, *Biomacromolecules*, **2007**, 8(8), 2337-2341.
95. O. Roger, S. Colliec-Jouault, J. Ratiskol, C. Sinquin, J. Guezennec, A.M. Fischer, and L. Chevolot, *Carbohydr. Polym.*, **2002**, 50, 273-278.
96. F.M. Winnik and S.T.A. Regismond, *Colloids Surf., A*, **1996**, 118, 1-39.
97. A.N. de Belder and K. Granath, *Carbohydr. Res.*, **1973**, 30(2), 375-378.
98. Y. Xu, X. Chen, and R. Pelton, *Tappi J.*, **2005**, 4(11), 8-12.
99. H. Holik ed. *Handbook of Paper and Board*, Wiley-VCH: Weinheim, 2006.
100. B.P.a.B.M. Association, *Paper Making: A General Account of Its History, Processes, and Applications*, William Clowes and Sons Limited: Great Britain, 1950.
101. C.J. Biermann, *Essentials of Pulping and Papermaking*, Academic Press, Inc.: San Diego, 1993.
102. M. Rice, *New Techniques of Continuous Chemical Analysis in the Pulp & Paper Industry*, PhD Thesis, Royal Institute of Technology: Stockholm, 2001.
103. A.-C. Engström, M. Ek, and G. Henriksson, *Biomacromolecules*, **2006**, 7(6), 2027-2031.
104. Y. Song, J. Zhou, Q. Li, A. Lue, and L. Zhang, *Carbohydr. Res.*, **2009**, 344(11), 1332-1339.
105. M. Zhang, B.-Z. Ju, S.-F. Zhang, W. Ma, and J.-Z. Yang, *Carbohydr. Polym.*, **2007**, 69(1), 123-129.

106. M. Watanabe, T. Gondo, and O. Kitao, *Tappi J.*, **2004**, 3(5), 15-19.
107. M.A. Hubbe, *BioResources*, **2006**, 1(2), 281-318.
108. S. Knez, D. Klinar, and J. Golob, *Chem. Eng. Sci.*, **2006**, 61(17), 5867-5880.
109. S. Bratskaya, S. Schwarz, G. Petzold, T. Liebert, and T. Heinze, *Ind. Eng. Chem. Res.*, **2006**, 45(22), 7374-7379.
110. E. Antunes, F.A.P. Garcia, P. Ferreira, and M.G. Rasteiro, *Chem. Eng. Res. Des.*, **2008**, 86(10), 1155-1160.
111. F.A. Messaud, R.D. Sanderson, J.R. Runyon, T. Otte, H. Pasch, and S.K.R. Williams, *Prog. Polym. Sci.*, **2009**, 34(4), 351-368.
112. J.C. Giddings, *Anal. Chem.*, **1995**, 67(19), 592A-598A.
113. R.J. White, *Polym. Int.*, **1997**, 43(4), 373-379.
114. J. Li, J. Ge, Y. Yin, and W. Zhong, *Anal. Chem.*, **2008**, 80(18), 7068-7074.
115. M.H. Moon, H. Kwon, and I. Park, *Anal. Chem.*, **1997**, 69(7), 1436-1440.
116. K.G. Wahlund and J.C. Giddings, *Anal. Chem.*, **1987**, 59(9), 1332-1339.
117. P.R.C. Gascoyne and J. Vykoukal, *Electrophoresis*, **2002**, 23(13), 1973-1983.
118. T.-S. Leu and C.-Y. Weng, *Mod. Phys. Lett. B*, **2009**, 23(3), 389-392.
119. X.-B. Wang, J. Yang, Y. Huang, J. Vykoukal, F.F. Becker, and P.R.C. Gascoyne, *Anal. Chem.*, **2000**, 72(4), 832-839.
120. W.-D. Hergeth, *On-Line Monitoring of Chemical Reactions*, Wiely-VCH: Weinheim, 2006.

Chapter 3: Experimental

3.1 Introduction

In this chapter the synthetic pathways for the preparation of spherical poly(vinyl pivalate) (PVPi) particles, the saponification/hydrolysis thereof, as well as the charging (ionic modification) and fluorescent labelling of these particles are introduced and described. A description of all characterisation/analytical techniques employed in this work is also presented. The results from the synthesis and characterisation of products are presented in the following chapter (Chapter 4).

3.2 Preparation of spherical PVPi particles via suspension polymerisation

The focus of this part of the study was to prepare cross-linked PVPi microspheres, via suspension polymerisation. These PVPi particles should ideally have narrowly dispersed particle sizes, within a 0.5–10 μm particle size range. Extensive research into suspension polymerised vinyl pivalate (VPi) and vinyl acetate (VAc) microspheres has been reported by Lee et al.,[1,2] Lyoo et al.,[3-5] Song and Lyoo,[6] and Chen and Burch.[7]

In this study, cross-linked PVPi microspheres were prepared via thermally initiated suspension polymerisation of VPi at a standard polymerisation temperature of 65 °C, using tri(ethylene glycol) divinyl ether (TEGDE) as cross-linking agent. The VPi monomer was suspension polymerised using 2,2′-azobis(isobutyronitrile) (AIBN) as free radical initiator, with poly(vinyl alcohol) (PVA) as the suspension agent and water as the suspending phase. A typical VPi polymerisation reaction is illustrated in Scheme 3.1. These suspension polymerisation reactions were carried out in much the same manner as the reactions reported by Lyoo et al.[3-5], Song and Lyoo[6] and Lee et al.[1,2] However, the particle sizes reported in the literature are in the order of tenfold (or more) larger than the desired particle sizes of 0.5–10 μm. Homogenation of the suspension solution prior to initiation was thus employed in an effort to create smaller and uniform particle sizes.

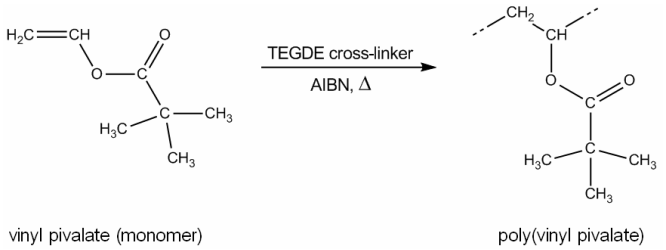

Scheme 3.1 Polymerisation of VPi with TEGDE as cross-linking agent/comonomer.

During this study, various polymerisation conditions were changed in attempts to achieve the desired particle size, and to improve the yield, particle size distribution and particle properties, such as strength, durability, morphology and stability. The following section describes the materials, experimental work and synthetic pathways used for the synthesis of the cross-linked PVPi microspheres.

3.2.1 Materials

Materials: The following materials were used: vinyl pivalate (VPi, Sigma-Aldrich), tri(ethylene glycol) divinyl ether (TEGDE, Sigma-Aldrich), 2,2′-azobis(isobutyronitrile) (AIBN, Riedel de Haën), poly(vinyl alcohol) (PVA, 87–89% hydrolysed, Sigma-Aldrich), Igepal CO890 (Sigma-Aldrich), Igepal CO520 (Sigma-Aldrich), Triton X-100 (OP 10, Sigma-Aldrich), calcium phosphate ($Ca_2O_7P_2 \cdot H_2O$, amorphous nanopowder, as assigned and supplied by Sigma-Aldrich), methanol (MeOH, Kimix), potassium hydroxide (KOH, Merck), anhydrous magnesium sulphate ($MgSO_4$, Saarchem), inhibitor remover column packing (Sigma-Aldrich).

Reagent purification: Vinyl pivalate monomer was washed with aqueous KOH solution and deionised water, and then dried over anhydrous $MgSO_4$. The inhibitor was then removed by passing the monomer through a packed inhibitor (stabiliser) removal column and the monomer was then stored over molecular sieve below 4 °C. The AIBN initiator was recrystallised from MeOH, then vacuum dried and stored below 4 °C. Other reagent grade materials were used as obtained from the suppliers.

3.2.2 Synthesis of spherical PVPi particles via thermally initiated (free radical) suspension polymerisation

The suspension polymerisation technique used was adapted from literature.[1,2,4] In a typical suspension polymerisation, an oil and aqueous phase were homogenised together, prior to the onset of the reaction. The AIBN initiator was dissolved in the VPi and TEGDE monomer mixture (oil phase).

The oil phase was then combined with the aqueous phase, which consisted of the PVA suspension agent, $Ca_2O_7P_2 \cdot H_2O$, non-ionic surfactant mixture (1.33 g/dL) and water. The non-ionic surfactant mixture comprised the Igepal CO890, Igepal CO520 and Triton X-100 surfactants in a 2:2:1 ratio, respectively. This combination ultimately provides a non-ionic surfactant mixture with a theoretical hydrophile lipophile balance (HLB) value of 13.5. The two-phase solution was then homogenised at ~8000 rpm for 4 min, and then transferred to a round-bottom reaction flask, equipped with condenser, magnetic stirrer and thermocouple. After degassing, the reaction was heated to 65 °C and allowed to proceed under nitrogen atmosphere with stirring at 400 rpm. After 24 hr, the reaction mixture was cooled and left overnight to allow the spherical particles to settle and sink. The PVPi sample was centrifuged and washed separately three times with warm water and MeOH, to eliminate any residues. The PVPi particles were then dried *in vacuo* at 40 °C overnight. Standard polymerisation conditions are tabulated in Table 3.1. For ease of future reference, the 'standard' cross-linked PVPi sample is assigned the general sample code **A**.

Table 3.1 Standard VPi suspension polymerisation conditions

Temperature	65 °C
Initiator concentration	7.57×10^{-3} mol/mol monomers
Suspension agent concentration	2.6 g/dL water
Water to monomer weight ratio (W/M)	VPi/water of 0.3 (L/L)
Stirring speed (rev min^{-1})	400 rpm
Cross-linking agent (comonomer) concentration	0.032 mol/mol VPi

In addition to the standard cross-linked PVPi particles (**A**), an uncross-linked PVPi sample was prepared in the same manner as described above. Furthermore, the cross-linking agent concentration was also varied in a sequence of suspension polymerisations, as shown in Table 3.2. The uncross-linked PVPi sample is of particular importance because it can be used as a reference, and for analyses (e.g. solution NMR), which is not the case with its cross-linked counterpart. Furthermore, it can be used to obtain a closer comparison to published data, and to also study and compare the properties of the cross-linked and uncross-linked samples.

3.2.3 Microsphere size and distribution

In a study carried out in order to obtain particles with the best combination of properties, such as size, distribution and morphology,[3,8] numerous suspension polymerisation reactions were carried out, in which various polymerisation conditions and parameters were varied. Such parameters include the

concentrations of initiator, cross-linking agent, suspension agent, dispersant and surfactant; as well as the monomer-to-solvent ratio; temperature and stirring speed. The suspension reactions, sample preparation and product purification for the various polymerisations were all carried out as described in Section 3.2.2. The suspension polymerisation conditions and parameters used are tabulated in Table 3.2.

Table 3.2 VPi suspension polymerisation conditions

Monomer	VPi	
Comonomer cross-linker	TEGDE	
Initiator	AIBN	
Type of suspension agent	PVA	
Initiator concentration	0.00038	mol/mol monomers
	0.00076	mol/mol monomers
	0.0038	mol/mol monomers
	0.0051	mol/mol monomers
	0.0076	*mol/mol monomers*
	0.0113	mol/mol monomers
Suspension agent concentration	1.3	g/dL of water
	2.6	*g/dL of water*
	3.9	g/dL of water
VPi/water	*0.3*	*L/L*
TEGDE/VPi	0.000	mol/mol
	0.006	mol/mol
	0.016	mol/mol
	0.032	*mol/mol*
	0.048	mol/mol
Non-ionic surfactant	0.66	g/dL of water
	1.33	*g/dL of water*
	2.00	g/dL of water
$Ca_2O_7P_2 \cdot H_2O$ (dispersant)	0.26	g/dL of water
	0.66	*g/dL of water*
	1.07	g/dL of water
Stirring speed (rpm)	300, *400*, 500	
Temperature	55 °C, *65 °C*, 75 °C	

Italic expressions represent the standard suspension polymerisation conditions used in this study.

Although many reactions (in which various variables and parameters were used), were carried out, only a selection is included in this table.

3.2.4 Analysis and characterisation

3.2.4.1 Conversion

Conversion studies were carried out on the standard VPi suspension reactions at the different polymerisation temperatures, 55 °C, 65 °C and 75 °C, respectively. The monomer conversion-versus-time data were determined gravimetrically, using equation 3.1. Sample fractions were extracted and collected at different time intervals during the reaction, for reactions at each of the three temperatures. The resulting polymer fraction masses were recorded prior to and after drying. The yield was then used to determine the conversion at the respective time intervals using equation 3.1, where the monomer and non-volatiles masses are a relative percentage of the extracted mass.

$$\text{Conversion}_{(\text{at time } t)}\,(\%) = \frac{\text{Yield (g) - Non Volatiles (g)}}{\text{Monomer (g)}} \qquad 3.1$$

Monomer loss by evaporation can be ruled out as the monomer boiling point is 110 °C, and the reaction set-up includes a condenser flushed with cold water (≤ 20 °C). A comparison between the monomer conversions versus time data for the suspension polymerisations carried out at the different reaction temperatures was made. Results are presented in Chapter 4 (Section 4.2.2).

3.2.4.2 Characterisation

Characterisation of the cross-linked PVPi particles was achieved with the aid of a variety of analytical techniques, including solid state NMR, FTIR, particle size analysis and SEM. The uncross-linked PVPi homopolymer was characterised with proton and carbon solution NMR, using $CDCl_3$ as solvent. The analytical techniques that were used, and the respective sample preparation methods, are described in Section 3.7. The results acquired using the various techniques are presented in Chapter 4. The standard cross-linked PVPi was characterised and proved to be an adequate precursor to PVA. Thus, the standard cross-linked PVPi particles, suspension polymerised at 65 °C and denoted **A**, was used in the subsequent synthetic pathways for the preparation of PVA.

3.3 Synthesis of PVA by saponification

Having successfully synthesised the spherical cross-linked PVPi particles, the next step in the synthetic pathway is saponification. Saponification is the process of hydrolysing ester bonds to form an alcohol derivative. The aim of this experimental work was, ideally, to synthesise core-shell PVA particles. This was to be done by surface saponification of the particles. Extensive work on the saponification of PVPi, poly(vinyl acetate) (PVAc) and PVPi/PVAc copolymer particles and/or fibres has been reported by Lyoo et al.[4,5,9-16] and several other authors.[2,6,17-19] Lyoo et al. reported mainly on reactions in which KOH is used as saponifying agent. However, to the author's knowledge, maintaining the spherical particle morphology during the KOH saponification is hardly reported. Lee et al.[1] reported on a skin-core heterogeneous saponification method, using an aqueous NaOH saponifying solution. In this study, the KOH and NaOH saponification techniques described by these authors, were used, with various hydrolysing reaction times.

3.3.1 Materials

The following materials were used: PVPi spherical particles (sample A; Section 3.2.2), tetrahydrofuran (THF, Kimix), methanol (MeOH, Kimix), potassium hydroxide (KOH, Merck), sodium sulphate (Na_2SO_4, Merck), distilled deionised (DDI) water. All solvent grade reagents were used as received.

3.3.2 Hydrolysis (Method A)

The technique used for the hydrolysis of the PVPi particles was adapted from literature.[4-6] Scheme 3.2 illustrates the conversion of PVPi to PVA.

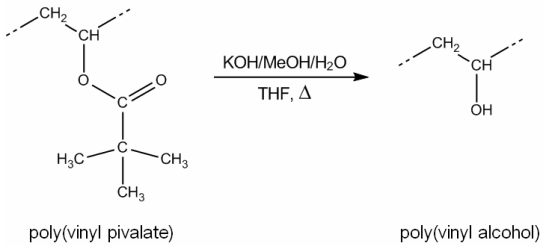

Scheme 3.2 PVPi saponification reaction to PVA, in THF solvent with KOH saponifying agent.

In a three-necked round bottom-flask equipped with condenser, dropping funnel, nitrogen inlet and magnetic stirrer, the spherical PVPi particles (3 g) were swollen in THF (300 mL). This mixture

was degassed and heated to 60 °C, whilst stirring at 400 rpm. In the dropping funnel, 60 mL of a 20% KOH/MeOH/H_2O (90/10 v/v) (with 1% Na_2SO_4) solution was flushed with nitrogen. The KOH solution, which was in a 0.20 v/v ratio with the PVPi solution, was added dropwise to the reaction mixture, whilst stirring at 60 °C. The saponification reaction was allowed to proceed under nitrogen atmosphere for predetermined lengths of time. Once the reaction had reached completion, the solid saponification product was centrifuged and washed several times with methanol combined with a small amount of water. The solid, surface hydrolysed particles were then dried under vacuum at 40 °C.

3.3.3 Heterogeneous surface saponification (Method B)

An alternative method of hydrolysis, described as the "heterogeneous surface saponification of the PVPi/PVAc microspheres" by Lee et al.[1] was also performed. In this procedure, an alkaline solution of sodium hydroxide and sodium sulphate (20 g of each) were mixed with 200 g of DDI water. This solution was mixed together and degassed at 50 °C in a three-necked round bottom-flask, equipped with condenser, dropping funnel, nitrogen inlet and magnetic stirrer. The PVPi particles (0.5 g), suspended in methanol (20 g) and separated via sonication, was then added to the reaction mixture. The reaction was allowed to run for 1 to 4 hr, thereafter the solution was filtered and the solid particles were washed several times with water. The particles were then dried at 40 °C under vacuum.

3.3.4 Analysis and characterisation

3.3.4.1 Characterisation

Using FTIR spectroscopy, it was observed that saponification via Method B was unsuccessful, whilst Method A proved to be highly successful. Method A is, however, a very robust saponification method and will, in the case of PVPi microspheres, destroy particle morphology and produce PVA fibres instead.[5] This was confirmed with hydrolysis of the uncross-linked sample. Exceptionally good results were obtained with the cross-linked particles, as they preserved their spherical structure and remained intact, whilst still having undergone saponification. This is described in more detail in the following chapter. Analytical techniques such as FTIR, SEM, TEM with iodine staining, solid state NMR (SS NMR), TGA and XRD were used to accurately characterise the hydrolysed samples. The techniques used, and the respective sample preparation methods, are described in Section 3.7.

3.3.4.2 Degree of saponification

After determining that hydrolysis of the PVPi particles was successful (using method A), efforts were made to determine the degree of saponification (DS). An array of saponification reactions were performed with varying saponification times in order to obtain particles with different degrees of hydrolysis. Hydrolysis times used varied between 2.5 min and 24 hr (2.5 min, 5 min, 7.5 min, 10 min, 15 min, 22.5 min, 30 min, 37.5 min, 45 min, 1 hr, 2 hr, 3 hr, 4 hr, 5 hr and 24 hr), as assigned with sample codes as tabulated in Table 3.3. Accurate quantitative results were difficult to obtain, due to the cross-linked nature, and hence, insolubility of the particles. A *relative* indication of the DS was acquired from solid state NMR analysis; the results are presented in the subsequent chapter. It was determined that the 15 min saponification time provided sufficient hydrolysis in terms of the PVA to PVPi ratio. As such, the 15 min hydrolysed cross-linked PVA/PVPi sample was deemed suitable and used for subsequent synthetic routes. For ease of future reference, the 15 min hydrolysed cross-linked PVPi sample is assigned the general sample code **B_5** (or just B).

Table 3.3 List of codes for the samples prepared at different saponification times

Sample code	Saponification time
A (B_0)	0 min (unhydrolysed PVPi)
B_1	2.5 min
B_2	5 min
B_3	7.5 min
B_4	10 min
B_5	15 min
B_6	22.5 min
B_7	30 min
B_8	37.5 min
B_9	45 min
B_{10}	60 min
B_{11}	2 hr
B_{12}	3 hr
B_{13}	4 hr
B_{14}	5 hr
B_{15}	24 hr

3.4 Ionic modification – anionic and cationic

The aim of this section of the study was to prepare surface modified spherical PVA particles. Earlier work, performed in our research group, on modified starches showed that modified cationic starch has an affinity towards the cellulose fibre and filler (precipitated calcium carbonate; PCC), while the modified anionic starch counterpart shows affinity towards the PCC particles. This can be explained by the fact that the fibre has a small negative surface charge, while the PCC particles have a surface of calcium atoms and hence can be complexed by anionic polymers or the calcium can be replaced by a strong cationic polymer. A cationic species would therefore have an affinity towards the fibre and also to the PCC, whilst the anionic species has a strong affinity towards the calcium atoms on the PCC. This idea was followed here: it was assumed that the cationically charged PVA particles would interact with the fibres and a charge attraction would become possible with the anionically charged PVA particles and PCC particles, in the same way that the corresponding modified starches interact with the fibres and PCC, respectively.

After the successful hydrolysis of the PVPi particles (see Section 3.3.2), the hydrolysed PVA/PVPi particles were then ionically functionalised with either a cationic or anionic group. Scheme 3.3 is a general illustration of the procedure used for the cationic and the anionic functionalisation reactions.

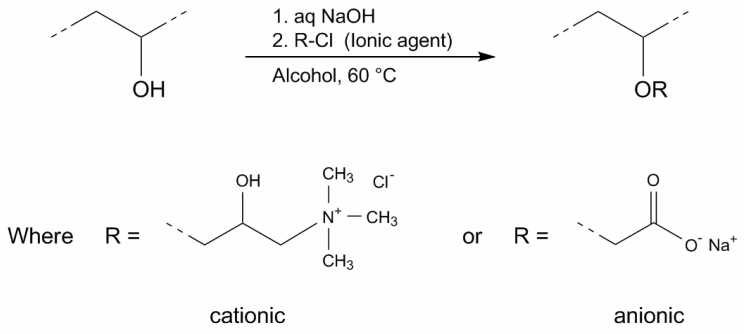

Scheme 3.3 General illustration of ionic modification of PVA by the two-step Williamson ether synthesis, showing the respective cationic and anionic functional groups.

Cationisation reactions were performed using 3-chloro-2-hydroxy-propyltrimethylammonium chloride (CHPTMAC)[20] as cationic agent, while carboxymethylation was performed using sodium monochloroacetate (SMCA)[21] as anionic agent. Ionic modification was carried out in order to investigate the interaction of the particles with the cellulose fibres.

Parallel to this study, fellow students have modified polysaccharides and starches into anionic and cationic particles for paper treatment.[22] These polysaccharides and starches are highly swellable and easily distorted materials in water and are cross-linked to stop solubility. In the present study, the interaction between the modified PVA particles with fibres is expected to be significantly reduced, due to the rigidity of the spherical particles which will hinder interaction with the fibre surface. Nonetheless, the use of rigid particles, as apposed to 'floppy' starches, ought to lead to a better understanding of where the charges are located on the surface of the fibres. Results are presented in Chapter 4 (Section 4.4 and 4.5).

3.4.1 Materials

3.4.1.1 Cationic modification

The following materials were used: PVA/PVPi particles (sample **B_5**, Section 3.3.2), 3-chloro-2-hydroxypropyltrimethylammonium chloride (CHPTMAC, 60% solution, Sigma-Aldrich), sodium hydroxide (NaOH, Merck), ethanol (EtOH, Sasol Solvents), hydrogen chloride (HCl, Merck) and DDI water. All reagents were used as received.

3.4.1.2 Anionic modification

The following materials were used: PVA/PVPi particles (sample **B_5**, Section 3.3.2), sodium monochloroacetate (SMCA, Fluka), sodium hydroxide (NaOH, Merck), isopropanol (IPA, Sasol Solvents), calcium oxide (CaO, Saarchem), glacial acetic acid (Saarchem), methanol (MeOH, Kimix), silver nitrate ($AgNO_3$, NT Laboratory Suppliers) and DDI water. Isopropanol was refluxed with CaO for an hour, then distilled and stored over molecular sieve. Other reagents were used as received.

3.4.2 Synthesis of ionic modified PVA/PVPi particles

3.4.2.1 Cationic modification

The cationisation procedure used was adapted from the procedure used by Haack et al.[20] The cationic modification was carried out in a reaction flask equipped with a condenser and nitrogen inlet. Dry PVA/PVPi particles (2.0 g) were suspended in an EtOH/water mixture (12 and 5 mL, respectively), and sonicated. An aqueous solution of NaOH (1.7 g) in water (2 mL) was prepared and added to the particle suspension, which was then degassed and heated to 60 °C, with stirring at 400 rpm. The cationic functionalising agent (CHPTMAC; 6.5 g, 35 mmol, calculated from 60% solution) and EtOH

(9 mL) were subsequently added to the reaction mixture and the cationisation reaction allowed to proceed for 6 hr. After cooling the reaction mixture to ambient temperature, it was neutralised with a 0.1 M HCl solution. The cationic modified PVA/PVPi product was centrifuged, washed several times with EtOH and then dried *in vacuo* at 40 °C.

3.4.2.2 Anionic modification

The anionic modification procedure used was adapted from Volkert et al.[21] It was carried out in a reaction flask equipped with condenser and nitrogen inlet. Dry PVA/PVPi particles (2.0 g) were suspended in isopropanol (25 mL) and sonicated. An aqueous solution of NaOH (1.7 g) in water (2 mL) was prepared and added to the particle suspension, which was then degassed and heated to 60 °C, with stirring at 400 rpm. The SMCA anionic functionalising agent (4.0 g, 35 mmol) mixed with water (5 mL) was subsequently added to the reaction mixture. The anionic functionalisation (carboxymethylation) reaction was run for 6 hr. The solution was cooled to ambient temperature and then neutralised with glacial acetic acid. The resulting slurry was washed with 80% aqueous methanol until no chloride ions were detected in the wash layer (by reaction with $AgNO_3$).[21] The anionic modified PVA/PVPi product was centrifuged, washed several times with pure MeOH and then dried *in vacuo* at 40 °C.

3.4.3 Analysis and characterisation

The cationic and anionic modified particles were characterised using FTIR and SS ^{13}C NMR spectroscopy. Zeta potential measurements were also recorded to determine the charges on the respective particles. The interactions of the cationic and anionic species with cellulose paper fibre were observed using SEM microscopy, and fluorescence imaging after labelling the respective ionic species with fluorescent tags. The process of fluorescent labelling is described in the following section (Section 3.5). Experimental details of the preparation of samples are described in Section 3.7. For simplicity in referring to the '6 hr cationic and anionic modified PVA/PVPi species', the samples are assigned with codes **C** (cationic) and **D** (anionic), respectively.

3.5 Preparation of fluorescent labelled cationic and anionic particles

Fluorescent labelling (fluorescent tagging) has proven to be a new and unique method in polymer analysis. It serves great purpose, by particularly showing the direct interaction between, for example, particles and fibres. There are different methods or techniques that can be used for the preparation of labelled (tagged) polymers. A few includes introducing the fluorophore either by means of copolymerisation with a dye-substituted comonomer, chemical modification of the polymer, or by preparing a polymer with the appropriate reactive functional groups and subsequent reaction with the dye.[23] In this study, a combination of the later two techniques was used, where the pendant hydroxyl groups are the appropriate reactive functional groups (introduced via saponification) (Section 3.3). Two different fluorescent probes, with complimentary fluorescent colours, were used to label the respective polymer particles. The chemical structures of the two fluorescent probes used, namely the red rhodamine B isothiocyanate (RBITC) and green fluorescein isothiocyanate (FITC), are shown in Figure 3.1 A and B, respectively.

A

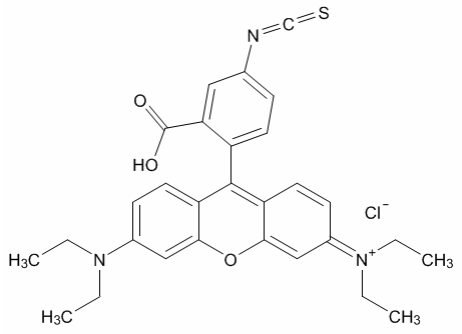

Rhodamine B isothiocyanate (red)
[RBITC]

B

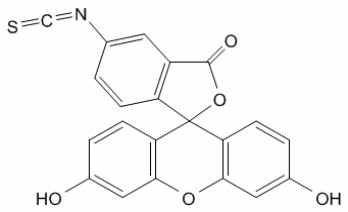

Fluorescein isothiocyanate (green)
[FITC]

Figure 3.1 Structures of the red and the green fluorescent dyes used to label the cationic and anionic PVA/PVPi particles, respectively.

3.5.1 Preparation of fluorescein isothiocyanate (FITC)

3.5.1.1 Materials

The following materials were used: 5-aminofluorescein (Sigma-Aldrich, ≥ 90%), thiophosgene (Sigma-Aldrich, ~ 90%), acetone, DDI water. Acetone was distilled and dried prior to use.

3.5.1.2 Method

FITC was prepared via the conversion of 5-aminofluorescein, in much the same manner as that performed by McKinney et al.[24] A solution of 7.8 g thiophosgene in 80 mL dry acetone was prepared, whereto a 1.71 g aminofluorescein in 60 mL acetone solution was added drop wise over 2 hr. Under nitrogen atmosphere, the reaction was allowed to proceed for an additional 2.5 hr. On completion, the product was precipitated and washed with acetone; the filtered product was then dried in a desiccator.

3.5.1.3 Analysis and characterisation

FTIR analysis proved that the synthesis of fluorescein isothiocyanate was successful. The synthesised FITC showed the characteristic cyano group absorption peak,[24] whilst the aminofluorescein precursor showed none, as seen in Figure 3.2.

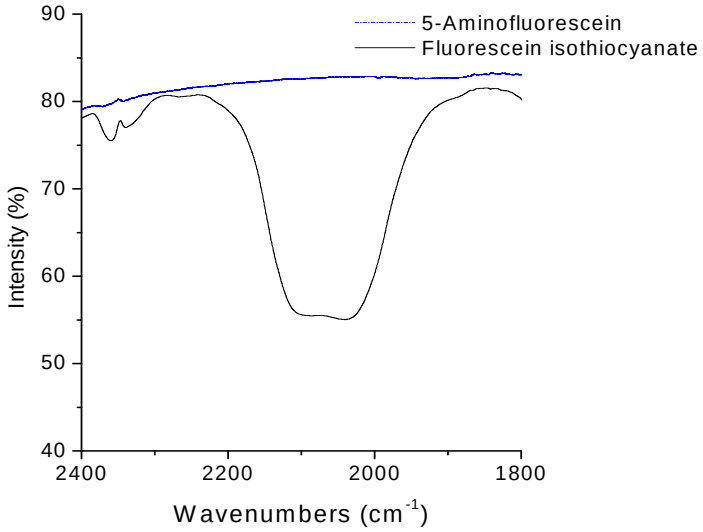

Figure 3.2 **FTIR spectra showing the absorption peak characteristic to the isothiocyanate group, present in FITC and absent in aminofluorescein precursor.**

3.5.2 Preparation of fluorescent labelled modified PVA/PVPi particles

The cationic (sample **C**) and anionic (sample **D**) modified PVA/PVPi particles were labelled with the rhodamine B tag (red dye) and fluorescein tag (green dye), respectively. In addition, a control set of unmodified particles, i.e. PVPi (sample **A**) and PVA/PVPi (sample $\mathbf{B_5}$), were tagged with the red rhodamine dye for comparison. Scheme 3.4 provides a general illustration of the reaction that takes place between the functional groups of the respective components. Both fluorophores are attached by

the addition and rearrangement reaction of the isothiocyanate and hydroxyl functional groups of the respective components.

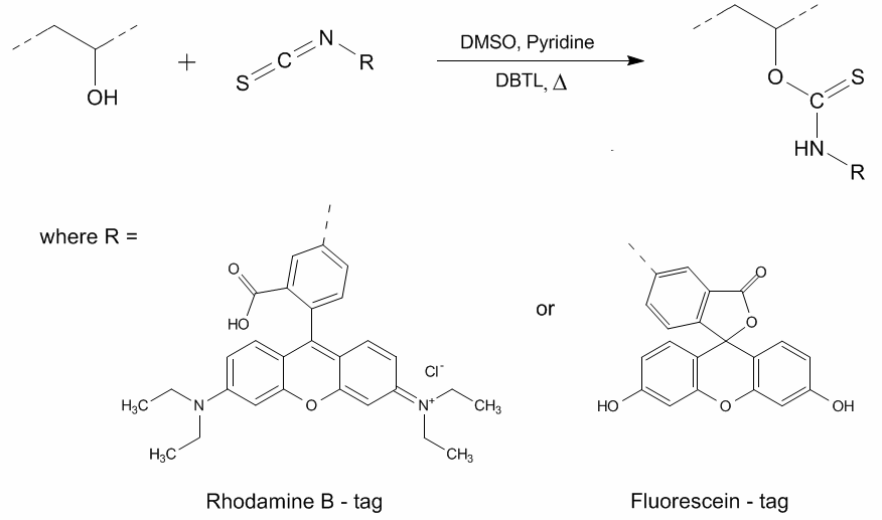

Scheme 3.4 Illustration of fluorescent labelling via reaction of the hydroxyl group on the polymer chain with the isothiocyanate functional group of the respective fluorophore.

The method used for the labelling of the modified particles with the functionalised rhodamine B dye and fluorescein dye was adapted from a procedure described by de Belder and Granath.[25] All reaction set-ups consisted of a three-neck round bottom flask, equipped with condenser, nitrogen inlet and magnetic stirrer.

3.5.2.1 Materials

The following materials were used: cationic modified PVA/PVPi particles (sample **C**, Section 3.4.2.1), anionic modified PVA/PVPi particles (sample **D**, Section 3.4.2.2), standard PVPi particles (sample **A**, Section 3.2.2), unmodified PVA/PVPi particles (sample $\mathbf{B_5}$, Section 3.3.2), rhodamine B isothiocyanate (RBITC, Fine Chemicals), fluorescein isothiocyanate (FITC, synthesised from Sigma-Aldrich reagents, Section 3.5.1), dibutyltin dilaurate (DBTL, Sigma-Aldrich), distilled pyridine (Saarchem), dimethylsulphoxide (DMSO; 99.7%, Sigma-Aldrich), ethanol (EtOH; 99.7–100%, chromatography grade, VWR Chemicals). All reagents were used as received.

3.5.2.2 Rhodamine B labelled cationic PVA/PVPi particles

The cationic particles (sample **C**, 1.5 g) were dissolved in DMSO (20 mL) at room temperature and sonicated for about 5 min to aid in efficient particle separation. A few drops of pyridine and the

RBITC (75 mg) were then added, followed by the addition of the dibutyltin dilaurate catalyst (15 mg). The mixture was heated to 95 °C and the reaction was run for 2 hr under a nitrogen atmosphere, with stirring at 400 rpm. The solid product was centrifuged and washed several times with ethanol until the wash layer was colourless. Once all the unreacted dye had been washed away, the rhodamine B labelled cationic PVA/PVi product was dried under vacuum at 60 °C.

3.5.2.3 Fluorescein labelled anionic PVA/PVPi particles

The anionic particles (sample **D,** 1.5 g) were dissolved in DMSO (20 mL) at room temperature and sonicated for about 5 min in order to aid in efficient particle separation. A few drops of pyridine and the FITC (75 mg) were then added, followed by the addition of the dibutyltin dilaurate catalyst (15 mg). The mixture was heated to 95 °C and the reaction was run for 2 hr under a nitrogen atmosphere, with stirring at 400 rpm. The solid product was centrifuged and washed several times with ethanol until the wash layer was colourless. Once all the unreacted dye had been washed away, the fluorescein labelled anionic PVA/PVPi product was dried under vacuum at 60 °C.

3.5.2.4 Control labelling: Rhodamine B labelled PVPi and PVA/PVPi particles

The PVPi particles (sample **A**) and the PVA/PVPi particles (sample $\mathbf{B_5}$) were tagged with the rhodamine B label using the same experimental procedure as described for the cationic particles (see Section 3.5.2.1). These samples were labelled as a control set, in order to ascertain whether the labelling process was successful. The PVPi particles should not be labelled because there are no hydroxyl functional groups present for the tagging reaction to occur (as illustrated in Scheme 3.4). The PVA/PVPi particles should however show fluorescence because hydroxyl groups, introduced via the saponification procedure (Section 3.3.2), are present.

3.5.3 Analysis and characterisation

Fluorescence images of the fluorescent tagged particles were obtained using fluorescence microscopy, as described in Section 3.7.10. Images of the labelled modified PVA particles with cellulose fibres, and a few images of these samples with a green FITC labelled cationic starch (prepared in the same way as described in Sections 3.4.2.1 and 3.5.2.3), were also obtained. Statistical information was also acquired using flow cytometry. The images and results are presented in the following chapter.

3.6 Product purification

Soxhlet extraction was performed on each of the samples, i.e. the PVPi cross-linked standard (sample **A**), the 15 min hydrolysed PVA/PVPi (sample $\mathbf{B_5}$), and the cationic and anionic modified PVA/PVPi samples (**C** and **D**, respectively). This was performed to eliminate any potential contaminants and determine sample purity. A general Soxhlet apparatus was used.[26] MeOH (200 mL) was used as extraction solvent. The system was arranged for continuous extraction over 24 hr at 90 °C. The solid residue (product) was washed and dried. These samples were analysed using SS NMR and FTIR spectroscopy. Zeta potential analysis was also carried out. Table 3.4 tabulates the sample codes for each step in the series.

Table 3.4 Summary of the overall PVA/PVPi particle series

Code[a]	Sample description	Acronym	Section
A	Unmodified, cross-linked PVPi, standard	PVPi	3.2.2
B_5	15 min hydrolysed PVA/PVPi	PVA/PVPi	3.3.2
C	Cationic modified PVA/PVPi (15 min hydrolysed)	C+PVA/PVPi	3.4.2.1
D	Anionic modified PVA/PVPi (15 min hydrolysed)	A-PVA/PVPi	3.4.2.2

[a] Soxhlet extraction was performed on at least one sample from each step in the synthesis series (A–D), where all samples are derived from the original cross-linked PVPi standard

3.7 Characterisation

Various analytical techniques were used for the characterisation and analysis of the various polymer particles synthesised. A description of the instrumentation, the experimental set-up and analytical conditions used in the analyses are now to be described.

3.7.1 Nuclear magnetic resonance spectroscopy (NMR)

All samples were purified and dried prior to NMR analysis. Solvents used were either $CDCl_3$ or deuterated DMSO, depending on the sample solubility. Once the suitable solvent was established, the proton (^1H) and carbon (^{13}C) NMR spectra were obtained using a 600 MHz Varian Unity Inova spectrometer.

3.7.2 Solid state nuclear magnetic resonance spectroscopy (SS NMR)

Solid state (SS) NMR spectroscopy, particularly ^{13}C (SS ^{13}C NMR), was used as routine analysis for molecular structure determination. SS NMR was used because the use of solution NMR analysis was severely limited due to the insolubility of the cross-linked samples. SS NMR spectra were obtained using a Varian VNMRS 500 MHz two-channel spectrometer with 6 mm zirconia rotors and a 6 mm Chemagnetics^{TM} T3 HX MAS probe.

The analytical method involved the use of cross-polarisation (CP) magic-angle-spinning (MAS). All CP spectra were recorded at ambient temperature with proton decoupling, using a 3.5 μs 90° pulse and a 3 s recycle delay time. The power parameters were optimised for the Hartman-Hahn match; the radio frequency fields were $\gamma_C B_{1C} = \gamma_H B_{1H} \approx 56$ kHz and a 2 ms contact time for cross-polarization was used. The Fourier transform was carried out with 0.5 Hz line broadening and the free induction decay had 2082 points. The MAS was performed at 5 kHz. Adamantane, with the downfield peak referenced to 38.3 ppm, was used as an external chemical shift standard. SS NMR was used for structural and compositional determinations. All samples were purified and thoroughly dried prior to analysis.

3.7.3 Fourier transform infrared spectroscopy (FTIR)

3.7.3.1 Attenuated total reflectance (ATR)

Attenuated total reflectance (ATR) is a simple technique that allows the FTIR analysis of samples without the need for meticulous sample preparation. Samples can simply be used in the powder form after purification and drying. FTIR analysis was accomplished using a Thermo Nicolet (Nexus model) instrument with an ATR attachment. The ATR attachment used was a Smart Golden Gate accessory, with ZnSe lenses and a diamond window.

3.7.3.2 Photoacoustic spectroscopy (PAS)

Photoacoustic spectroscopy (PAS) is an alternative to ATR, where the spectrometer is equipped with a PAS attachment. A Perkin Elmer Paragon 1000 PC FTIR spectrometer, equipped with photoacoustic MTEC 300 cell, was used to record PAS-FTIR scans. Once again, no tedious sample preparation is necessary; samples, in a sample holder, are simply placed inside a sealed chamber, which is then flushed with helium in order to promote the acoustic waves. The instrument resolution, number of scans and mirror speed used were 8 cm^{-1}, 128 and 0.15 cm/s, respectively.

3.7.4 Scanning electron microscopy (SEM)

SEM produces high resolution images of surface structures by using electron back scattering. The electron micrographs obtained provide useful information regarding the surface structure and/or topography of the sample.

Imaging was accomplished using a Leo® 1430VP Scanning Electron Microscope. Samples were prepared for imaging by dispersing the respective particles in a suitable solvent and then spreading over a smooth sheet of foil, allowing the particles to settle individually instead of in an agglomeration. Once the solvent had evaporated, the foil sheets were cut to size, mounted on stubs with double-sided carbon tape, and coated with a thin layer of gold to make the surfaces electrically conducting. Beam conditions (volts, spot size and working distance) used during surface analysis and imaging, were changed accordingly to suit the sample and obtain the best image.

For the particle-fibre images, the purified and dried particles were sonicated in EtOH/MeOH to separate the particles efficiently, then centrifuged and sonicated in DDI water. The particles were then mixed with a 1% cellulose fibre solution in a 2% dry additive (particle) to fibre ratio. The particle-fibre suspensions were then spread out on a smooth foil sheet and dried at 40–60 °C, then they were cut to size and gold coated. It should be noted that mechanical attrition during handling can reduce the number of particles on the surface, especially at low adhesion densities.

3.7.5 Particle size analysis by laser diffraction spectrometry (LDS)

A HELOS laser diffraction spectrometer (Particle Size Analyser) was used for particle size and distribution analysis. The instrument is equipped with a Sympatec SUCELL HELOS/BF-OM laser diffraction sensor. It is a universal wet dispersion system that provides accurate particle size distributions of suspensions and emulsions. The R1 and R3 lenses, with a range of operational measurements from 0.1–35 μm and 0.5–200 μm, respectively, were used for particle size detection. Sample preparation involved the preparation of aqueous particle suspensions of each sample (0.1 g per 3.5 g H_2O), using a non-ionic surfactant and suspension agent (at ± 1.5%) to aid the dispersion. Samples were sonicated (for a minimum of 3 × ½ hour sonication periods) prior to analysis in order to break up any potential agglomerations. Where necessary, samples were subjected to extended periods of sonication of up to 3 hours (6 × ½ hour cycles).

The mean diameters obtained from this analysis were the number-average (D_n) and volume-average diameter (D_{vad}), calculated using WINDOX software. The particle diameters, for the standard suspension particles (sample A), were also measured directly from SEM images (Section 3.7.4), where

at least 300 particles (N) were counted. The counted number-average diameter (D_n) and the weight-average diameter (D_w) were calculated using equations 3.2 and 3.3,[4] respectively.

$$D_n = \frac{\sum N_i D_i}{\sum N_i} \qquad 3.2$$

$$D_w = \frac{\sum N_i D_i^4}{\sum N_i D_i^3} \qquad 3.3$$

3.7.6 Thermal analysis

3.7.6.1 Differential scanning calorimetry (DSC)

The glass transition and crystalline melting temperatures (T_g and T_m, respectively) were determined using a TA Instruments, Q100 Series, Differential Scanning Calorimeter. Samples (4–7.5 mg) were weighed and analysed, under a nitrogen atmosphere, at a heating rate of 10 °C/min. DSC data analysis was achieved using TA Instruments Universal Analysis 2000 software.

The reader should note that here T_m does not refer to the melting temperature of the whole polymer, as a cross-linked polymer (by definition) cannot melt. Instead, T_m refers to the melting or rearrangement or orientation of the crystalline segments between the cross-links of the polymer. The percent crystallinity also refers to the crystalline or crystallisable domains between the cross-links.

The percentage crystallinity of each sample was determined by comparing the observed heat of fusion/melting ($\Delta H'_m$) for each respective sample with that of 100% crystalline PVA (ΔH_m), using equation 3.4. For the 100% crystalline PVA, the literature ΔH_m value of 161.4 J/g[27] was used (alternative sources indicate ΔH_m = 156.0 J/g[28,29] or 156.2 J/g[30]).

$$\text{Degree of crystallinity } (\%) = \frac{\Delta H'_m}{\Delta H_m} \times 100 \qquad 3.4$$

3.7.6.2 Thermogravimetric analysis (TGA)

Besides sample purification and drying prior to analysis, no further sample preparation for TGA was necessary. The thermogravimetric analyser used was a Perkin Elmer Pyris TGA-7 instrument. Samples were heated, under a nitrogen atmosphere, from 20 °C to 900 °C at a rate of 20 °C/min.

3.7.7 X-ray diffraction (XRD)

X-ray powder diffraction (XRPD), or simply X-ray diffraction (XRD), studies were conducted to obtain additional information regarding sample crystallinity. The diffractograms were acquired on a PANanalytical X'Pert Pro Multi Purpose Diffractometer, with Bragg-Brentano geometry, providing intensity versus 2θ diffraction patterns. A Cu-K_α radiation source was used (λ = 1.5418 Å) and intensity data were acquired from multiple 2θ scans using an X'Celerator detector with flat-stage configuration. A scan speed of 42 s per step, with a step size of 0.017°, over a 2θ range of 3–80°, was utilised for data collection. Besides routine purification and drying, sample preparation for XRD analysis only required that the dry samples be ground into a fine powder.

3.7.8 Transmission electron microscopy (TEM)

Transmission electron microscopy (TEM) is a high magnification, high resolution imaging technique, useful in the study of material morphology. An electron beam is focused on a sample specimen and an enlarged image is developed by detecting the differences in electron densities. TEM images were obtained from a JEOL 1200 EXII instrument (Electron Microscopy Unit, University of Cape Town). In this case, the particles were stained with a 2% KI/H_2O solution (with 1.3% I_2),[31] for 12 hr, then washed with a little MeOH (dilute) and excess amount of water. After drying, the particles were set in resin for 16 hr at 60 °C. After microtoming, the resin-set sample slices were finally placed on copper TEM grids for imaging.

3.7.9 Zeta potential measurements

The zeta potential is the electrical potential that exists a small distance from the shear plane of a particle surface. Ionic and dipolar characteristics of colloidal particles that are suspended in solution result in electric charge on the particles. When in solution, a particle carrying a net surface charge will be surrounded by oppositely charged (counter) ions in the 'Stern' layer. The counter ions (ions opposite in charge to the particle) are distributed in the interfacial region with highest concentration closest to the particle surface. In this manner, an electrical double layer is formed in the particle–liquid interfacial region, consisting of an inner and outer (diffuse) region.[32,33]

The zeta potential is the potential at the shear plane between the particle's ion atmosphere and its surrounding medium. The zeta potential is therefore a function of the particles' surface charge, the composition and nature of the surrounding suspension medium, and the adsorbed interfacial layer. It can be calculated using the Henry equation,[34,35] which takes into account electrophoretic mobility, the

medium's viscosity and dielectric constant, and a correction factor for the particle diameter and double layer thickness. In this case, the zeta potential is determined by the instrument.

If the prepared and modified particles are to be used as paper additives or fillers, they would have to be incorporated or adsorbed onto the cellulose fibre surface. The extent of this adsorption will depend on the functional groups. Zeta potential measurements provide information on the overall particle charge. The surface charges of the various modified spherical PVA/PVPi particles were investigated. The zeta potentials of the respective particles were measured using a Malvern Zetasizer Nano ZS90 instrument, with disposable capillary cuvettes for analysis. Samples were prepared by first sonicating the purified dry particles in EtOH/MeOH in order to separate the particles efficiently. After removing excess alcohol by centrifuging and washing with water, the particles were sonicated and then suspended in DDI water solution, with a 1% solid content. Samples were further diluted (to approximately 0.05%) with water until the solution was transparent.

3.7.10 Fluorescence imaging and statistical analysis

Fluorescence microscopy, a technique which uses fluorescence light and a series of lenses to obtain magnified fluorescence images, was used to image the fluorescing (fluorescent labelled) samples. Fluorescence images were obtained with an IX-81 inverted fluorescence microscope, fitted with an F-view-II cooled CCD camera (Soft Imaging Systems), coupled with attached Olympus Cell^{R} imaging software. Images were excited with 472 nm and 572 nm excitation filters. The emissions were collected using a UBG triple-bandpass emission filter cube (Chroma), and the images were obtained and collected with an Olympus Plan Apo N (60x/1.4) oil immersion objective lens and the Cell^{R} imaging software. The Cell^{R} software was used to process and background-subtract the images obtained. Transmission mode optical (visible) light images and the fluorescence light mode images were obtained.

Statistical fluorescence data were acquired via a BD FACSAria flow cytometer, using an event rate of 500–1000 events/s. A total of 50 000 events were recorded and analysed with BD FACSDiva and FlowJo software.

Fluorescent labelled particles, i.e. samples **A** (PVPi), **B** (PVA), **C** (cationic PVA) and **D** (anionic PVA), were prepared for fluorescence imaging and flow cytometry in aqueous sample suspensions (using DDI water). Purified and dried samples were sonicated in EtOH/MeOH in order to separate the particles efficiently. After solvent extraction via centrifugation, the particles were sonicated in DDI water at 2% concentration.

Where cellulose paper fibres were studied for adhesion of the above particles, a 1% aqueous fibre solution was mixed with the 2% aqueous particle mixture (2% dry particles to dry fibre ratio), then centrifuged and washed twice with water. The aqueous particle–fibre solution was then submitted for fluorescence studies.

In a follow up investigation, a fluorescein labelled (FITC) cationic starch (previously synthesised) was added to the particle–fibre mixture used above. The starch was first added to the 1% cellulose fibre solution, in a 0.8% dry starch to dry fibre ratio; the solution was mixed well, then centrifuged and decanted, and then redispersed in aqueous medium (water). The labelled modified PVA/PVPi particles (prepared and sonicated in aqueous medium as above; 2% dry particles to dry fibre ratio) were then added to this FITC cationic starch–fibre solution and mixed well.

3.7.11 Field-flow fractionation (FFF)

The principles of field-flow fractionation (FFF) have been described in Section 2.8. For this investigation, the asymmetric flow FFF (AsFl-FFF or AF4) technique was employed, using an AsFl-FFF instrument coupled to a PN3000 XPT Particle Analyzer (both instruments were obtained from Postnova Analytics, Landsberg, West Germany). Samples **A** (PVPi particles) and $\mathbf{B_5}$ (15 min hydrolysed PVA/PVPi particles) were used for comparison. Pure samples were suspended in a THF solvent system (in 3 mg/mL or 5 mg/mL ratios), with added surfactants (Igepal CO890) to aid in suspension. Samples were injected either with only an injection flow rate of 1 mL/min and no cross-flow, or with an injection flow rate of 0.2 mL/min, a 2 min focus period and exponentially decreasing cross-flow rate of 0.5 mL/min to 0.01 mL/min (decreases from 2–5 min). The particle size analyser was used to detect the particles eluting from the FFF channel and establish particle size elution and distribution curves. Comparison in terms of the surface charge of the modified particles would have been ideal, but could not be accomplished as only AsFl-FFF was available.

3.8 References

1. S.G. Lee, J.P. Kim, W.S. Lyoo, J.W. Kwak, S.K. Noh, C.S. Park, and J.H. Kim, *J. Appl. Polym. Sci.*, **2005**, 95(6), 1539-1548.
2. S.G. Lee, J.P. Kim, I.C. Kwon, D.S. Shin, S.S. Han, and W.S. Lyoo, *J. Appl. Polym. Sci.*, **2006**, 101(6), 4064-4070.
3. W.S. Lyoo, C.S. Park, K.H. Choi, J.W. Kwak, W.S. Yoon, and S.K. Noh, *Polym. Plast. Technol. Eng.*, **2005**, 44(3), 475-487.
4. W.S. Lyoo, J.W. Kwak, J.H. Yeum, B.C. Ji, C.J. Lee, and S.K. Noh, *J. Polym. Sci., Part A: Polym. Chem.*, **2005**, 43(4), 789-800.
5. W.S. Lyoo, C.S. Park, J.H. Yeum, B.C. Ji, C.J. Lee, S.S. Lee, and J.Y. Lee, *Colloid Polym. Sci.*, **2002**, 280(12), 1075-1083.
6. D.H. Song and W.S. Lyoo, *J. Appl. Polym. Sci.*, **2007**, 104(1), 410-414.
7. T. Chen and E.L. Burch. Use and Preparation of Crosslinked Polymer Particles for Inkjet Recording Materials. United States Patent: US007507439B2, 2009.
8. B.V. Kichatov, A.M. Korshunov, and P.V. Assorova, *Theor. Found. Chem. Eng.*, **2003**, 37(3), 306-309.
9. W.S. Lyoo and W.S. Ha, *Polymer*, **1999**, 40(2), 497-505.
10. W.S. Lyoo, S.S. Han, J.H. Kim, W.S. Yoon, C.J. Lee, I.C. Kwon, J. Lee, B.C. Ji, and M.H. Han, *Angew. Makromol. Chem.*, **1999**, 271(1), 46-52.
11. W.S. Lyoo and H.W. Lee, *Colloid Polym. Sci.*, **2002**, 280, 835-840.
12. W.S. Lyoo, J. Blackwell, and H.D. Ghim, *Macromolecules*, **1998**, 31(13), 4253-4259.
13. W.S. Lyoo, H.D. Ghim, J.H. Kim, S.K. Noh, J.H. Yeum, B.C. Ji, H.T. Jung, and J. Blackwell, *Macromolecules*, **2003**, 36(14), 5428-5431.
14. W.S. Lyoo, J.H. Yeum, B.C. Ji, H.D. Ghim, S.S. Kim, J.H. Kim, J.Y. Lee, and J. Lee, *J. Appl. Polym. Sci.*, **2003**, 88(6), 1482-1487.
15. W.S. Lyoo, J.H. Kim, and H.D. Ghim, *Polymer*, **2001**, 42(14), 6317-6321.
16. W.S. Lyoo, J.H. Kim, J.H. Choi, B.C. Kim, and J. Blackwell, *Macromolecules*, **2001**, 34(12), 3982-3987.
17. R. Baudry and D.C. Sherrington, *Macromolecules*, **2006**, 39(16), 5230-5237.
18. J.H. Yeum, B.C. Ji, S.K. Noh, H.Y. Jeon, J.W. Kwak, and W.S. Lyoo, *Polymer*, **2004**, 45(12), 4037-4043.
19. T.L. Uyen Nguyen, B. Farrugia, T.P. Davis, C. Barner-Kowollik, and M.H. Stenzel, *J. Polym. Sci., Part A: Polym. Chem.*, **2007**, 45(15), 3256-3272.

20. V. Haack, T. Heinze, G. Oelmeyer, and W.-M. Kulicke, *Macromol. Mater. Eng.*, **2002**, 287(8), 495-502.
21. B. Volkert, F. Loth, W. Lazik, and J. Engelhardt, *Starch-Stärke*, **2004**, 56(7), 307-314.
22. A. Kornherr, F. Eder, B. Janse, R. Sanderson, J. Terblanche, and M. Zou. Process for Preparing Polysaccharide Gel Particles and Pulp Furnish for Use in Paper Making. European Patent Application: 09450061.8 – 2115, 2009.
23. F.M. Winnik and S.T.A. Regismond, *Colloids Surf., A*, **1996**, 118, 1-39.
24. R.M. McKinney, J.T. Spillane, and G.W. Pearce, *Anal. Biochem.*, **1964**, 7(1), 74-86.
25. A.N. de Belder and K. Granath, *Carbohydr. Res.*, **1973**, 30(2), 375-378.
26. L.M. Harwood, C.J. Moody, and J.M. Percy, *Experimental Organic Chemisty: Standard and Microscale*, 2nd edn., Blackwell Science Ltd: Cornwall, 1999.
27. H.F. Mark, *Encyclopedia of Polymer Science and Technology*, ed. J.I. Kroschwitz, 3rd edn., Vol. 12, John Wiley & Sons, Inc.: Hoboken, 2003, pp. 168-169.
28. Y. Nagara, T. Nakano, Y. Okamoto, Y. Gotoh, and M. Nagura, *Polymer*, **2001**, 42(24), 9679-9686.
29. H. Ohgi, T. Sato, S. Hu, and F. Horii, *Polymer*, **2006**, 47(4), 1324-1332.
30. H. Chirowodza, *Synthesis and Characterization of Cationically and Anionically Modified Poly(Vinyl Alcohol) Microfibrils*, MSc Thesis, Stellenbosch University, 2009.
31. A.I. Vogel, *A Text-Book of Quantitative Inorganic Analysis; Including Elementary Instrumental Analysis*, 3rd edn., Longmans Ltd: London, 1961, pp. 343-357.
32. C. Werner, H. Körber, R. Zimmermann, S. Dukhin, and H.-J. Jacobasch, *J. Colloid Interf. Sci.*, **1998**, 208(1), 329-346.
33. M. Löbbus, J. Sonnfeld, H.P. van Leeuwen, W. Vogelsberger, and J. Lyklema, *J. Colloid Interf. Sci.*, **2000**, 229(1), 174-183.
34. A. López Valdivieso, J.L. Reyes Bahena, S. Song, and R. Herrera Urbina, *J. Colloid Interf. Sci.*, **2006**, 298(1), 1-5.
35. A. Wiącek and E. Chibowski, *Colloids Surf., A*, **1999**, 159(2-3), 253-261.

Chapter 4: Results and Discussion

4.1 Introduction

This chapter presents the results and data acquired from the synthetic and experimental procedures and the respective analytical techniques used throughout this study for each step of the synthetic pathway. These steps essentially comprise the initial vinyl pivalate (VPi) suspension copolymerisation with tri(ethylene glycol) divinyl ether (TEGDE) as cross-linking comonomer to prepare cross-linked poly(vinyl pivalate) (PVPi) microspheres, the hydrolysis of these microspheres to poly(vinyl alcohol) (PVA), and their subsequent ionic functionalisation and fluorescent labelling, and respective fluorescence imaging of these particles.

4.2 Suspension polymerised spherical PVPi particles

The main objective of this section of the work was to prepare cross-linked PVPi microspheres via suspension polymerisation, as described in Chapter 3 (Section 3.2). Emphasis was placed on the synthesis of PVPi microspheres with close to uniform particle sizes, ideally with diameters in the range 0.5–10 μm, in contrast to the larger spheres and wider distributions presented in the literature.[1-3] Scheme 4.1 shows the general reaction pathway used for the polymerisation of VPi.

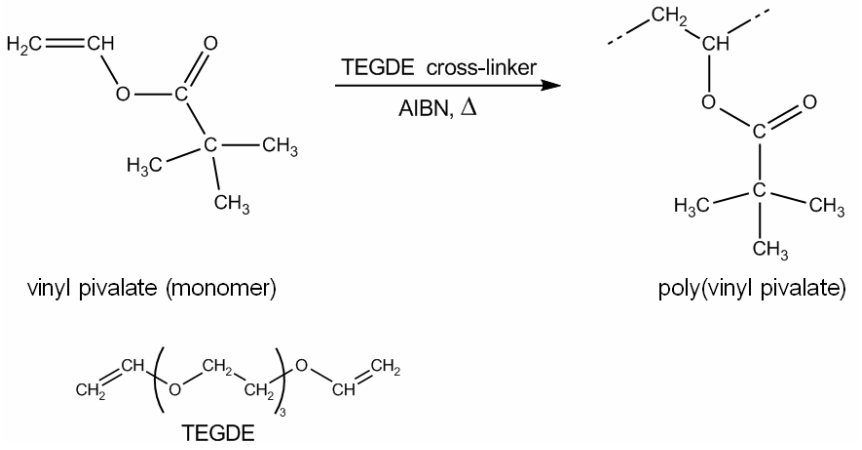

Scheme 4.1 VPi polymerisation with TEGDE as comonomer cross-linking agent, yielding cross-linked PVPi.

4.2.1 Characterisation

PVPi microspheres were successfully synthesised via the thermo-initiated radical suspension polymerisation procedure described in (Chapter 3, Section 3.2). Nuclear magnetic resonance (NMR) and Fourier transform infrared (FTIR) spectroscopy were used to characterise the polymer particles. A comparison was made between the standard PVPi (cross-linked) polymer and its uncross-linked homopolymer counterpart. The uncross-linked PVPi was prepared according to standard suspension polymerisation conditions, without cross-linking agent. The uncross-linked PVPi homopolymer was characterised with solution NMR, with $CDCl_3$ as solvent.

The ^{1}H NMR spectrum of the PVPi homopolymer, Figure 4.1, shows three resonance signals attributed to the three chemically distinct types of protons in the PVPi repeat unit. The resonance shifts at 1.75 ppm (a) and 4.8 ppm (b) correspond to the methylene (-C**H**$_2$-) and methine (-C**H**-) protons, respectively, whilst the signal at 1.2 ppm (e) is attributed to the chemical shift of the methyl protons (-C**H**$_3$).[4-6] The additional signals seen around 3.6 ppm (weak) are likely to be due to contaminants, from grafted or hydrogen bonded surfactant (a possible side reaction). The surfactant carries free hydroxyl groups which may result in covalent attachments to the particles.[7] The stereochemistry gives insight into the multiple peaks (a) and (b). Full conversion took place, as no vinyl methine (-C**H**-) peak, at 7.28 ppm, was observed.

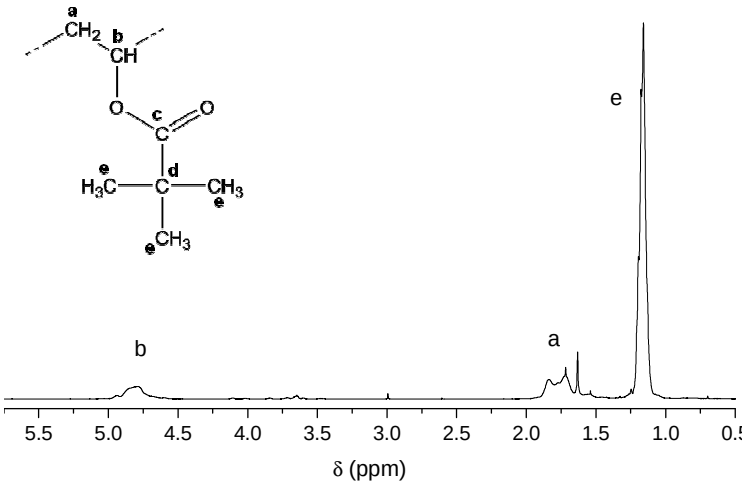

Figure 4.1 ^{1}H NMR spectrum of uncross-linked PVPi ($CDCl_3$ solvent).

The characterisation of the cross-linked PVPi samples was not as simple, due to the obvious fact that cross-linking limits the solubility of the polymer. Consequently, techniques such as solution NMR, and even size exclusion chromatography (SEC), are impractical for cross-linked polymer characterisation. Solid state nuclear magnetic resonance (SS NMR) spectroscopy is a viable

alternative.[8,9] SS NMR spectroscopy, specifically ^{13}C, proved to be a valuable and efficient characterisation technique for these cross-linked polymers. Solid state ^{13}C NMR (SS ^{13}C NMR) studies were conducted on these cross-linked samples. The SS ^{13}C NMR spectra were used to characterise and compare the cross-linked and uncross-linked samples, and their derivatives (presented later). Figure 4.2 is an example of a cross-polarization magic-angle-spinning (CP/MAS) SS ^{13}C NMR spectrum of standard cross-linked PVPi particles. Assignments (indicated on the spectrum) of signals a–e are listed in Table 4.1. The minor signal seen at 105.8 ppm is likely to be the Teflon background signal.

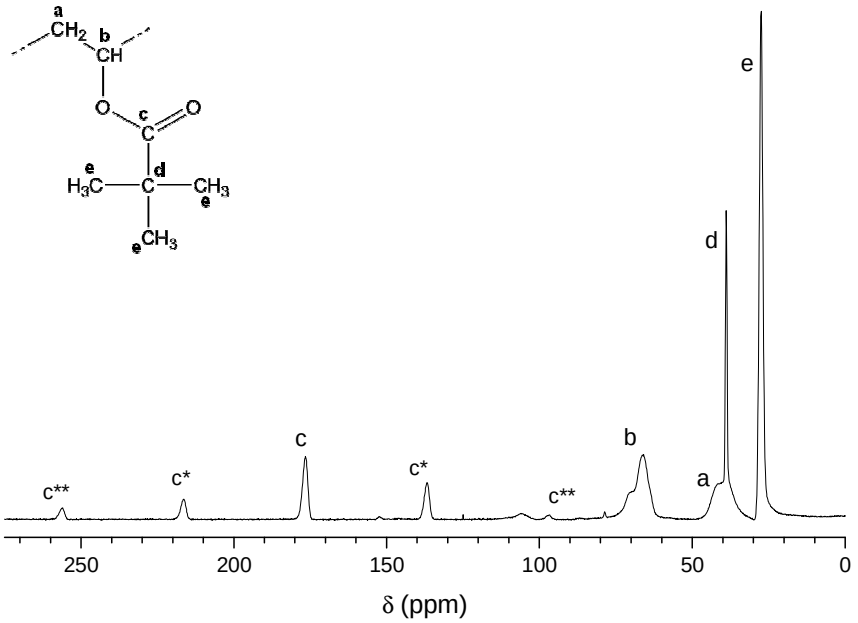

Figure 4.2 **SS ^{13}C NMR spectrum of cross-linked PVPi microspheres; c* and c** represent the spinning and secondary spinning side bands of the carbonyl chemical shift, respectively.**

The methylene (-**C**H_2) carbons of the ethylene glycol units in the cross-linking agent (TEGDE) should resonate at ca. 70.5 ppm, due to their chemical environment (ether bonds, -O-). On the other hand, the shoulder seen at 70.5 ppm on peak "b" could possibly be due to differences in stereoregular arrangements of the methine (-**C**H) carbon (b) and that of its pendant group.[8-10] A comparison was made between the SS ^{13}C NMR spectra of the cross-linked PVPi and uncross-linked PVPi homopolymer samples (see Appendix A.1). The shoulder is also observed in the uncross-liked sample, where TEGDE was not used and the ethylene glycol carbons are thus absent, which suggests that the shoulder is due to stereoregular arrangement of the methine carbons (b). However, there are differences in the shoulder intensities at 70.5 ppm (b), where in the cross-linked sample a larger

shoulder intensity is observed than in the uncross-linked sample. Hence, it is likely that both ideas are valid and may both contribute to the shoulder.

Table 4.1 Resonance signal assignments[i] in the solid state ^{13}C NMR spectrum of cross-linked PVPi

Label	Chemical shift (ppm)	Assignment[4,5]
a	42.0	-**C**H_2
b	66.3	-**C**H
c[ii]	176.5	-**C**=O
d	39.0	-**C**-
e	27.5	-**C**H_3

[i] The references mentioned and NMR prediction software provided assistance in the assignments of the carbon shifts;
[ii] Peaks c* and c** represent the primary and secondary spinning side bands of the carbonyl chemical shift, respectively.

Single-pulse-excitation magic-angle-spinning (SPE/MAS) NMR was performed on the standard PVPi particles and compared with the CP/MAS spectrum (Appendix A.2). Besides noting an increase in signal intensity and detail, no new information was obtained from the SPE/MAS data. Thus, there is no valuable information gained from the prolonged SPE/MAS measurements; the CP/MAS analysis provides adequate information.

Further characterisation included attenuated total reflectance-Fourier transform infrared spectroscopy (ATR-FTIR). Results showed that very few differences were seen in the FTIR spectra of the cross-linked and uncross-linked PVPi. Typical ATR-FTIR spectra of uncross-linked and cross-linked PVPi, with main absorption band assignments,[5,11] are seen in Appendix B.1.

SS ^{13}C NMR and ATR-FTIR analyses were performed on the standard cross-linked PVPi samples, and its derivatives (subsequent sections), before and after Soxhlet extraction. No change was observed in the samples, proving that the standard washing process (using MeOH and water) provided sufficient sample purification.

4.2.2 Conversion

A comparison between the monomer conversions versus time data for the suspension polymerisations carried out at different reaction temperatures was made. The conversion-versus-time data was determined gravimetrically,[12,13] using equation 4.1. Figure 4.3 shows the monomer conversions for the polymerisations conducted at 55 °C, 65 °C and 75 °C, respectively.

$$\text{Conversion}_{(\text{at time } t)}\,(\%) = \frac{\text{Yield}\,(g) - \text{Non Volatiles}\,(g)}{\text{Monomer}\,(g)} \qquad 4.1$$

The monomer conversion versus time plots, Figure 4.3, clearly illustrate that a high monomer conversion is obtained at higher temperatures. The 65 °C and 75 °C polymerisations reach approximately 90% conversion, while the 55 °C polymerisation reaches a plateau at 80% conversion. The conversion rate (slope) of monomer conversion is clearly seen to be fastest at 75 °C, and slowest at 55 °C, as is expected. The temperature has an effect on the rate of conversion due to the relationship between temperature and initiator activation. In other words, the higher the temperature the larger the concentration of radicals produced, and vice versa. Hence, at lower temperatures there are fewer free radicals present, and consequently slower propagation and lower conversions. Thus, the 65 °C polymerisation provides a balance between the highest conversion and a stable propagation rate. The total monomer conversions and total polymer yields for the VPi suspension samples polymerised at different polymerisation temperatures are tabulated in Table 4.2. Scanning electron microscopy (SEM) and particle size distribution analysis aid in establishing whether the rate of propagation has an effect on the size and distribution of the particles (Section 4.2.3, Figure 4.6).

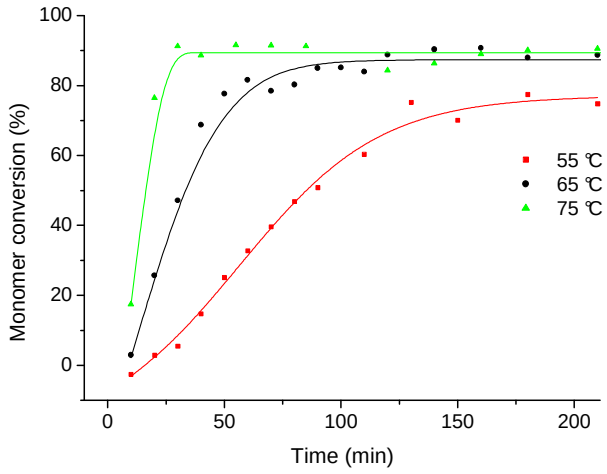

Figure 4.3 **Monomer conversion versus time plot for a VPi suspension polymerisation at 55 °C (red), 65 °C (black) and 75 °C (green), respectively. (Standard polymerisation conditions, [AIBN] = 0.0076 mol/mol monomer.)**

The effect of the polymerisation temperature on the particle morphology and size distribution is discussed in Section 4.2.3.2.

Table 4.2 Monomer conversions and polymer yields of PVPi polymerised at 55 °C, 65 °C and 75 °C

Sample code	Polymerisation temperature (°C)	Maximum monomer conversion (%)[a]	Polymer dry yield (%)[b]
AT_3	55	77.5	-
AT_2	65	90.7	-
AT_4	75	91.5	-
AT_6	55	-	51.3
AT_5[c]	*65*	-	74.1
AT_7	75	-	72.3

[a] The maximum monomer conversion value obtained with sampling during polymerisation using equation 4.1; [b] Dry yields of washed and dried samples after 24 hr of undisturbed polymerisation, where dry yield is calculated as a weight percent (minus initiator) of the total initial monomer and non-volatiles are assumed to be removed by washing; [c] *Standard PVPi* (A), with an average yield for 9 repeat standard samples of 76.4%.

4.2.3 Particle morphology and size analysis

SEM and a HELOS laser diffraction spectrometer were used to study the particles in terms of size, distribution and morphology. Laser diffraction spectrometry (LDS) provides particle distribution curves and the number- and volume-average particle diameters (D_n and D_{vad}, respectively). Samples were prepared for SEM and particle size analysis (LDS) as described in Sections 3.7.4 and 3.7.5, respectively. SEM images of the standard suspension polymerised PVPi particles are shown in Figure 4.4. It is clearly seen that the particles are perfectly spherical and are in the size range of approximately 1–5 μm.

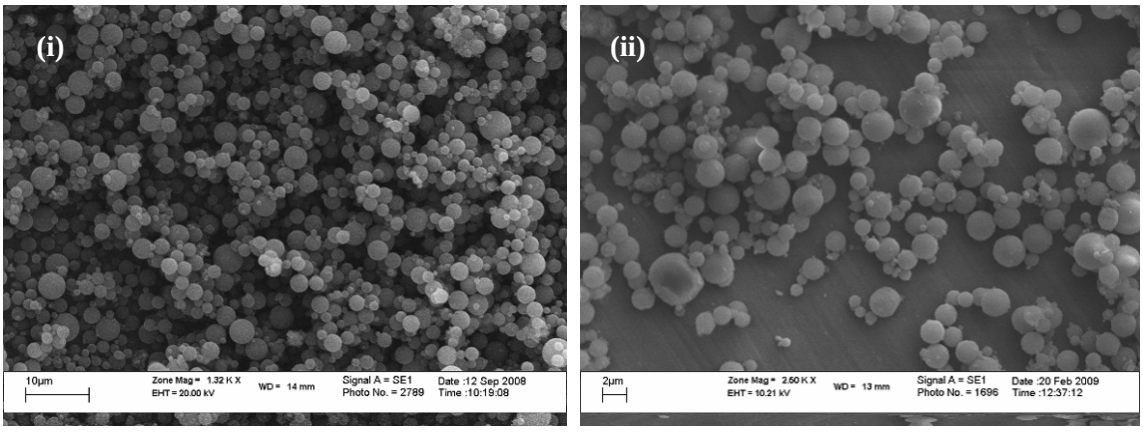

Figure 4.4 SEM images of the standard cross-linked PVPi suspension particles (prepared at 65 °C) at (i) ×1320 and (ii) ×2500.

Particle size analysis was carried out using a HELOS laser diffraction spectrometer. Comparisons between a few repeat standard samples were first carried out to establish the reproducibility of the suspension polymerisations. The distribution curves[†] for repeat standard PVPi samples are presented in Figure 4.5. The particle size distribution of a preliminary standard sample indicates that the suspension polymerisation for the standard conditions is successful in attaining particles of narrow size distribution, in the range of 1 μm to 5 μm in diameter (between the desired 0.5–10 μm); see Figure 4.5 (A). Figure 4.5 (B) shows the particle size distributions of three repeat standard reactions (prepared and analysed at least twice with LDS), illustrating that the suspension polymerisation reactions yield reproducible results and particle sizes.

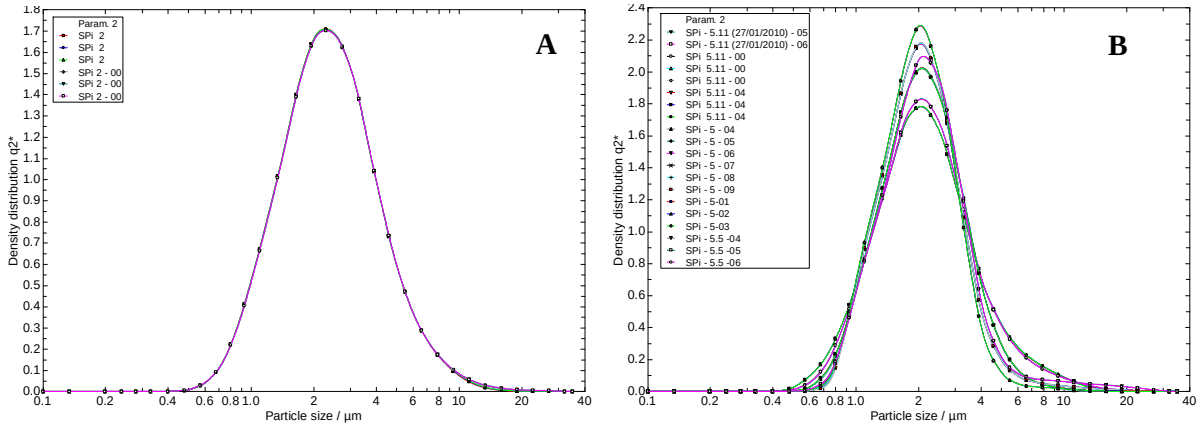

Figure 4.5 **Particle size distribution curves of (A) a preliminary PVPi polymerisation reaction, and (B) multiple distribution curves for three repeat samples of standard PVPi particles, prepared by standard suspension polymerisation conditions (i.e. 65 °C, cross-linked).**

As indicated in the previous chapter, for ease of reference, the standard cross-linked PVPi particles are assigned the sample code: "**A**" (sample A). The standard polymerisation conditions used are described in Section 3.2.2 and 3.2.3.

4.2.3.1 Particle sizes and average diameters

The HELOS laser diffraction spectrometer also provides data regarding the number- and volume-average particle diameter (D_n and D_{vad}, respectively). The particle size results for four repeat standard PVPi samples (codes numbers A_1–A_4) prepared by standard suspension polymerisations conditions are

[†] Particle size distribution graphs were obtained using a HELOS laser diffraction spectrometer. Please note, due to program restrictions, the font size of the captions on the axes is rather small (an effort to achieve increased font size led to fewer tick labels being visible).

listed in Table 4.3. The repeat samples have an average D_n of 2.49 μm, with a standard deviation of 0.2.

Table 4.3 Average particle diameters for standard PVPi particles

Sample (A) code	D_n (μm) [a]	D_{vad} (μm) [b]
A_1	2.79	3.93
A_2	2.22	2.88
A_3	2.52	4.21
A_4	2.44	3.34
Average	2.49	3.59

[a] Number-average particle diameter (D_n); [b] volume-average particle diameter (D_{vad}).

Results of particle size analysis, NMR and FTIR analysis, for the set of repeat standard VPi polymerisations provided evidence that the suspension polymerisation reactions are relatively reproducible. For the standard VPi suspension polymerisations, the D_n is 2.49 μm compared to the manually counted D_n of 2.29 μm. Generally, for such situations, the homogeneity of particle size would be evaluated by determining the polydispersity index (PD)[1-3,13] of the particles diameter. The PD is a ratio of the weight- and number-average particle diameters, D_w and D_n, respectively; see equation 4.2. Typically, a PD within the range of 1.0–1.1 is classified as monodisperse.

$$\mathrm{PD} = \frac{D_w}{D_n} \qquad 4.2$$

The particle diameters of the standard PVPi samples were determined from SEM, using the number-average diameter (D_n) and weight-average diameter (D_w) equations below (equations 4.3 and 4.4).[2]

$$D_n = \frac{\sum N_i D_i}{\sum N_i} \qquad 4.3$$

$$D_w = \frac{\sum N_i D_i^4}{\sum N_i D_i^3} \qquad 4.4$$

At least 300 particles (*N*) were counted and the PD of the standard cross-linked PVPi particles was experimentally calculated to be 1.4.

A variation in D_n and D_w (and hence PD) can be expected because there are many factors that can influence the particle diameter and their distribution. The homogenation, removal of the solution from the homogeniser and transfer to reaction vessel, stirring and bringing the reaction medium (and particles) to the required polymerisation temperature, are all factors that may affect the particle size and distribution. Ideally, an automated computerised sequence should replace manual operations, however, the method used was sufficient for this study.

4.2.3.2 Effect of polymerisation temperature on particle morphology and size distribution

A sharp Gaussian-type shaped distribution curve is observed for most of the particles of the various polymerisation conditions (discussed in detail in Section 4.2.5). Figure 4.6 compares the SEM images and distribution curves of the 55 °C, 65 °C and 75 °C PVPi particles. The volume average diameter, D_{vad}, has proportional relationships with the initiator, monomer and suspension agent concentrations, the polymerisation temperature and agitation speed.[2]

The distribution curves of these PVPi particles (Figure 4.6, (ii)) show that there are some differences in the size distribution of the respective samples. Whereas the 65 °C sample (B) shows uniform distribution, the 55 °C and 75 °C samples (A and C, respectively) show tailing in the larger diameter region. The 55 °C sample has a shoulder in the particle distribution (Figure 4.6 A(ii)), which is likely to be the result of particle coagulation during polymerisation as a result of the slower conversion rate (Figure 4.3, red curve). Lyoo et al.[2] have reported similar findings: at higher polymerisation temperatures the probability of droplet separation is "more frequent". Although the overall particle size (i.e. D_{vad}) decreases at higher temperatures, the PD increases. This is to be expected, since at higher temperatures, the suspension viscosity is reduced and the probability of droplet separation is greater.

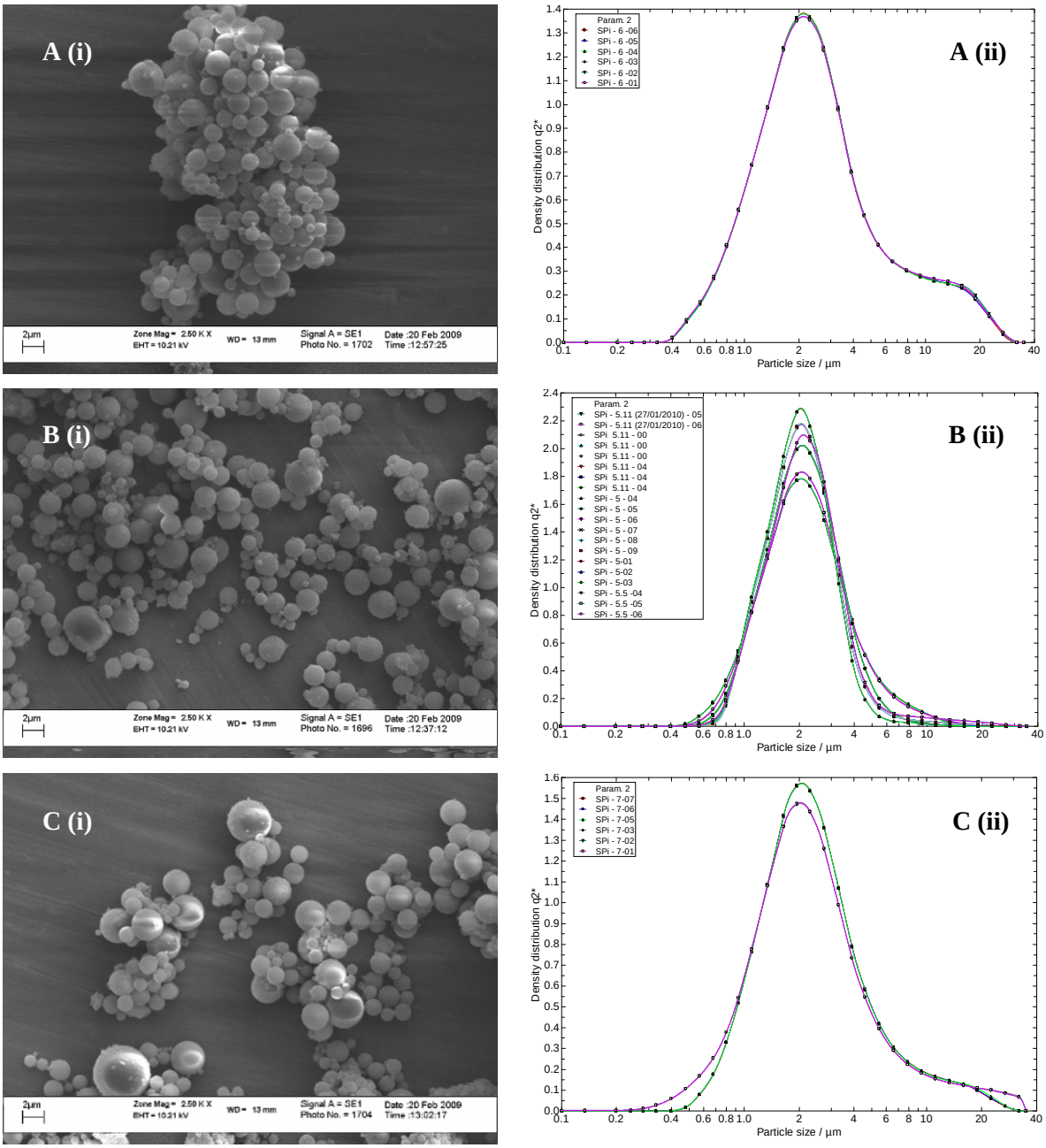

Figure 4.6 **PVPi particles polymerised at different reaction temperatures, (A) 55 °C, (B) 65 °C and (C) 75 °C: (i) SEM images (×2500) and (ii) particle distribution curves.**

Figure 4.7 compares the particle morphologies of the respective PVPi particles polymerised at the various temperatures. The 55 °C particles show collapsed morphology compared to PVPi particles resulting from the 65 °C and 75 °C polymerisations. This could be due to loss of monomer: the monomer conversion was lower, hence there is more free monomer that is able to leach out. In SEM analysis one must always be vigilant for possible artefacts of the heat generated by the SEM beam. In

Figure 4.7, a higher voltage was used, 20.0 kV, when compared to the lower voltage used in Figure 4.6 (i) (10.21 kV). When lower voltages were used, this collapsed particle effect disappeared, as seen in the electron micrographs in Figure 4.6.

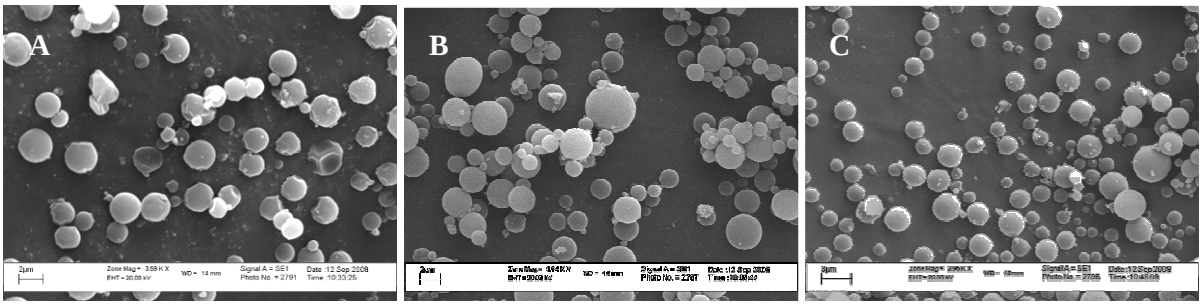

Figure 4.7 SEM image comparison of PVPi particles synthesised at (A) 55 °C (i) ×3690, (B) 65 °C (i) ×3040 and (C) 75 °C (i) ×2690.

4.2.4 Degree of cross-linking of PVPi

A particular polyfunctional vinyl ether, tri(ethylene glycol) divinyl ether (TEGDE), was used as cross-linking agent during polymerisation to ensure the particles maintain their shape and size. The ether linkage was chosen because an ether is more chemically stable than an ester linkage and ethers are supposedly resistant to most organic reactions. Cross-linking was performed during polymerisation to ensure the particles were cross-linked throughout, as opposed to cross-linking post-polymerisation.[14-16] The cross-linking via copolymerisation with VPi as described, to the best of the author's knowledge, has not yet been reported in literature, besides a very recent patent that appeared during the course of this study (2009),[17] which mentioned divinylbenzene in the examples. The concept is therefore no longer novel, but the structures being created are. The cross-linked nature of the particles prove to be a valuable trait of the PVA precursor, as the cross-linked particles maintain their shape during saponification (discussed later in Section 4.3.4.1).

Cross-linking using a divinyl monomer takes place by means of the reaction illustrated in Scheme 4.2, where two double bonds are available for propagation on the TEGDE monomer. When incorporated into the growing polymer chain, this monomer provides two active sites for propagation (double bond and free radical species, red arrows). This results in rapid branching and cross-linking.[18] In this manner, the TEGDE monomer cross-links the polymer network into a single molecule by linking different chains together in a complex matrix.

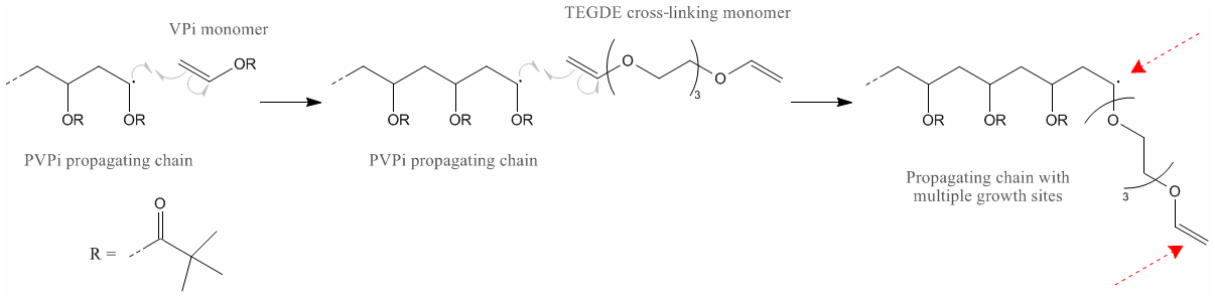

Scheme 4.2 **The proposed reaction of the free radical propagating PVPi chain with the TEGDE cross-linking monomer.**

In the present study, a series of VPi polymerisation reactions, with different cross-linking concentrations, was carried out to study the effect of the cross-linking concentration and degree of cross-linking on the sample morphology, particle size, etc. The experimental conditions and the concentrations used are described and listed in Chapter 3, Table 3.2. It was assumed that the reactivities of the cross-linker and VPi are similar. Accordingly, it was assumed that both the VPi and the cross-linking agent were depleted during polymerisation, and hence the degree of cross-linking can be represented as a percentage cross-linking agent to VPi monomer ratio (TEGDE:VPi).

4.2.4.1 DSC data and the determination of T_g values of cross-linked PVPi particles

DSC analysis was carried out on the PVPi samples with varying degrees of cross-linking. The DSC thermograms of the series of PVPi samples with the varying degrees of cross-linker concentration (TEGDE, as a percentage of the VPi monomer concentration) are shown in Figure 4.8. PVPi is non-crystalline, and no crystalline melting endotherm was observed in the DSC thermograms for any of the PVPi samples.

Table 4.4 tabulates the glass transition temperature (T_g) values of each cross-linked PVPi sample. Literature sources indicate that pure uncross-linked PVPi has a T_g value of 86 °C.[19,20]

The uncross-linked PVPi has a relatively low T_g of 80 °C, in comparison to the literature value of 86 °C. This is probably a result of the shorter chain length and more chain ends in the experimental sample, attributed to the high initiator concentration used in polymerisation. The PVPi samples were cross-linked with relatively low cross-linking concentrations of 0.6%, 1.6%, 3.2% and 4.8% ([TAGDE]/[VPi]). As cross-linking agent is added and the degree of cross-linking increases, there is a corresponding decrease in the T_g, from 80 °C to 71 °C.

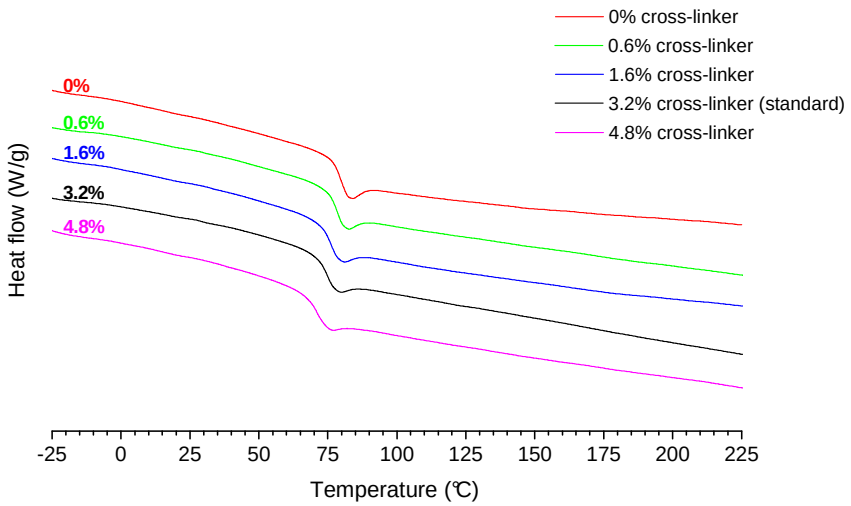

Figure 4.8 **DSC thermograms of PVPi prepared with various cross-linker concentrations (cross-linker concentration represented as a percentage [TEGDE]/[VPi]).**

Generally, with cross-linking and an increase in cross-linking concentration, there is an expected increase in the T_g values as cross-linking results in less flexibility within the polymer chains. This trend is not observed here, and instead an unusual decrease in the T_g values are observed with increasing cross-linking concentration. This is not entirely understood and cannot be explained. Possible contributions to this effect may be that an increase in cross-linking concentration, results in shorter PVPi block lengths, decreasing molecular weight (sequence length of the repeating VPi units) and thereby causing a decrease in the T_g. Additionally, the added ether linkages (three repeat ethylene glycol units) of the cross-linking agent may impart a certain amount of flexibility within the sample.

Table 4.4 **DSC data of the PVPi particles prepared using different cross-linker concentrations**

Sample code	% TEGDE (mol/mol) [a]	TEGDE/VPi (wt%)	T_g (°C) [b]
AC1[c]	0.0	0.0	80
AC2	0.6	1.0	78
AC3	1.6	2.5	76
AC4[*]	*3.2*	*5.0*	*75*
AC5	4.8	7.5	71

[a] Percent cross-linking agent (tri(ethylene glycol) divinyl ether) concentration (mol/mol VPi); [b] Glass transition temperature observed from DSC data; [c] uncross-linked PVPi fibres [*] average of 5 samples; *italics* relates to the standard PVPi sample

The T_g of the standard PVPi sample (with 5.0 wt% cross-linking agent, [TEGDE] = 0.032) is 75 °C, much lower than the literature values. The low T_g value was, nonetheless, considered useful for use as expandable/foaming particles (for possible future application). A plot of the degree of cross-linking versus T_g shows the decrease in T_g with increasing cross-linker concentration; see Appendix C.1.

4.2.4.2 Effect of cross-linking agent concentration on particle size distribution

The particle size distributions of the PVPi samples prepared using different TEGDE cross-linker (or comonomer) concentrations were determined by LDS, and are compared in Figure 4.9 below.

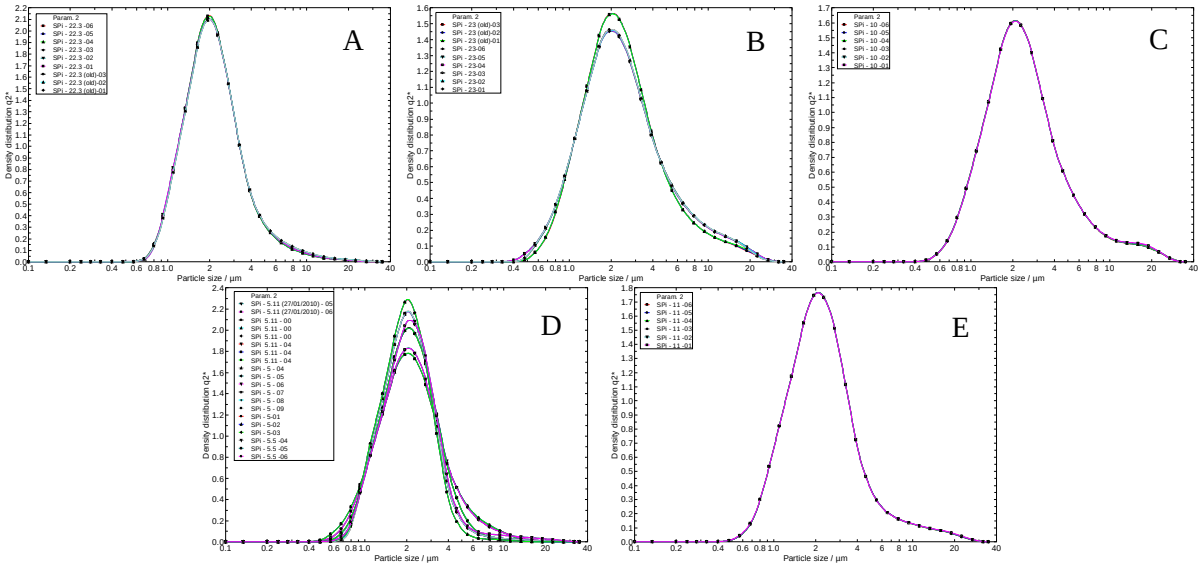

Figure 4.9 **Particle distribution curves of PVPi samples prepared using different TEGDE cross-linker concentrations: (A) *uncross-linked* (0%), (B) 1 wt% (6.3×10^{-3}/mol VPi), (C) 2.5 wt% (1.6×10^{-2}/mol VPi), (D) *standard 5 wt%* (3.2×10^{-2}/mol VPi), and (E) 7.5 wt% (4.8×10^{-2}/mol VPi).**

Under standard conditions, a very narrow distribution was obtained, similar to the case of 0% (zero) cross-linking agent (i.e. uncross-linked PVPi). The distributions of all samples were very similar. It was interesting to note the small shoulder that occurs if either more or less cross-linking agent is added (Figure 4.9 B, C and D). A comparison between the particle distributions of two uncross-linked samples is shown in Appendix D.1.

4.2.5 The effect of polymerisation conditions on particle size distributions

Many factors can influence particle size and distribution,[1,21,22] such as the dispersion phase viscosity, agitation speed, monomer/water ratio and suspension agent concentration. The effects of the polymerisation conditions on the particle size distribution curves (obtained with the HELOS laser diffraction spectrometer) of the PVPi particles are described in Section 4.2.5.1 – 4.2.5.4. The effects of PVPi polymerisation temperature and cross-linking concentration on particle size distribution have been discussed in Sections 4.2.3.2 and 4.2.4.2, respectively.

With regards to the synthesis using the different suspension polymerisation conditions, unless otherwise stated (i.e. for standard PVPi particles and uncross-linked PVPi), a single reaction of each condition was carried out. Hence, the distribution curves obtained are that of single run samples, except in the case of the standard and uncross-linked PVPi particles. Samples were prepared and sonicated as described in Section 3.7.5, and initial analysis established that with sufficient sonication, particles were adequately separated and portrayed a uniform distribution curve, see Appendix D.2. For each of the following discussions, the specified polymerisation condition was varied as listed in Table 3.2 (Chapter 3) and indicated here in the respective figures.

4.2.5.1 Effects of initiator concentration on particle size distribution

Various initator concentrations were used in the preparation of PVPi particles and the resulting particle distribution graphs are compared in Figure 4.10. The lower initiator concentrations yielded very poor distributions (Figure 4.10, A and B) and were put aside in terms of being used as standards. A good particle distribution was obtained for PVPi prepared using 50% less initiator (3.8×10^{-3}/mol monomer, Figure 4.10 C), but a 25–30% higher product yield was achieved for PVPi prepared using (what was chosen as) the standard initiator concentration (Figure 4.10 D). High PVPi product yields were also obtained when using a larger initiator concentration (Figure 4.10 E), however, the distribution showed a shoulder in the larger particle size range of the distribution graph. At the high initiation concentration (and hence faster propagation rate), the larger particles may have coalesced and become fixed in shape and they were not easily broken up again. In this case, it might have been better to use a slightly higher agitation speed.

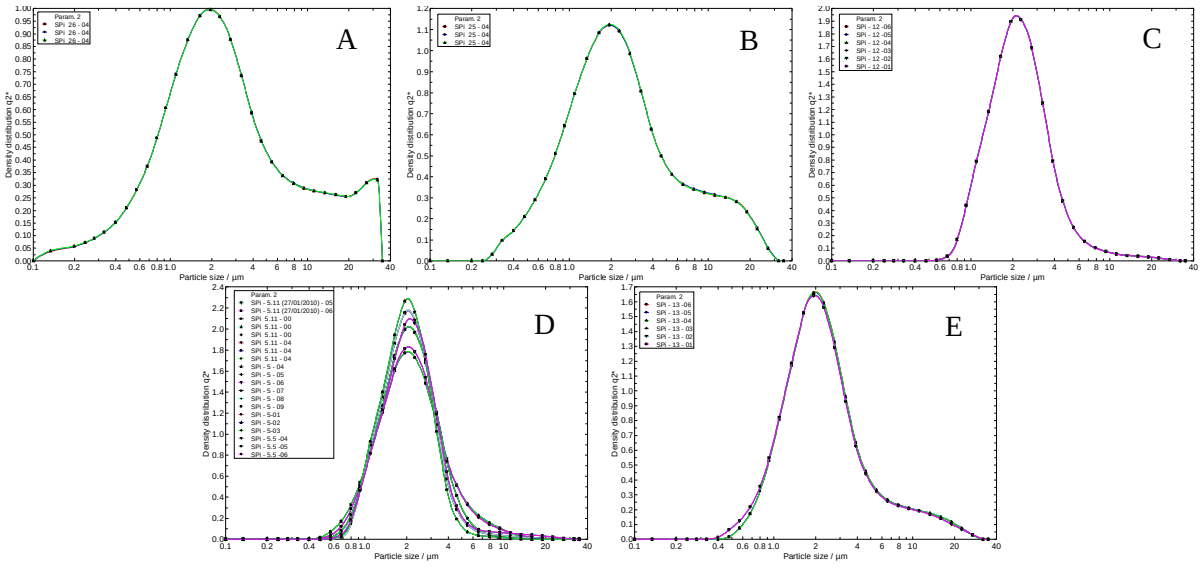

Figure 4.10 **Particle distribution curves of PVPi particles prepared using different initiator concentrations: (A) 3.8×10^{-4}, (B) 7.6×10^{-4}, (C) 3.8×10^{-3}, (D) *standard* 7.6×10^{-3} and (E) 1.13×10^{-2}, per mol monomer.**

The curves in Figure 4.10 show that PVPi particles prepared with the lower initiator concentrations (graph A and B) have a broader distribution than the standard particles (graph D). Sample C shows a good distribution, but has 25% less product yield, when compared to the standard (D), while the opposite is true for sample E, which has a poor particle distribution, but good yield (similar to that of the standard: about 77–80% yield). Nevertheless, the chosen standard initiator concentration (D) seemed to offer the best distribution and yield, and was therefore considered suitable for use in this study.

In this study, the concentrations used were chosen based on the assumption that the sonication of the PVPi samples adequately separated and decoagulated the particles. However, sonication may not have been adequate for complete separation, and therefore in some cases, stirring would assist in separating the particles efficiently. This was confirmed later in an additional investigation into why the lower initiator concentrations yielded insufficient broad particle distributions. The particle distributions of the samples prepared using lower initiator concentrations were re-tested. In addition to the normal sample preparation and extended sonication times, the samples were now also stirred prior to particle size analysis. Results are shown in Figure 4.11. This second stirring step resulted in successful re-dispersion of the particles and breaking up coagulates (previously thought to be whole colloids and larger particles, due to low reaction rates). The particle size distributions of these low initiator PVPi particles were very symmetric, but were however, still broader than the distribution of

the standard PVPi sample. Overall, the additional stirring step during sample preparation did improve the results. It is however not clear why more force is needed to separate the particles here.

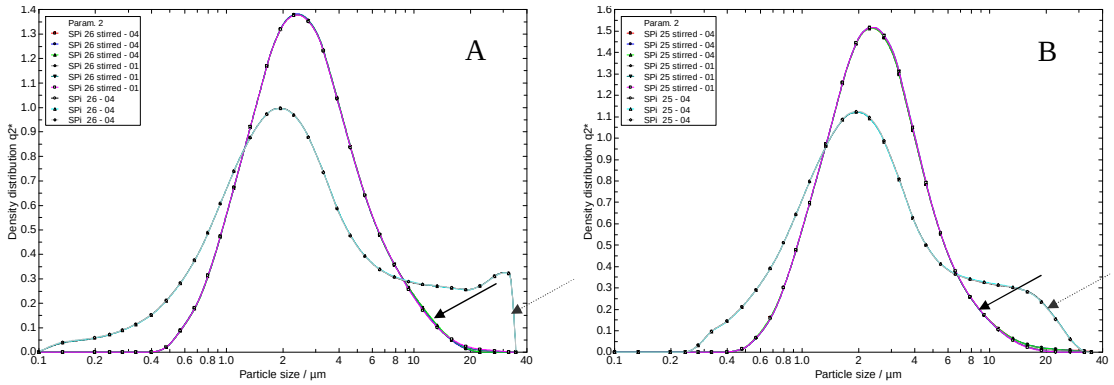

Figure 4.11 **Particle distribution curves of PVPi samples without and with additional stirring, prepared using initiator concentrations: (A) 3.8×10^{-4}/mol monomer and (B) 7.6×10^{-4}/mol monomer. The arrows indicate differences in the samples prior to magnetic stirring (dotted grey) and with additional stirring (solid black) in sample preparation.**

4.2.5.2 Effects of dispersant ($Ca_2O_7P_2$) concentration on particle size distribution

Figure 4.12 shows the distribution graphs of the PVPi particles prepared using different dispersant ($Ca_2O_7P_2$) concentrations. It is apparent that (theoretically) there is a critical value at which the dispersant concentration becomes too high and begins to interfere with the particle distribution. There were no significant differences in the distributions of the PVPi particles prepared with the lower dispersant concentration and the standard (Figure 4.12 A and B, respectively). When a higher dispersant concentration was used (C), there was a slight shift to a lower particle size, but there was also an increase in the broadness of the particle distribution and larger particles and agglomerates were formed (Figure 4.12 C).

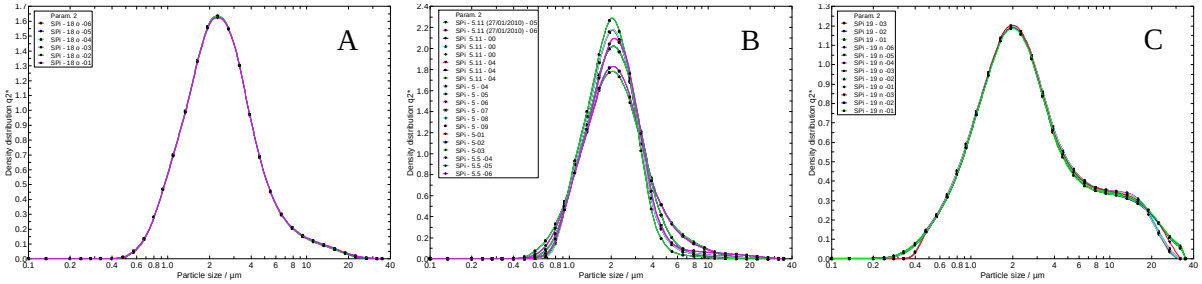

Figure 4.12 **Particle distribution curves of PVPi samples prepared using different dispersant ($Ca_2O_7P_2$) concentrations: (A) 0.10 g, (B) *standard* 0.25 g and (C) 0.40 g.**

The amount of dispersant used to prepare the standard PVPi sample is sufficient for the required application, but lower concentrations could also be considered. In an attempt to remove the shoulder seen in the PVPi sample prepared with a higher dispersant concentration (C), the sample was subjected to extended periods of sonication. This was however, to no avail as the shoulder was still present in the PVPi sample.

4.2.5.3 Effects of the stirring speed (rpm) on particle size distribution

Figure 4.13 shows the distribution graphs of the PVPi particles prepared using different stirring speeds. The narrowest particle distribution is achieved when using a stirring speed of 400 rpm (Figure 4.13 B). Besides a few slightly larger particles, there were no significant differences in the particle distribution of PVPi prepared using a slower stirring speed (A, 300 rpm), compared to the standard stirring speed (B, 400 rpm). Interestingly, the distribution curve of the PVPi particles prepared at a faster stirring speed (C, 500 rpm) showed a wider distribution and a shoulder in the larger size range, indicating particle coalescence.

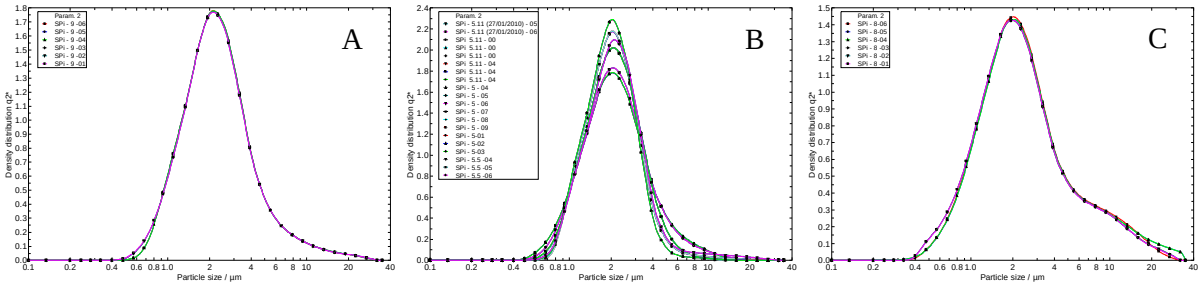

Figure 4.13 Particle distribution curves of PVPi prepared using different stirring speeds: (A) 300 rpm, (B) *standard* 400 rpm, and (C) 500 rpm.

4.2.5.4 Effects of the suspension agent concentration on particle size distribution

Figure 4.14 shows the distribution graphs of PVPi particles prepared using different suspension agent concentrations; Figure 4.14 B shows the distribution curves of PVPi prepared using the standard suspension agent concentration. When less suspension agent was used in the preparation of PVPi particles (A), the solution was less stable, and hence, particles coalesce together forming larger particles. It is unclear why the PVPi particles prepared using a higher suspension agent concentration (C) show a slightly wider base distribution on the larger particle size.

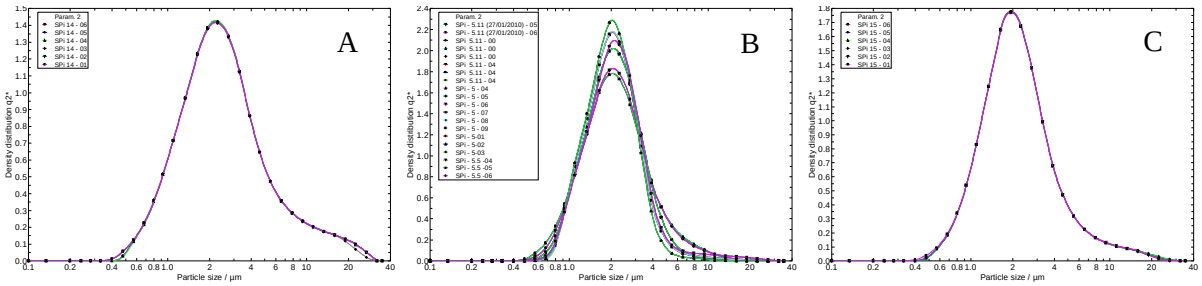

Figure 4.14 **Particle distribution curves of PVPi prepared using different suspension agent concentrations: (A) 1.3 g/dL water, (B) *standard* (2.6 g/dL water) and (C) 3.9 g/dL water.**

4.2.5.5 Effects of the non-ionic surfactant concentration on particle size distribution

Figure 4.15 shows the distribution graphs of PVPi particles prepared using different non-ionic surfactant concentrations. The PVPi sample prepared using less non-ionic surfactant (A) showed minor broadening in the base (and slight sharpening) of the distribution compared to PVPi prepared with the standard non-ionic surfactant concentration (B). A significant broadening in the distribution of the PVPi sample prepared with a higher non-ionic surfactant concentration (C) is clearly evident (compared to the distribution of PVPi prepared using the standard surfactant concentration (B)), even after extended sonication (green curve).

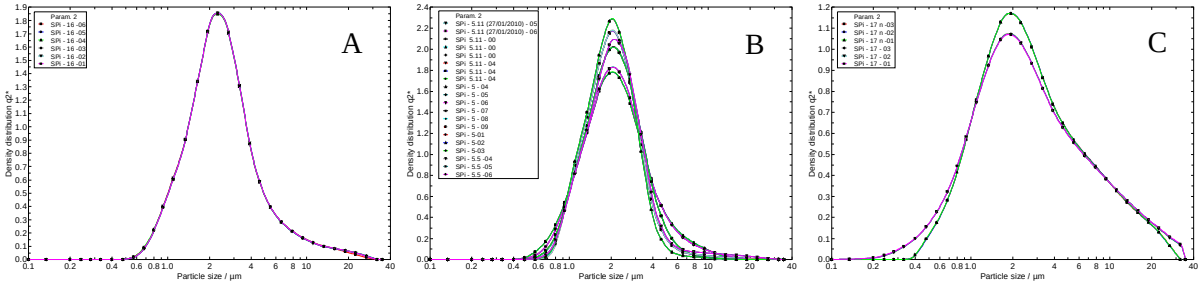

Figure 4.15 **Particle distribution curves of PVPi prepared using different non-ionic surfactant concentrations: (A) 0.25 g (0.66 g/dL water), (B) *standard* 0.50 g (1.33 g/dL water) and (C) 0.75 g (2.00 g/dL water).**

In the present study, the preparation of narrowly distributed PVPi particles via suspension polymerisation of VPi is dependent on the stirring speed, suspending agent concentration, and a mixture of three surface active agents (surfactants) to give an HLB of 13.5; all of which influence particle size. The surfactant is used to stabilise the particles once formed. It is unclear why the use of more surfactant causes a larger spread of particles.

4.2.6 Summary

The suspension polymerisation of VPi (with and without cross-linking) to afford PVPi was successfully carried out, as confirmed by SS ^{13}C NMR. The cross-linked and uncross-linked PVPi particles were characterised using SS ^{13}C NMR and FTIR analysis. SEM was used to observe the PVPi spherical particle morphology. The monomer conversions, determined for the different polymerisation reactions carried out at different temperatures, showed that the higher polymerisation temperatures (65 °C and 75 °C), were better than the lower polymerisation temperature (55 °C) in terms of obtaining higher conversions and a faster rate of polymerisation. This is because the system is thermally initiated, and at lower temperatures, fewer active initiating radicals are present, leading to a slower rate of monomer conversion. SEM analysis showed that the particles polymerised at higher temperatures (i.e. at 65 °C and 75 °C) and thus faster rate, had more stability in terms of maintaining their spherical form. However, an in-depth investigation into the temperature effects of particle stability is necessary, as the temperature variations/jumps used in this study were quite large.

The suspension polymerisations afforded relatively uniformly distributed spherical cross-linked PVPi particles, of about 1–5 μm, within the desired range of 0.5 μm to 10 μm in diameter. A PD for the standard PVPi particles was manually calculated to be 1.4. The standard cross-linked PVPi particles prepared at 65 °C (sample **A**) were considered suitable PVA precursors and used for the subsequent experimental procedures, i.e. surface saponification and modification.

Preparation of cross-linked particles via the free radical copolymerisation of the VPi and using the divinyl cross-linking agent proved to be successful in maintaining the particles' spherical morphology, in comparison to the uncross-linked samples. The cross-linking agent reduced the effective T_g of the PVPi, relative to its percentage concentration (TEGDE composition). This cannot be explained and it is not in agreement with the generally expected increase in T_g with increasing cross-linking concentration and decreasing flexibility.

With regards to particle size distributions, it is clear that each of the various polymerisation conditions have an effect on the particle dispersion (and hence, on liquid monomer droplets dispersion). The selected standard suspension polymerisation conditions of the standard PVPi sample were suitable for the preparation of samples with a reasonably narrow particle size distribution.

4.3 PVA preparation by PVPi saponification

The next step after the successful synthesis of the PVPi particles, was the surface saponification (or hydrolysis). This involved chemical modification of the polymer: the pendant ester group was saponified to a hydroxyl group. As previously mentioned, comprehensive studies on the saponification of poly(vinyl esters) have been reported by Lyoo et al.[2,23-26] and Lee et al.[3] They have reported on the suspension polymerisation of vinyl acetate (VAc) and VPi, and the subsequent particle saponification in THF, predominantly using a potassium hydroxide or sodium hydroxide solution as saponifying agent. To the author's knowledge, this saponification technique results in the modification of the particles both chemically and morphologically, affording syndiotactic PVA fibres. Most recently, Lee et al.[3] and Lyoo and Lee[25] have reported on a heterogeneous surface saponification technique used on VPi and VAc copolymer microspheres. This hydrolysis was conducted in an aqueous alkali solution of sodium hydroxide/sodium sulphate/alcohol with PVAc microspheres and poly(vinyl pivalate/vinyl acetate) (P(VPi/VAc)) copolymer microspheres.

The main objective of the present study was to prepare partially hydrolysed PVPi microspheres or PVPi-core PVA-shell particles, in order to preserve an almost 1:1 copy of the particle but change the surface characteristics. The cross-linked spherical PVPi particles (sample **A**), prepared by the standard polymerisation procedures (described in Section 4.2), were used for all saponification/hydrolysis procedures, unless otherwise stated. The experimental procedures were described in Chapter 3, Section 3.3.

4.3.1 Characterisation by FTIR and NMR

Two saponification methods were used for the surface hydrolysis of the PVPi particles. The two methods differ in terms of the solvent solution used. For Method A, the saponifying agent comprised KOH (or NaOH), methanol and water, with THF as solvent. In Method B, the saponifying agent comprised equal amounts of sodium hydroxide, sodium sulphate and methanol, but with water as solvent.

Method A (see Scheme 4.3) proved to be very successful, as confirmed by FTIR analysis of the product (see Figure 4.16). Method B, adapted from a technique used by Lee et al.[3] was, however, less successful. FTIR spectra of the product(s) of the reaction carried out using this saponification method showed no absorption band in the 3400–3200 cm^{-1} frequency range of O-H vibrations. The hydrolysis of PVPi was always difficult to achieve, until it was found successful using a THF based solvent solution.[27] It is important to note that in the literature reported saponification (using Method

B), a copolymer of VAc and VPi was used. It is assumed that saponification occurred more readily on the VAc units of the P(VPi/VAc) copolymer, and the VPi would be more difficult to hydrolyse. VAc was not used in this study, but the difficulty in hydrolysing PVPi was experienced in that no hydrolysis was achieved when using the aqueous based system (Method B). This is in agreement with the above statement that PVPi is essentially 'unhydrolysable' in any solvent other than THF. Additionally, as observed experimentally, the PVPi particles are very hydrophobic, limiting the polymer-solution contact area and hindering possible hydrolysis. Lyoo and Lee[25] also reported on the successful hydrolysis of PVAc homopolymer microspheres via this method. Yet, to the author's knowledge, there are no reports on the heterogeneous saponification (Method B) of PVPi homopolymer microspheres, strengthening the idea that PVPi can only be hydrolysed in THF or a similar swelling medium.

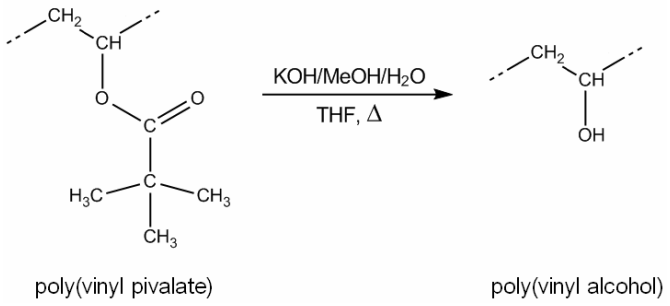

Scheme 4.3 Synthesis of PVA via PVPi saponification (Method A).

The saponification reactions of PVPi in THF, with KOH/MeOH/H_2O saponifying agent (described in Chapter 3, Section 3.3.2), were carried out for various time periods, from 2.5 min to 24 hr. The various samples with their respective saponification times, and their respective reference codes were tabulated in Table 3.3 (Section 3.3.4.2). Only a select few will be presented here, specifically those that had saponification times of 15 min (B_5), 30 min (B_7), 45 min (B_9) and 60 min (B_{10}).

Figure 4.16 shows the ATR-FTIR spectra of a few of the hydrolysed PVA/PVPi samples (i.e. unhydrolysed PVPi, 15 min, 30 min, 45 min and 60 min hydrolysed PVA/PVPi). The carbonyl peak (C=O, 1724 cm^{-1}) is present and the hydroxyl peak/band[3,5,11] (O-H, 3400–3200 cm^{-1}) is absent in the unhydrolysed PVPi sample. It is seen that as the saponification time increases, the O-H absorption band increases, while the C=O peak decreases. This confirmed that saponification occurred successfully, and also illustrated the progression of hydrolysis over time, from unhydrolysed to partially and then fully hydrolysed forms. Fully assigned FTIR spectra of fully hydrolysed PVA are reported in literature.[28]

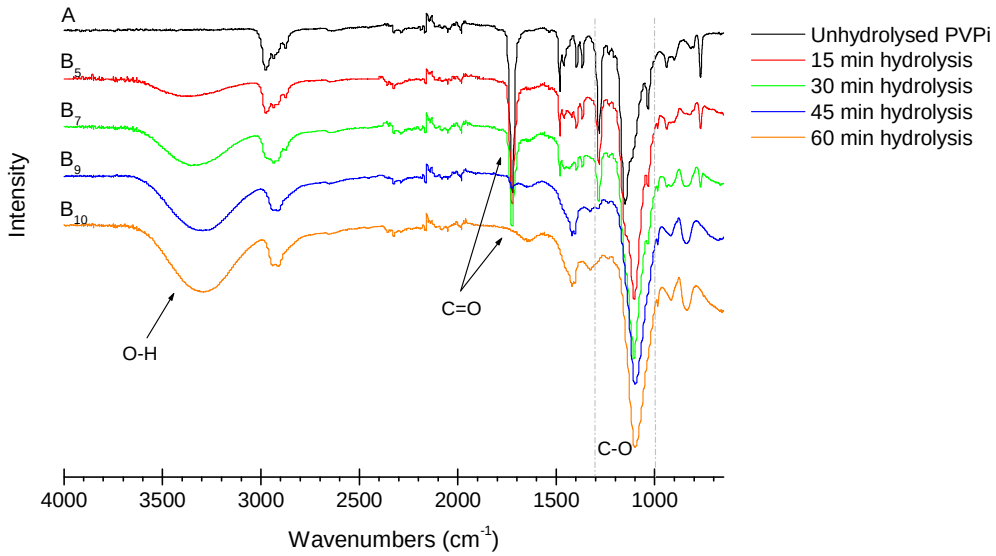

Figure 4.16 **ATR-FTIR spectra for the saponification series of the PVPi conversion to PVA, showing the unhydrolysed PVPi (black), and the 15 min, 30 min, 45 min and 60 min hydrolysed PVA/PVPi samples (red, green, blue and orange, respectively).**

The degree of saponification (DS) provides an indication of the extent of conversion from poly(vinyl ester) to PVA. It is clear that as the saponification reaction time increases, so too does the extent of hydrolysis, and hence the DS (as observed). By comparing the DS of the samples, the conversion from PVPi to partially and then fully hydrolysed PVA (see Figure 4.17) can be studied sequentially. After incomplete or partial hydrolysis (Figure 4.17 B), the resulting PVA/PVPi material will typically portray a mixture of the properties attributed to both the hydrolysed and the unhydrolysed polymers.

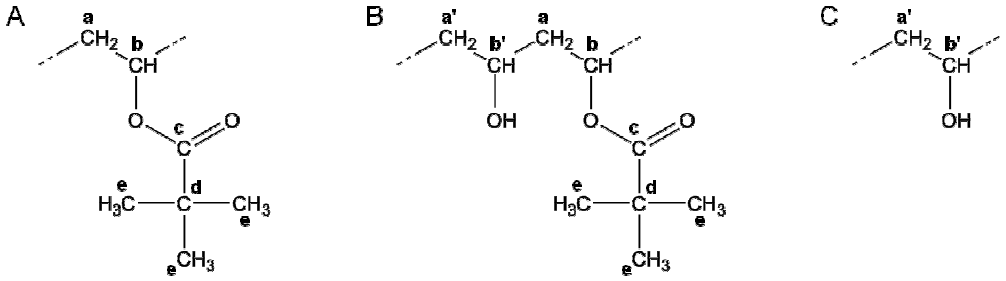

Figure 4.17 **Poly(vinyl pivalate) (A), and poly(vinyl alcohol): (B) partially hydrolysed and (C) fully hydrolysed.**

Determining the DS normally involves a very simple comparison of the PVPi methylene protons (a) before and after hydrolysis. However, ^{1}H NMR studies, both solution and solid state, have

proven to be impractical for the analysis of the cross-linked PVPi and PVA/PVPi samples. Since ^{1}H NMR was futile and only SS ^{13}C NMR analysis of the cross-linked samples was achieved, it was not possible to determine the DS by proton assignment and comparison. SS ^{13}C NMR was successfully used to observe the changes in the cross-linked PVPi and PVA/PVPi samples as the extent of hydrolysis (time) increases (see Figure 4.18). The relative DS was determined by comparing the changes in the carbon signal intensities of the respective PVA/PVPi samples. Thus, a relative DS comparison between PVPi and the consecutively hydrolysed PVA/PVPi samples could be made.

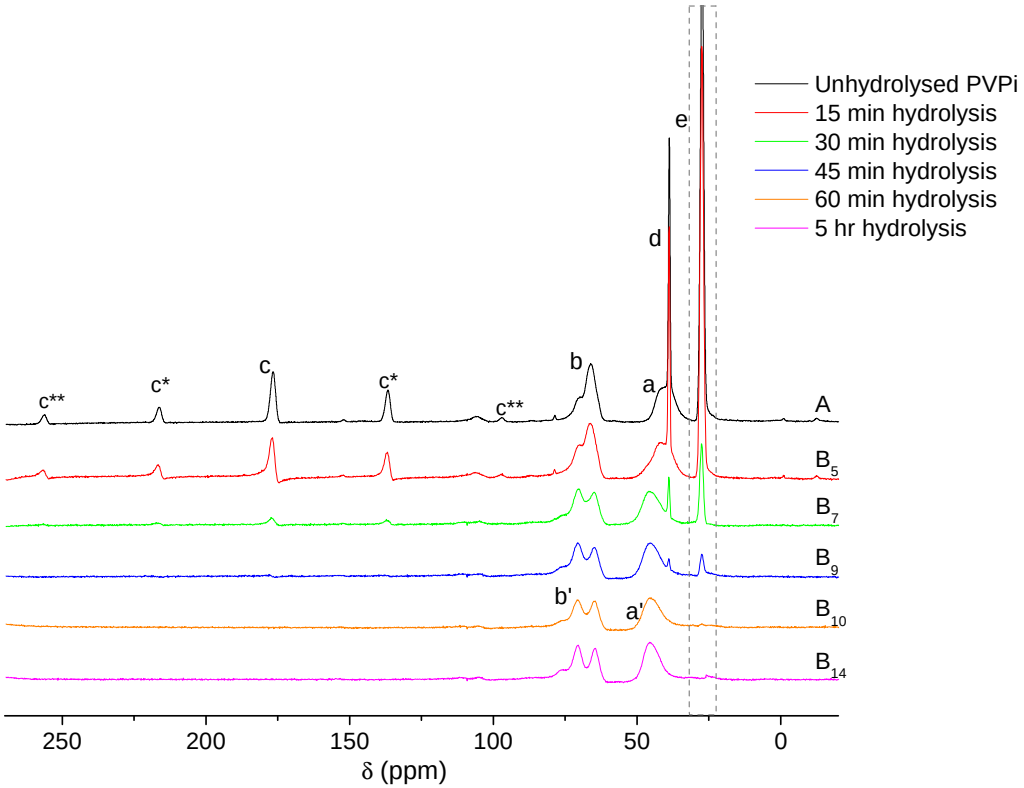

Figure 4.18 **SS ^{13}C NMR spectra of the unhydrolysed PVPi (black) and hydrolysed PVA/PVPi particles, obtained after hydrolysis times of 15, 30, 45 and 60 min (red, green, blue and orange, respectively), as well as after 5 hr hydrolysis (pink).**

Detailed ^{13}C NMR data pertaining to PVPi were reported in Section 4.2.1, in Figure 4.2 and Table 4.1. Figure 4.18 shows the SS ^{13}C NMR spectra of PVA/PVPi for the series of saponification times. The DS was determined from SS ^{13}C NMR analysis; it was based on a relative comparison of the pivaloyl groups' methyl carbon signals of the samples (labelled e in Figure 4.17 A, and seen at 27.5 ppm in Figure 4.18). Accordingly, clear progression in saponification from the unhydrolysed PVPi sample (intense peak at 27.5 ppm) to the fully hydrolysed PVA sample (no peak at 27.5 ppm), was noted. In the spectra of the samples where the signals of the methyl (e), carbonyl (c) and tertiary

(d) carbons of the pivaloyl group were absent, it was assumed that the samples had > 99% hydrolysis. Hence, after 60 min saponification time, the PVPi polymer had (within the accuracy of resolution) been entirely hydrolysed to PVA.

The DS (and degree of hydrolysis) could not be determined by ^{1}H NMR but it could be comparatively studied using SS ^{13}C NMR (see Figure 4.18). During saponification, the samples undergo progressive changes, and by the time hydrolysis has reached completion (fully hydrolysed sample), the original PVPi pivaloyl groups' carbons (i.e. methyl (e), carbonyl (c) and tertiary (d) carbons) will have disappeared and only the methylene (-**C**H$_2$) and methine (-**C**H) carbons remain (labelled a′ and b′ respectively, Figure 4.17 C). The resonance signals of the methylene carbons (a′) shift slightly downfield to ca. 45 ppm, while the methine carbon (b′) resonance signal splits into two peaks, at ca. 65 ppm and 70 ppm, and there is a shoulder peak at ca. 75 ppm. This is a result of the change in the chemical environment of these carbons, brought about by the new pendant hydroxyl group on the methine carbon (b′). Furthermore, the splitting seen in the methine carbon peak (b and b′) is attributed to the different stereoregular arrangements,[29,30] and corresponds to the characteristic triad configuration of syndiotactic PVA (where the three peaks are assigned mm, mr and rr, from low to high frequency, with a small mm and larger mr and rr intensities, indicative of syndiotacticity[29-31]). These changes are seen to progress from the PVPi to the fully hydrolysed PVA samples (60 min, B_{10} and 5 hr, B_{14}).

A relative indication of the DS can be obtained by comparing the peak intensities (or change therein) of the methyl pivaloyl carbons (three equivalent methyl carbons at 27.5 ppm) of the different samples. The methine carbon peak (b or b′) was used as a common reference between samples, as the number of methine carbons are not altered during saponification. The changes in the methyl peak (e) intensities of the PVA/PVPi samples of various saponification times were compared to with those of the unhydrolysed PVPi sample. The percentage hydrolysis is thus based on the difference in methyl intensity (e) of the hydrolysed PVA/PVPi sample relative to that of the unhydrolysed PVPi sample, using the methine (b or b′) carbons as a common reference intensity. Figure 4.19 shows the percentage hydrolysis, relative to the unhydrolysed sample, versus time relationship. A sigmoidal relationship (sigmoidal fit, red curve) was observed.

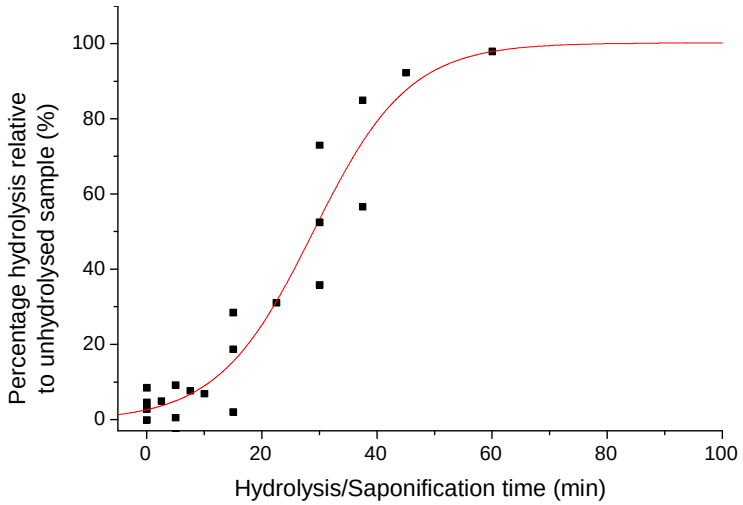

Figure 4.19 **Percentage saponification versus time plot of the various hydrolysed PVA/PVPi samples, showing the conversion from unhydrolysed PVPi to fully hydrolysed PVA; determined from changes in methyl peak intensities (e, 27.5 ppm), using the methine intensity (b or b′) as a reference carbon.**

The relative DS of each sample was determined by extrapolating the values off the sigmoidal fit of the percentage saponification versus time graph (Figure 4.19). It should be borne in mind that the SS ^{13}C NMR analysis technique is not entirely quantitative because no standard reference was included, but this technique nonetheless provided a good indication of the DS.

4.3.2 Thermal analysis

4.3.2.1 DSC of PVA/PVPi particles

DSC analysis provides information on crystallinity, crystalline melting temperature (T_m^*)[‡] and T_g. The DSC thermograms of the PVA/PVPi samples (B_5, B_7, B_9 and B_{10}) with different degrees of saponification are shown in Figure 4.20. (The asterisk indicates the number of analyses carried out for the respective samples and hence the number of curves obtained, which were then averaged into the single curve shown: ** two; *** three.) The averaged DSC results of samples are tabulated in Table 4.5. The percentage crystallinity of each sample was calculated as described in Chapter 3, Section 3.7.6.1.

[‡] Note: By definition, a cross-linked polymer cannot melt and thus it will not have a melting temperature. Syndiotactic PVA derived from PVPi is crystalline and will therefore exhibit crystalline melting. Cross-linking restricts crystallinity, but because in this study only a very low percentage of cross-linking was used (i.e. 3.2%), crystallinity is still possible between the cross-linking points. Therefore, the T_m^* here refers to the melting temperature (or endotherm peak temperature) of the crystalline segments between the cross-links. These crystalline segments undergo thermal transition (seen in the endo- and exo-therms in the DSC thermograms). Crystallinity of the sample is confirmed by XRD analysis, see Section 4.3.3.

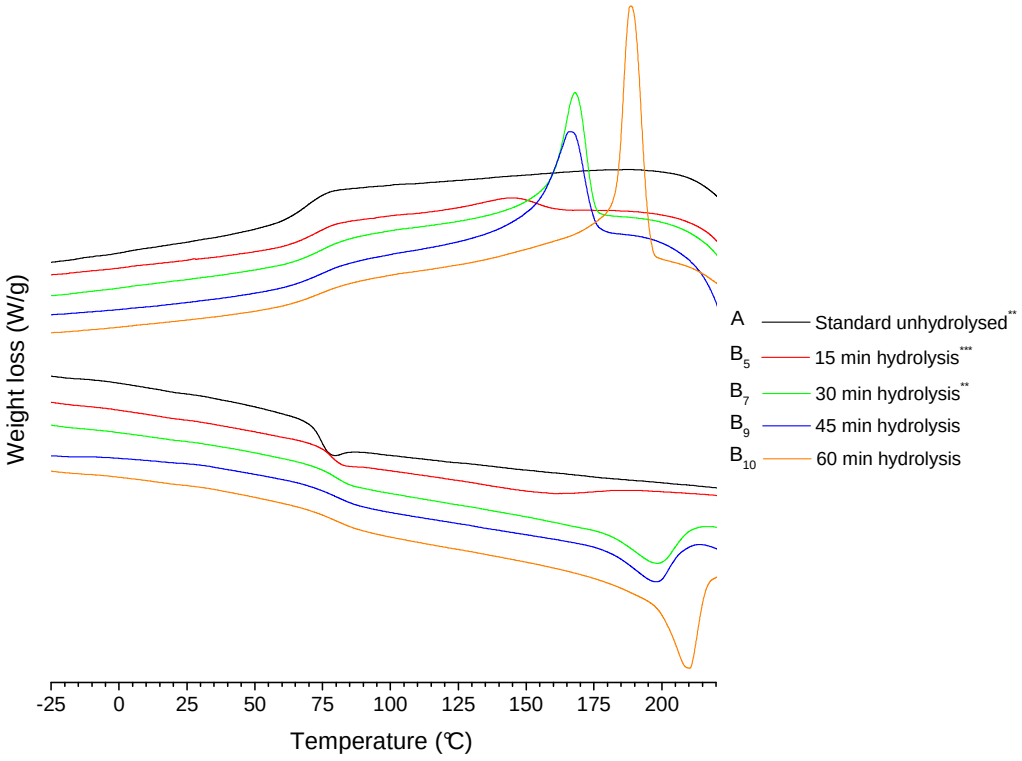

Figure 4.20 DSC thermograms of PVA/PVPi particles, for the saponification series comparison.

When the samples are compared, the differences brought about by the various degrees of saponification are very clear. The partially hydrolysed, 15 min PVA/PVPi sample (B_5, red curve) is different to that of the unhydrolysed standard PVPi sample (A, black curve). The 15 min (B_5) sample has a higher T_g than the PVPi standard (A) (Table 4.5) and a small broad crystalline melting peak, between about 120 °C and 165 °C. This indicates that only a few (consecutive) alcohol groups have replaced the pivaloyl groups, resulting in small crystalline segments.

The DSC thermograms (Figure 4.20) show the sequential changes that occur in the samples' thermal properties as the DS (or hydrolysis time) increases. It is clear that there are differences in the crystallinity, T_m^* and T_g of the samples. For example, the 60 min hydrolysed PVA/PVPi sample (orange curve, sample code B_{10} Table 4.5), with a high DS (≥ 98%), exhibits a sharp crystalline melting endotherm and the highest T_m^*. This indicates a more ordered and perfect crystal PVA lattice structure, compared to the 15 min, 30 min and 45 min hydrolysed samples (sample codes B_5, B_7 and B_9, respectively).

Table 4.5 DSC data of the PVA/PVPi particles with different degrees of saponification

Sample (Saponification time)	DS (%) [a]	T_m * [b] (°C)	Crystallinity [c] (%)	T_g [d] (°C)
A – Standard PVPi (unhydrolysed)	0	-	-	75
B_1 – PVA/PVPi (2.5 min)	4	Not detectable		75
B_5 – PVA/PVPi (15 min)	9	157	2	78
B_7 – PVA/PVPi (30 min)	53	198	5	80
B_9 – PVA/PVPi (45 min)	87	198	6	79
B_{10} – PVA/PVPi (60 min)	≥ 98	210	13	81
B_{14} – PVA/PVPi (5 hr)	> 99	198	9	77

[a] Degree of saponification (DS) estimated from percentage hydrolysis versus time graph (Figure 4.19); [b] Crystalline segment melting temperature observed from DSC data; [c] Crystallinity determined from the enthalpy of fusion of PVA crystals; [d] Glass transition temperature observed from DSC data

As the samples' DS increases, and as they approach the state of being fully hydrolysed PVA, a sequential increase in T_g values is observed. The T_g values increase, approaching the T_g of a fully amorphous (fully hydrolysed) PVA sample, at 85 °C.[19,20,32] One should bear in mind that the T_g is influenced by a variety of factors, including chain length, mobility and the tacticity of the sample. The T_g observed for the standard PVPi sample (A) is lower than the literature value of 86 °C,[19] (discussed previously in Section 4.2.4.1). Thus, the cross-linked hydrolysed PVA/PVPi samples derived from the cross-linked PVPi have lower T_g values compared to the literature T_g value.

The 5 hr hydrolysed sample (B_{14}, Table 4.5), fully hydrolysed and with a DS of ≥ 99%, shows a decrease in T_g when compared to the 60 min hydrolysed sample (B_{10}). This could be a result of polymer chain scission when subjected to the harsh hydrolysis conditions for extended time periods, resulting in shorter chain lengths and ultimately a lowering the T_g.

With regards to tacticity, Nagara et al.[33] found that syndiotactic PVA had a higher crystallisation temperature, T_m and T_g than that of amorphous PVA. The mm, mr and rr NMR configurations of atactic PVA and syndiotactic PVA are very similar, with a low mm, and high mr and rr peak intensities. However, syndiotactic PVA generally has a higher rr peak intensity than atactic PVA[29-31,33] (which is in some cases equivalent to its mm intensity[31]). These differences are, however, not easily seen in the SS NMR spectra of these samples (see Figure 4.18), and, because PVPi was used as precursor, it is expected that syndiotactic PVA[27] was prepared. Therefore a higher T_g than that of

amorphous PVA should have been obtained, confirming the above idea that there is a loss of cross-linking and a shortening of chains, resulting in the very low T_g observed (for B_{14}).

The T_g values of the various samples of both the unhydrolysed PVPi and hydrolysed PVA/PVPi samples, observed in DSC data, were compared. See Figure 4.21. The results were generally reproducible and the T_g values of repeat samples were within marginal error (0.4) of each other. As the DS increases (with increasing hydrolysis time) and as more pivalate groups are replaced by hydroxyl groups, there is a shift in the T_g from a lower T_g (T_g closer to the T_g of unhydrolysed PVPi) to a higher T_g (T_g closer to that of PVA, i.e. 85 °C[19,20,32]).

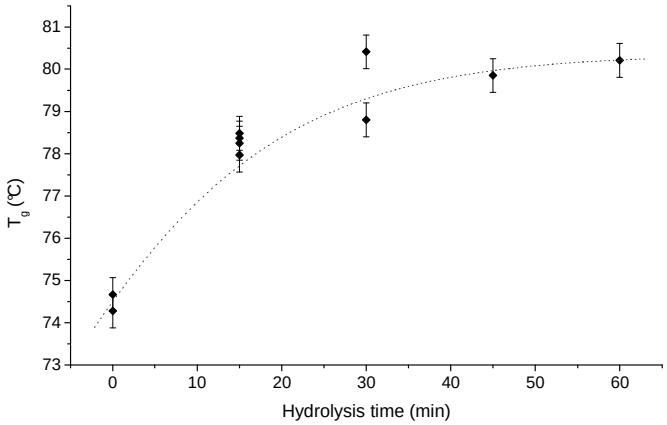

Figure 4.21 Comparison of the T_g values of cross-linked PVPi and hydrolysed PVA/PVPi samples prepared with different hydrolysis times.

4.3.2.2 TGA of PVA/PVPi particles

The thermal degradation behaviour of the standard PVPi and selected hydrolysed PVA/PVPi samples was studied using thermogravimetric analysis (TGA). Thermal decomposition of the PVPi standard (A) and partially and fully hydrolysed PVA/PVPi samples are shown in Figure 4.22, where multiple curves for repeat samples, indicated by the asterisk (*), have been averaged into the single curve shown. The thermal decomposition of PVA involves two steps of pyrolysis.[34,35] The first stage includes the dehydration and depolymerisation of PVA, commencing around 200 °C, while the second stage is that of pyrolysis via main chain scission or intramolecular cyclisation, commencing around 400 °C. The DS, molecular structure, method of polymer preparation and tacticity are all factors that influence the thermal degradation of PVA. Differential TGA (DTGA, see Appendix E) was performed, and the mass loss data, and the onset temperature of thermal decomposition (T_{onset}) of each sample (A, B_3, B_5, B_7, B_9, B_{10}, B_{12}, B_{14}) are tabulated in Table 4.6.

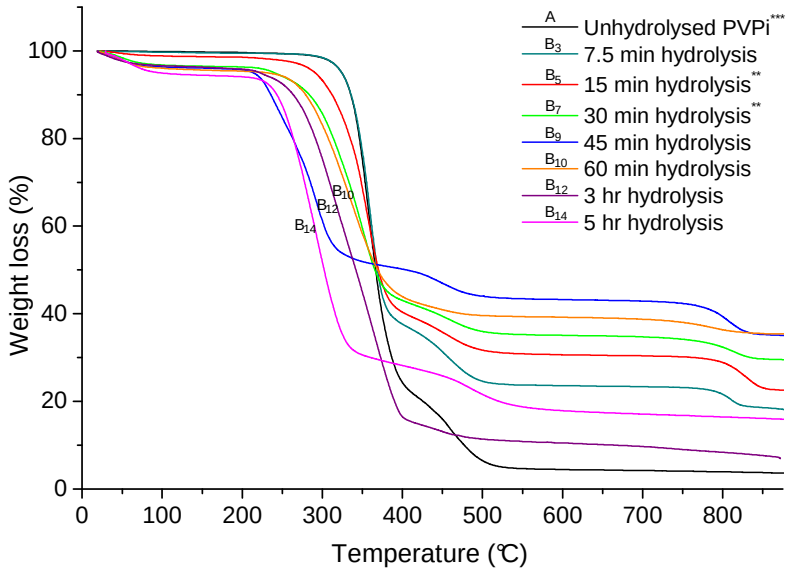

Figure 4.22 TGA thermograms of PVPi and the PVA/PVPi samples with different DS (hydrolysis times, as indicated), showing changes in thermal stability over the hydrolysis range.

The slight weight loss observed below 100 °C is attributed to water loss. For the standard cross-linked PVPi (A), thermal degradation also takes place via the two-step decomposition, with dehydration and main chain pyrolysis occurring at 354 °C and 459 °C, respectively. For the partially hydrolysed samples (B_3, B_5, B_7, B_9), dehydration occurs at 290–359 °C, while main chain pyrolysis occurs at 447–453 °C. In the fully hydrolysed (DS ≥ 98%) samples (B_{10}, B_{12}, B_{14}), the dehydration occurs at 295–364 °C, while main chain pyrolysis occurs at 439–486 °C. With an increase in DS, there is a progressive decrease in thermal stability of the samples. Although fully hydrolysed, the samples B_{10}, B_{12} and B_{14} show a progressively lower dehydration temperature with the length of the reaction (saponification) time. This is interesting, in that, as all three samples are fully hydrolysed, there must be some form of chemical damage with extended reaction times, as is seen in the loss of spherical shape (see Section 4.3.4.1).

Ohgi et al.[30] established that for atactic PVA, thermal decomposition occurs at 220–275 °C and 300–350 °C for the first and second weight loss steps, respectively. It has been reported that syndiotactic PVA has improved thermal stability over the atactic PVA,[30,36] which is attributed to the larger degree of crystallinity (higher chain compactness) as a result of a higher degree of stereoregularity and stronger intermolecular hydrogen bonds. Lyoo and Ha[36] also suggest that, for syndiotactic rich PVPi, there is an improvement in thermal decomposition temperature with increasing DS.[36] This is however, not in accordance with the results obtained here, where with longer

saponification times (and hence increased DS), a reduction in T_{onset} is observed. This could possibly be attributed to chain scission with longer saponification times.

Table 4.6 TGA data of the hydrolysed PVA/PVPi particles with varying degrees of saponification

Sample (Saponification time)	DS (%) [a]	T_{onset} (°C) [b]	DTGA peak (°C) [c]	Weight loss (%) [d]	Residue at 870 °C (%) [e]
A – Standard PVPi (unhydrolysed)	0	332	354	73.4	3.7
			459	21.4	
B_3 – PVA/PVPi (7.5 min)	7	334	358	59.0	18.3
			453	16.3	
			809	4.3	
B_5 – PVA/PVPi (15 min)	9	318	44	1.0	22.6
			359	56.0	
			448	11.3	
			834	7.3	
B_7 – PVA/PVPi (30 min)	53	290	41	3.5	29.6
			352	51.4	
			451	9.3	
			808	4.7	
B_9 – PVA/PVPi (45 min)	87	242	45	3.6	35.1
			290	42.5	
			447	9.4	
			814	7.3	
B_{10} – PVA/PVPi (60 min)	98	280	48	3.9	35.4
			340	50.4	
			439	4.9	
			793	3.3	
B_{12} – PVA/PVPi (3 hr)	>99	269	30	3.0	7.2
			364	79.1	
			439	4.7	
B_{14} – PVA/PVPi (5 hr)	>99	248	56	5.1	16.0
			295	62.3	
			486	13.3	

[a] Degree of saponification (DS) estimated from percentage hydrolysis versus time graph (Figure 4.19); [b] Onset temperature of thermal decomposition; [c] Differential mass loss peak maxima (as seen in Appendix E.1); [d] Weight loss at DTGA peak max; [e] Carbon residue at 870 °C

The presence of catalyst residue by-products of the hydrolysis reactions, such as alkali hydroxides or alkali acetate (for PVAc), are known to decrease the thermal stability of PVA.[34] These contaminates can be removed by washing or by converting them into more inert compounds. In this study, three washings with MeOH, and only a small amount of H_2O were carried out, which could have an effect on the TGA char results. A late check for potassium using SEM-EDX (Energy-

Dispersive X-ray analysis conducted by means of SEM) to determine chemical composition showed a small but definite amount of potassium (K) residue in one of the 15 min hydrolysed samples. This indicates that the MeOH wash used without an adequate H_2O wash, was not sufficiently effective in removing all contaminants. The thermal stability of the samples, in the 250–450 °C range, may thus be influenced, depending on the presence and amount of catalyst by-products.

The unhydrolysed PVPi (A) has a very high thermal stability, with a T_{onset} of 332 °C, and hardly any residue remaining at 870 °C. The partially hydrolysed 15 min sample (B_5, DS 9%) possesses crystallinity, and showed a decrease in the T_{onset} and more remaining residues when compared to PVPi (A). This progression continues with the increasing DS in the 30 min and 45 min samples (B_7 and B_9, respectively), until the fully hydrolysed samples, where there are decreases in the residual content (B_{12}, B_{14}), and increases in the T_{onset} (B_{10}, B_{12}) compared to the 45 min sample (B_9). It is unclear why the amount of residues increase with increasing DS, or why B_{12} and B_{14} show less residues. This is difficult to explain, as we know from the loss of pivaloyl carbons (from the NMR data, Figure 4.18) that the 60 min sample is fully hydrolysed with a high DS ≥ 98%. This is confirmed by the absence of pivaloyl carbons in the 5 hr fully hydrolysed sample (DS > 99%).

The changes in thermal stability could be attributed to loss of cross-linking in the fully hydrolysed samples (B_{10}, B_{12}, B_{14}) compared to the partially hydrolysed samples. Loss of cross-linking corresponds to the discussion of T_g changes in Section 4.3.2.1, but also gives a possible explanation as to the flattening of particle morphology with extended saponification times, seen in the SEM images of the 60 min, 5 hr and 24 hr hydrolysed samples (discussed in Section 4.3.4.1 later). This could be an interesting study for the future, in that the TGA behaviour is anomalous in the three fully hydrolysed samples (B_{10}, B_{12}, B_{14}) in terms of T_{onset} and remaining residues. This is strange as once hydrolysis has reached completion, the hydrolysis or DS cannot change. NMR results indicate that by 60 min hydrolysis a DS of 98% is obtained. Therefore, there should not be any difference in the DS of the 3 hr (B_{12}) and 5 hr samples (B_{14}), and it is thus proposed that extended exposure to the harsh saponification conditions could influence the chain length by chain scission or loss of cross-linking, supported by the observed loss of shape of the particles. In addition, the catalyst residues that are not fully removed play a major role in the degradation.

4.3.3 Crystallinity of PVA/PVPi

The PVPi precursor will always yield syndiotactic PVA upon hydrolysis, as a result of the very specific nature of the pivalate pendant groups. Due to the bulky pivaloyl pendant groups, the PVPi polymer chains are able to undergo ordered packing and thus crystallisation. Hence, the crystallinity

of the hydrolysed samples and the unhydrolysed PVPi sample (A) were investigated by means of X-ray diffraction (XRD). Figure 4.23 shows the XRD patterns resulting from crystal scattering, indicating some form of structured orientation. Narrow peaks indicate a more ordered packing and hence a sample with high crystallinity. Very sharp crystalline reflections are observed in the XRD profiles of the hydrolysed PVA/PVPi particles (B_1, B_3, B_5, B_7, B_{10}), with strong maxima at approximately $2\theta = 31°$. The diffraction patterns show a characteristic PVA peak (crystalline reflection[37]) at $2\theta = 21°$, close to the reported values for PVA resin,[38] films,[39] hydrogels[37] and membranes[40] ($2\theta = 18–21°$).

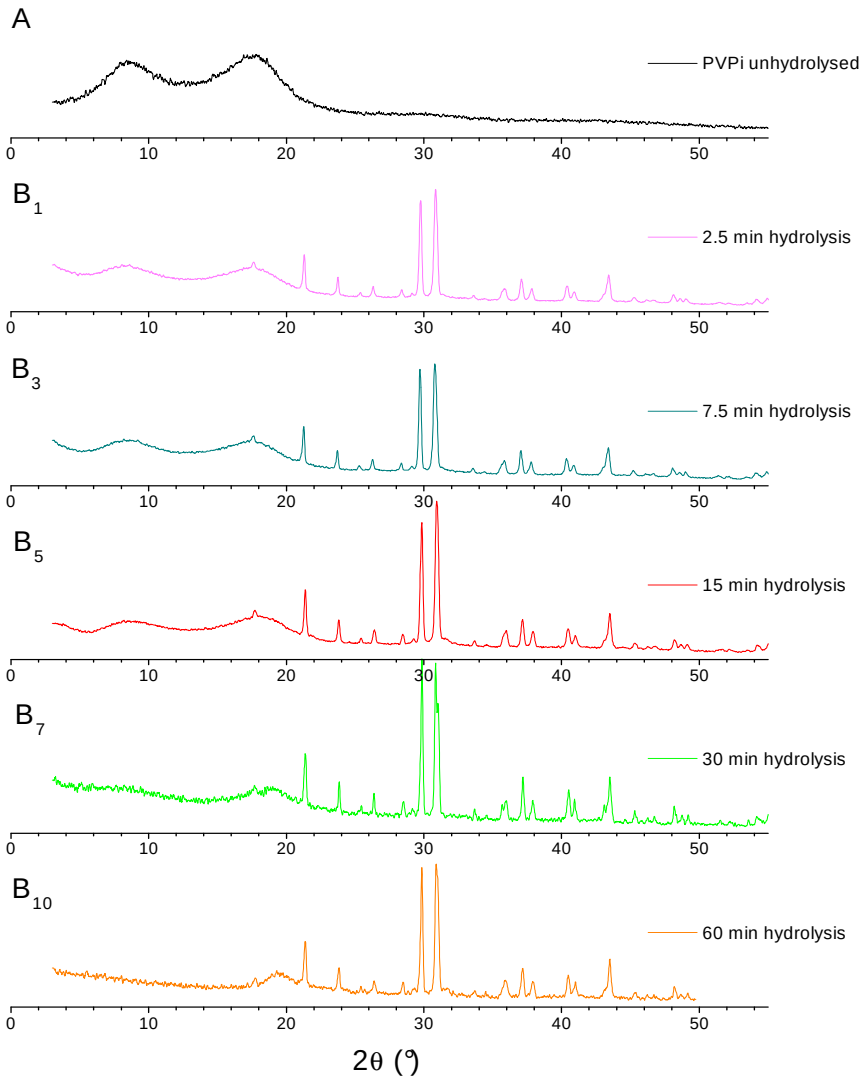

Figure 4.23 **X-ray powder diffraction profiles (diffractograms) of the unhydrolysed PVPi (A), partially hydrolysed PVA/PVPi (B_1, B_3, B_5, B_7) and fully hydrolysed PVA (B_{10}).**

With regards to the XRD peak signals, it is known that the sharper or narrower the peaks are the more highly syndiotactic the sample is.[41] This corresponds to the syndiotactic PVA hydroxyl groups formed during PVPi saponification, and DS thereof. This also confirms the syndiotactic triad assignment of the methine carbon in the SS ^{13}C NMR spectra of the fully hydrolysed PVA samples (Figure 4.18). Moreover, very broad peaks (or an "amorphous halo") is seen for the unhydrolysed sample (A) indicates that there may be some form or degree of crystallity, but that ordered packing is greatly hindered.[42] Thus, the PVPi polymer chains tend towards ordered packing, but bulky pivalate pendant groups, no doubt, obstruct and limit ordering of polymer chains.

The degree of crystallinity can be affected by the thermal history of the material, and a higher temperature and extended periods of heat treatment can cause a higher degree of crystallinity.[27,34] However, to avoid discrepancies in crystallinity between the different samples with different DS, all samples were subjected to the same thermal history and sample preparation processes. As seen in the diffraction patterns of the 2.5 min (B_1) and 7.5 min (B_3) hydrolysed samples (Figure 4.23), very sharp peaks are observed, similar to the peaks in the other partially (B_5, B_7) and fully (B_{10}) hydrolysed samples. It appears that crystallinity takes place immediately at the surface, even after, for instance a 2.5 min hydrolysis, yet no crystalline melting peak is observed in DSC analysis (Table 4.5 B_1), as crystalline segments are presumably too small for detection. This does however indicate that the saponification reaction is specific to the surface layers, and proceeds immediately from the outer layers of the particle towards the inner core. Even at 9% hydrolysis (B_5, 15 min hydrolysis) or less, the sharp peaks indicate that the hydrolysis product (hydrolysed portion) is ultra-crystalline, suggesting that the hydrolysis occurs from the outer shell inwards. An intermediate PVA–PVPi interface layer must be present, but it (the PVA–PVPi interface) shows little crystallinity, and it could be associated with the observed reduction in T_m^* (DSC data) for the 15 min sample, as well as for the 30 and 45 min samples, when compared to the 60 min hydrolysed sample.

A comparison between the XRD patterns of repeat samples of B_5 (15 min hydrolysis PVA/PVPi sample) was made (Appendix F). The two XRD patterns illustrated that the results are reproducible.

4.3.4 Imaging and charge measurements

4.3.4.1 SEM

As previously described, saponification via method B, using water as solvent and NaOH solution as saponifying agent, proved to be unfruitful. The SS ^{13}C NMR and FTIR results prove that method A (in THF) was successfully carried out on the cross-linked PVPi microspheres. However, in the case of

the uncross-linked PVPi microspheres, this hydrolysis technique destroys the original PVPi morphology and produces syndiotactic PVA fibrils instead. This has been reported in literature[23,43-45] for PVPi and P(VPi/VAc) copolymers, but was also observed experimentally with the hydrolysis of the uncross-linked PVPi homopolymer (Appendix G.1). This is a more robust hydrolysis method as THF is used, which in all likelihood, is the reason the particles lose their structure. Lyoo and Ha[43] propose a formulation mechanism for the syndiotactic PVA fibrils, produced via method A. PVPi undergoes saponification in THF, using an alkali saponifying agent containing water (i.e. base/alcohol/water). The new PVA hydroxyl groups interact with the water, forming an oriented gel structure. The microfibrillar structure is said to form with the collapse of the water-hydroxyl interbridges and consequential PVA chain packing between molecules.[43]

Unique results were obtained with regards to the cross-linked sample; the particles maintained their spherical nature after saponification. SEM imaging shows that the cross-linked particles preserved their spherical morphology and remained intact, whilst still having undergone saponification, whether partially or fully. Examples of 15 min and 30 min saponified PVA/PVPi samples (i.e. partially hydrolysed) are shown in Figure 4.24 (A and B, respectively). It is therefore clear that the cross-linked samples were stable in comparison to the uncross-linked sample. The PVA particles (especially the higher saponification time (DS > 99%) particles), were seen to show morphological disturbances, when prepared in water. In the higher DS PVA, the particles somewhat morph into each other, showing loss of structure with longer reaction times (See Appendix G.2).

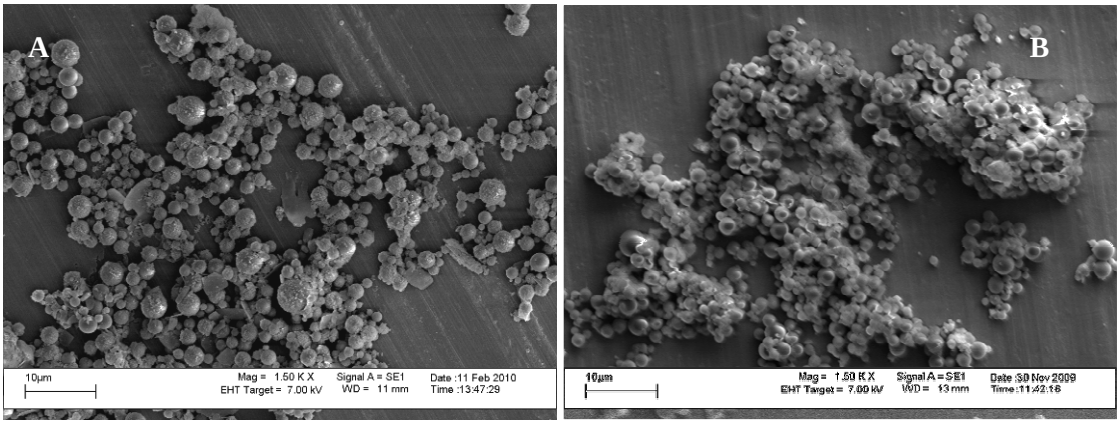

Figure 4.24 SEM images of hydrolysed PVA/PVPi samples exposed to (A) 15 min and (B) 30 min saponification times, ×1500. (Particles have maintained their spherical morphology.)

The specific cross-linking agent used in this study, i.e. TEGDE, is a divinyl ether and is thus supposedly not susceptible to saponification. Ethers are inert and unreactive to many organic reagents and are generally only cleaved by strong acids.[46] Saponification involves the reaction of an ester with

an aqueous base (or acid), ultimately yielding a carboxylic acid and alcohol.[46] Neither of these functional groups are present in the TEGDE cross-linker, thus the cross-linked bonds ought not be severed or affected during saponification. The particles consequently retain the spherical morphology, making TEGDE an ideal cross-linking agent for such applications. However, for reasons not yet clear, at extended saponification times of 3 hr, 5 hr and 24 hr (B_{12}, B_{14} and B_{15}) the spherical structure is somewhat lost, potentially due to very strong hydrogen bonding interaction or chain scission, see Appendix G.2.

4.3.4.2 Zeta potential

Zeta potential measurements were carried out on the 15 min, 30 min and 5 hr hydrolysed PVA/PVPi samples, as well as the original unhydrolysed PVPi particles (samples prepared as described in Section 3.7.9). Results are tabulated in Table 4.7. The unhydrolysed PVPi sample has a very strong negative value of (-) 34 mV. It was observed that the zeta potential values increased with increasing saponification times.

Table 4.7 Comparison of zeta potential results of PVA/PVPi prepared using different saponification times

Sample (saponification time)		Zeta potential (mV)
A	PVPi	-34.0
B_5	PVA/PVPi (15 min)	-30.0
B_7	PVA/PVPi (30 min)	-21.5
B_{14}	PVA/PVPi (5 hr) [a]	-14.4

[a] Fully hydrolysed with DS ≥ 99%

The reasons for the charge and change in charge measurements are not entirely understood.

4.3.4.3 TEM

Transmission electron microscopy (TEM) is a useful imaging technique which allows for high magnification and resolution of sample morphology. TEM imaging of the various samples was carried out to detect differences in morphology and PVA/PVPi layers. The samples were stained and prepared for TEM imaging as described in Section 3.7.8. SEM images of three samples, standard PVPi, and partially and fully hydrolysed PVA/PVPi, are shown in Figure 4.25. No distinct PVA/PVPi layers can be distinguished between the different samples.

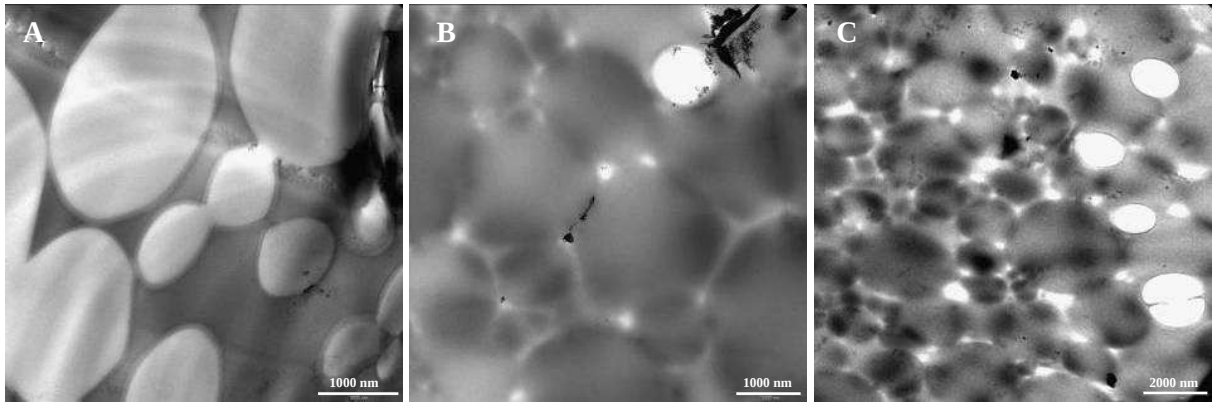

Figure 4.25 TEM images of iodine stained particles: (A) unhydrolysed PVPi, (B) partially hydrolysed 30 min PVA/PVPi, and (C) fully hydrolysed 60 min PVA/PVPi.

Fully hydrolysed PVA forms a complex with iodine which exhibits a characteristic blue colour, similar to that formed by a starch-iodine complex.[34] Iodine staining is a useful technique, used in many areas, particularly with starches, and provides information in terms of colour, intensity ('blue value') and wave length of peak light absorption,[47] characterisation[48] or even distinguishing between phenotypes and genotypes in grain and pollen.[49] Iodine staining may be used in titration and calorimetric methods for PVA characterisation. In terms of the PVA-iodine complex, the colour intensity is affected by factors such as the extent of branching, molecular weight, 1,2-glycol content, reagent composition, stereoregularity and degree of hydrolysis.[34] For example, a weaker colour is obtained with lower molecular weight. Iodine and partially hydrolysed PVA forms a red complex, which is influenced by the sequence distribution of the residual acetate groups, where the intensity of the colour increases with increasing "*blockiness*"[34] (sequence length). In other words, the differences in sequence length are visibly observed as colour changes. Hence, the colour intensity increases with an increase in the PVA sequence length, as the DS increases and as the crystallising segments grow larger.

In the present experimental study, the iodine stained PVPi and hydrolysed PVA/PVPi particles became darker with increasing hydrolysis time; as seen in Figure 4.26. Thus, the increase colour intensity indicates an increase in PVA sequence length, which agrees with the crystallinity differences in DSC. This confirms the idea that, while DSC data show little or no crystallinity, XRD results verifies crystallinity for these short segments. XRD observes crystallinity in even small sequences, as seen in the yellow to redish-brown colour of the samples. Results of these colour tests are very important as they show the increasing PVA sequences from the shortest saponification time (i.e. 2.5 min, B_1) to the longest (60 min, B_{10}), whereas DSC only sees observable changes in crystallinity (melting endotherm) from about 15 min saponification time (B_5, DS 9%).

Figure 4.26 **Iodine stained samples showing the change in colour with increasing hydrolysis times (and hence DS): (A) unhydrolysed PVPi, (B_1–B_9) partially hydrolysed PVA/PVPi of 2.5 min, 5 min, 7.5 min, 10 min, 15 min, 22.5 min, 30 min, 37.5 min and 45 min, respectively, and (B_{10}) 60 min fully hydrolysed PVA/PVPi.**

Figure 4.26 shows a series of samples after iodine staining, and the progression from unhydrolysed PVPi (A) to partially hydrolysed (B_1–B_9), and then to fully hydrolysed (B_{10}). The intensity of the blue colour of the iodine-PVA complex increases as the degree of hydrolysis increases. There is no complex formation with unhydrolysed PVPi and no colour was observed (A). In the case of the partially hydrolysed samples a reddish/brown colour complex is obtained (B_1–B_5). The colour of the iodine complex is sensitive towards the residual pivaloyl groups. The colour of samples B_8 (37.5 min) and B_9 (45 min) appear to be less vivid than the colours observed for the other samples. However, the intensities were strong and vibrantly blue, in sequence with the increasing hydrolysis en route to the intensely blue fully hydrolysed PVA/PVPi (B_{10}).

4.3.5 Summary

The PVPi particles were successfully hydrolysed to various degrees in THF using an alkali saponification agent, i.e. KOH/MeOH/H_2O solution. Determining the DS proved to be difficult due to the limited analysis of cross-linked particles. The uncross-linked PVPi sample lost all its spherical morphology during the saponification process (Appendix G.1). The cross-linked PVPi particles generally maintained their spherical shape during saponification. This specific technique of preparing spherical PVA particles by saponification of cross-linked PVPi particles has, to the best of author's knowledge, not yet been reported in an academic publication but has been claimed in a recent patent.[17]

Thus, cross-linking during VPi polymerisation and subsequent PVPi saponification is a relatively new and innovative technique for the synthesis of spherical syndiotactic PVA microspheres.

Determining whether the particles are surface hydrolysed or hydrolysed throughout, proved to be slightly more challenging than originally anticipated. It is likely that the particles are exponentially hydrolysed from the outside inwardly, as the method of hydrolysis (using THF as solvent), allowed for the sample to be hydrolysed throughout, instead of only on the surface. This is because the THF caused the particles to swell, allowing the core to come in contact with the hydrolysing agent. Had the alternative heterogeneous saponification method (method B) been successful, the particles would have been hydrolysed only on the surface, as reported by Lee et al.[3] This approach, in the present study, proved less successful, because the PVPi particles are extremely hydrophobic and therefore very difficult to dissolve or suspend in the aqueous solution, hence restricting saponification. Nevertheless, partial and full hydrolysis was achieved, as confirmed by SS ^{13}C NMR, FTIR.

It was decided that the 15 min saponification time provided a sufficient DS, to provide the proposed core-shell particle and these samples were therefore used for further experimentation. PVA/PVPi is the abbreviation created and used for these partially hydrolysed PVPi particles and, unless otherwise indicated, will always represent a 15 min hydrolysed PVPi sample (also indicated as sample **B** or $\mathbf{B_5}$). Since the hydrolysis is only partial, yet the crystallinity of the PVA is well developed, surface-biased hydrolysis is feasible. There will be an intermediate layer as well, but the thickness of this is difficult to measure. The XRD results suggests that it is very thin; the crystals form almost immediately on hydrolysis, as seen in the immediate sharp peaks of the 2.5 min and other partially hydrolysed samples. There are no real intermediate stages where the peaks grow narrower or shift, indicating that there is a very thin intermediate PVA/PVPi layer.

Whereas the recent patent claimed a cross-linked porous PVA particle, the core-shell particles obtained in the study are different, and therefore new.

4.4 Surface modification of PVA particles by cationic and anionic functionalisation

Ionic modification is a well known and extensively used process, both for cationic[50-52] and anionic[53-56] functionalisation. Ionic modification of starch has been used in the paper industry to enhance flocculation properties and the interaction of the starch molecules with the cellulose fibres.[50] It is generally known in the trade that cationic starch has a higher affinity towards negatively charged cellulose fibres than anionic starch.

In this study, ionic modification was carried out in order to investigate the interaction of the particles with the cellulose fibres (the spherical cross-linked particles will have limited deformation, and therefore limited contact for interaction with the cellulose fibres). Cationic (cationisation) and anionic (carboxymethylation) modification reactions were separately carried out on the PVA/PVPi (15 min hydrolysis, sample **B_5**). A general illustration of the predicted surface ionisation is given in Scheme 4.4. The cationic and anionic modification reactions were carried out as described in Section 3.4.

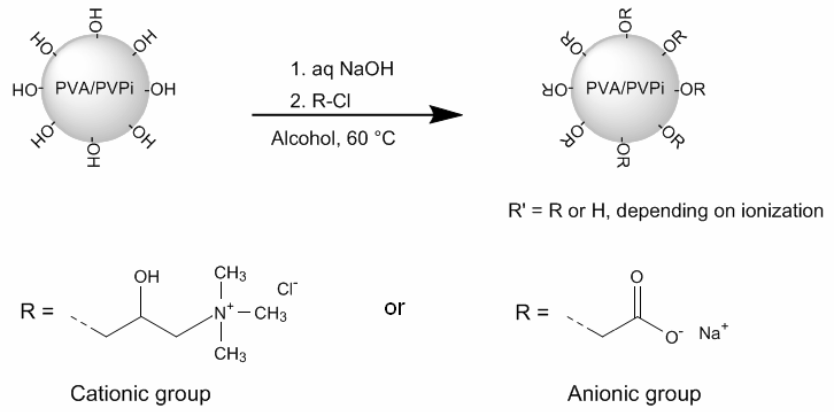

Scheme 4.4 Schematic representation of ionic modification, showing ionic substitution of PVA/PVPi spheres with active hydroxyl groups.

4.4.1 Characterisation of modified particles

4.4.1.1 Evidence of cationisation (cationic modification)

Figure 4.27 illustrates the cationic modified PVA/PVPi, prepared using CHPTMAC as cationic agent, as described in Section 3.4.2.1.

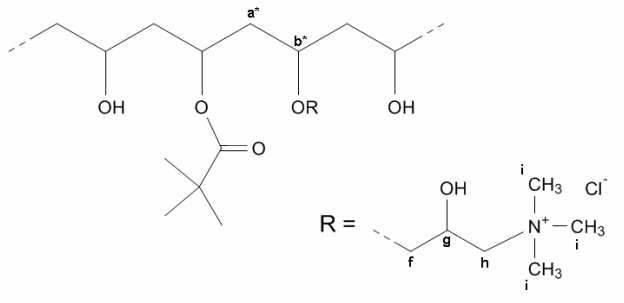

Figure 4.27 PVA/PVPi polymer chain with cationic substitution (actual arrangements of the various pendant groups may vary).

The cationic modification of the hydrolysed PVA/PVPi particles (sample $\mathbf{B_5}$) was confirmed by SS ^{13}C NMR spectroscopy. See Figure 4.28. In addition to having all the characteristic resonance signals of the unmodified PVA/PVPi (sample $\mathbf{B_5}$, see Section 4.3.1) the cationic sample has a new resonance signal at 55 ppm. This peak is attributed to the methyl carbons (-**C**H$_3$) of the cationic species[50] (as labelled in Figure 4.27, i). The samples that were analysed were obtained after Soxhlet extraction and drying, so the probability of the presence of any unreacted cationic species is unlikely. Hence, the cationic modification was successfully achieved.

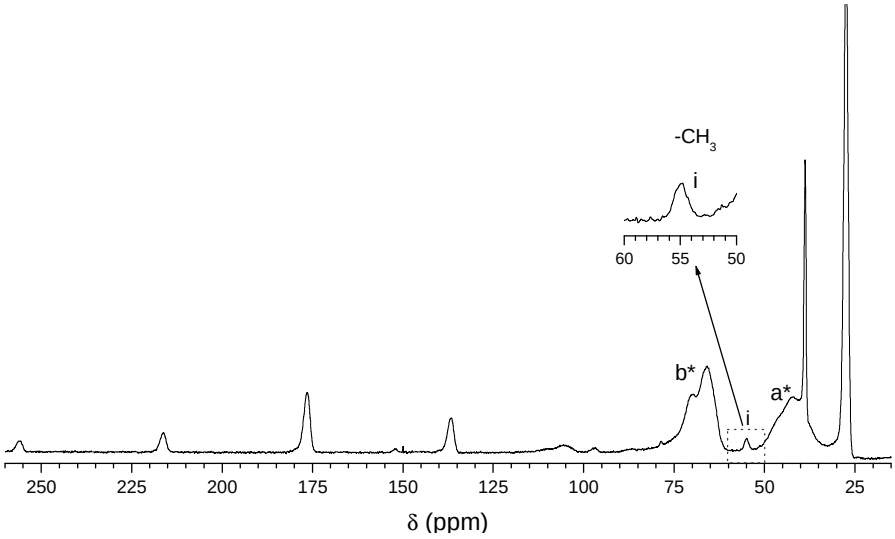

Figure 4.28 SS ^{13}C NMR spectrum of cationic modified PVA/PVPi particles, with inset showing the methyl carbon peak (55 ppm) for the cationic species (post Soxhlet extraction).

It is noticeable that the methylene (-**C**H$_2$) and methine (-**C**H) peaks of the polymer backbone, seen at 42 ppm (a*) and 66 ppm (b*), respectively, were slightly broadened. This is attributed to the fact that the methylene and methine carbons adjacent and in close proximity to, the newly bonded

cationic group would be subjected to a new chemical environment. The resonance signals of these few carbons change slightly; they tend to shift slightly downfield. The signals of the carbons labelled f, g and h (see Figure 4.27), are in the same chemical shift region as, and therefore overlap with, the backbone methine carbon (-**C**H) peak, labelled b* (see Figure 4.28).

The ATR-FTIR spectra of the cationic functionalised PVA/PVPi particles did not yield any significant information on the new cationic functional groups. However, changes were observed in the absorption bands intensities, seen in Appendix H.1.

4.4.1.2 Evidence of carboxymethylation (anionic modification)

Anionic modified PVA/PVPi (see Figure 4.29) was prepared via the Williamson etherification using SMCA anionic monomer and PVA/PVPi particles (15 min hydrolysed, sample $\mathbf{B_5}$), as described in Chapter 3, Section 3.4.2.2. After Soxhlet extraction and drying the anionic modified particles were analysed via ATR-FTIR and SS ^{13}C NMR. FTIR spectroscopy showed differences between the unmodified PVA/PVPi particles and the anionic modified PVA/PVPi, see Figure 4.30. Of particular importance are the two new absorption bands in the anionic modified PVA/PVPi sample, compared to the unmodified PVA/PVPi sample, occurring at 1605 cm^{-1} and 1355 cm^{-1}. These signals are attributed to the asymmetric and symmetric stretch vibrations of the carboxylate salt (**C**OO$^-$), respectively. There is also carbonyl overtone at 3350 cm^{-1},[5] but this could also just be due to the hydroxyl groups.

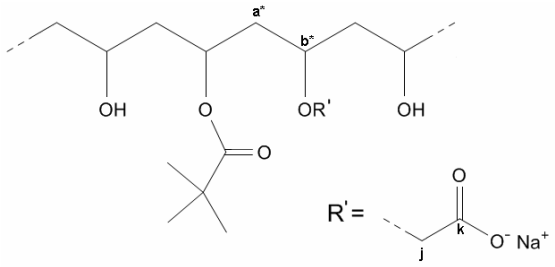

Figure 4.29 PVA/PVPi polymer chain with anionic substitution (actual arrangements of the various pendant groups may vary).

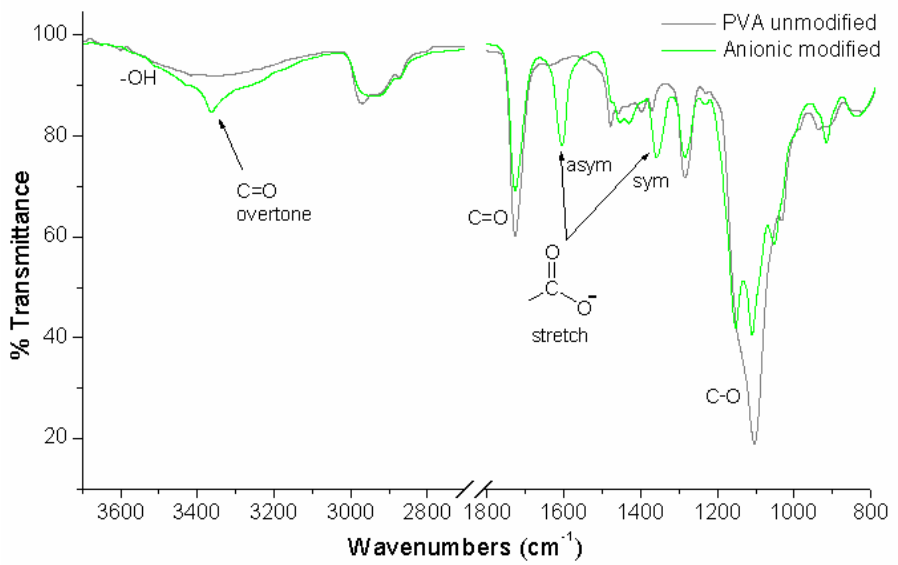

Figure 4.30 ATR-FTIR spectra of the 15 min hydrolysed PVA/PVPi particles (grey, B_5) and the anionic modified PVA/PVPi particles (green).

SS ^{13}C NMR spectrum also showed that the anionic modification was successful (see Figure 4.31). The anionic species has a new resonance shift at 181 ppm, in addition to other characteristic PVA/PVPi resonance signals. This resonance signal is attributed to the carbonyl carbon (**C**=O) of the anionic species,[55] assigned k in Figure 4.29. Furthermore, like the carbonyl of the pivalate group, this carbonyl carbon also has spinning side bands, assigned k*. Like its cationic counterpart, the anionic modified PVA/PVPi sample is seen to have slightly broader methylene (-**C**H_2) and methine (-**C**H) resonance signals, a* and b*, respectively. Again, this is due to the new chemical environment these carbons have been introduced into, specifically those in or in close proximity to the repeat unit where anionic substitution has occurred. The resonance shift of the methylene carbon of the anionic species, labelled j in Figure 4.29, is concealed by the methine carbon shift, b*, of the polymer. This peak increases in size, relative to the two carbon peaks a* and b*. The b* resonance signal now represents the methylene (-**C**H_2-) carbons of PVA/PVPi and the anionic species.

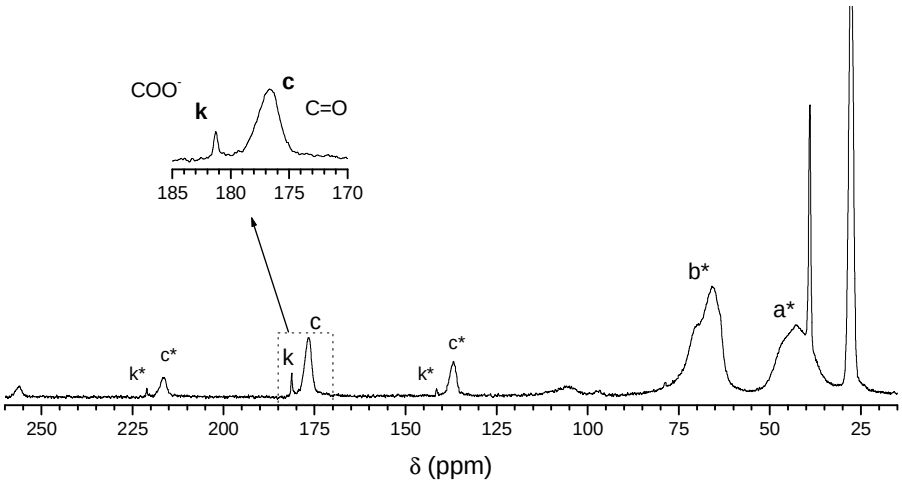

Figure 4.31 **SS ^{13}C NMR spectrum of anionic modified PVA/PVPi particles, inset showing the carbonyl peak (181 ppm) for the anionic species (post Soxhlet).**

4.4.2 Properties of ionic modified PVA/PVPi particles

4.4.2.1 Charge measurements (zeta potential)

Ionic modified particles with only one degree of ionic charge (i.e. either cationic or anionic) were synthesised. Zeta potential measurements performed on the cationic and anionic modified PVA/PVPi, and a variety of other samples, were carried out in order to determine the charge of the particles. Samples were prepared as described in Section 3.7.9 and the zeta potentials of each sample (i.e. unhydrolysed PVPi; hydrolysed PVA/PVPi; cationic and anionic modified PVA/PVPi) were measured. The average zeta potentials of all the samples analysed are listed in Table 4.8.

Table 4.8 **Zeta potential average measurements of the various samples (PVPi, PVA/PVPi, cationic and anionic modified PVA/PVPi)**

Sample code	Sample description	Zeta potential (mV)
A	PVPi (unhydrolysed)	-34.0
B_5	PVA/PVPi (15 min hydrolysed)	-30.0
B_{14}	PVA/PVPi (5 hr hydrolysed)	-14.4
C	Cationic (6 hr)[i] PVA/PVPi	19.6
C_{12}	Cationic (12 hr)[ii] PVA/PVPi (5 hr)	26.5
D	Anionic (6 hr)[i] PVA/PVPi	-39.3

[i] Cationic and anionic modifications of the 15 min PVA/PVPi particles were carried out for 6 hr; [ii] Cationic modification of the 5 hr hydrolysed PVA/PVPi sample was carried out for 12 hr.

These zeta potential results show that both the cationic and anionic modification reactions were successful. Introducing positive charges via cationic modification of PVA/PVPi (15 min hydrolysed, B_5), increases the zeta potential from an initially very low value of -30 mV (B_5), to a relatively strong positive charge of 19.6 mV for the 6 hr cationic modified PVA/PVPi. Similarly, carboxymethylation, and hence the addition of negatively charged anionic species, decreases the charge to -39.3 mV, as would be expected.

An investigation into whether the Soxhlet extraction was successful in removing impurities and any unreacted components was carried out. The zeta potential measurements of the PVA/PVPi sample series was performed before and after Soxhlet extraction. This sample series included one sample from each synthetic step mentioned thus far, i.e. unhydrolysed PVPi (A), 15 min hydrolysed PVA/PVPi (B_5), 6 hr cationic modified PVA/PVPi (C) and 6 hr anionic modified PVA/PVPi (D). Results showed that there were unreacted species in all but the initial PVPi sample (see Table 4.9). Therefore, Soxhlet extraction was successful and necessary for total sample purification. Furthermore, each of the samples maintained its "characteristic charge change". From PVPi (A) to PVA/PVPi (B_5) there is an increase in the charge and from the PVA/PVPi (B_5) to cationic (C) and anionic (D) modified PVA/PVPi, there is a corresponding increase and decrease in the charge, respectively.

Table 4.9 Zeta potential data of the PVPi, PVA/PVPi and modified PVA/PVPi particles, before and after Soxhlet extraction

Sample code	Sample description	Zeta potential (mV)	
		Before	After
A	PVPi	-33.0	-33.3
B_5	PVA/PVPi (15 min)	-31.8	-28.0
C	Cationic PVA/PVPi	19.3	14.8
D	Anionic PVA/PVPi	-39.2	-35.6

Cationic and anionic modifications were prepared by 6 hr modification reactions, as described in Section 3.4.

Due to the limitations and restrictions with regards to ^{1}H NMR analysis of these samples (or the lack thereof), the zeta potential provides additional valuable information to confirm that the corresponding ionic modification was successful.

4.4.2.2 Thermal properties of ionic modified PVA/PVPi particles

DSC and TGA were performed on the complete PVPi samples series: PVPi, 15 min PVA/PVPi, cationic and anionic modified PVA/PVPi particles (A–D, respectively). The T_g and T_m^* results from the DSC analysis of the samples are tabulated in Table 4.10, while TGA data is tabulated in Table 4.11. The corresponding DSC and TGA thermograms for the complete sample series (A-D) are presented in Appendices I.1 and I.2, respectively.

Table 4.10 DSC data (T_g and T_m^*) of the complete PVA/PVPi modified series, before and after Soxhlet extraction

Sample code	Description	T_m^* (°C) [a]	T_g (°C) [b]	
			Before	After
A	PVPi (standard)	-	75	75
B_5	PVA/PVPi (15 min)	157	78	78
C	Cationic (6 hr)[c] PVA/PVPi	146	80	81
D	Anionic (6 hr)[c] PVA/PVPi	-	84	85

[a] Crystalline melting temperature observed from DSC data; [b] Glass transition temperature observed from DSC data before and after Soxhlet extraction; [c] Ionic modification reaction carried out for 6 hr, as described in Section 3.4.

When comparing the DSC data (Table 4.10) and thermograms (see Appendix I.1), there are very clear differences in the new cationic (C) and anionic (D) modified particles, in comparison to the PVA/PVPi precursor (B_5). There is an increase in T_g for both modified species (i.e. cationic and anionic); a decrease in the crystalline melting endotherm (T_m^*) for the cationic particles, while there is no observable crystallinity for the anionic particles. The carboxymethylation and cationisation affect the crystallinity of the PVA/PVPi samples. The loss of crystallinity (and T_m^*) of the anionic modified PVA/PVPi (D) indicates that the carboxymethylation affects the crystalline structure of the PVA. The crystallisation of PVA is disrupted by the large carboxylic acid group (large in comparison to the hydroxyl group), and thereby reduces the crystallinity (and T_m^*). The cationic modified sample (C), which contains newly introduced bulky (hydroxy-propyltrimethylammonium) groups, shows a slightly less severe disruption. It is unclear as to why the crystallinity disappears entirely for the anionic modified sample (D). This is possibly due to the charged acidic groups that offer more repulsion, thereby disrupting the crystal lattice packing structure between polymer chains of the particle to a large extent.

Results for the TGA and DTGA data (Table 4.11) of the modified series shows distinct differences in the cationic (C) and anionic (D) modified PVA/PVPi particles compared to the PVPi (A) and PVA/PVPi (B_5) precursors. The T_{onset} of the cationic and anionic modified species shows an

increase in thermal stability (higher T_{onset}) compared to the PVA/PVPi (B_5). The increase in thermal stability, at least for the carboxymethylated PVA/PVPi (D), could be attributed to hydrogen bond interactions between the newly introduced carboxylic acid groups,[54] causing a slight improvement in thermal stability of the modified PVA/PVPi samples. A decrease in the remaining residues at 890 °C is observed for samples C and D; possibly corresponding to the slight decrease in crystallinity (T_m^*) for the cationic particles (± 13.8% decrease of residuals), and complete absence thereof for the anionic particles (± 20.3% residual decrease); see Table 4.11 and TGA thermograms in Appendix I.2.

Table 4.11 TGA data of the complete PVA/PVPi modified series

Sample code	Description	T_{onset} (°C) [a]	DTGA peak max (°C) [b]	Weight loss (%) [c]	Residue at 890 °C (%)[d]
A	PVPi	332	354	73.4	3.5
			459	21.4	
B_5	PVA/PVPi (15 min)	318	44	1.0	21.7
			359	56.0	
			448	11.3	
			834	7.3	
C	Cationic PVA/PVPi [e]	337	42	2.0	7.9
			364	56.3	
			468	23.7	
			801	7.3	
D	Anionic PVA/PVPi [e]	340	86	3.0	1.4
			375	68.7	
			470	22.9	
			774	2.2	

[a] Onset temperature of thermal degradation/decomposition; [b] Differential mass loss peak maxima; [c] Weight loss at DTGA peak max; [d] Carbon residue at 890 °C; [e] Ionic modification reaction carried out for 6 hr, as described in Section 3.4.

4.4.3 Summary

ATR-FTIR and SS ^{13}C NMR analysis confirmed that cationic and anionic modifications of PVA/PVPi (B_5, 15 min hydrolysed) were successful. In the FTIR spectrum of the anionic modified PVA/PVPi (D), two new IR absorption bands, attributed to the carboxylic acid functional group, were observed at 1605 cm^{-1} and 1355 cm^{-1}. No new structural information was obtained from the FTIR spectrum of the cationic PVA/PVPi (C), but, when compared to the unmodified PVA/PVPi (B_5), a decrease in the characteristic C=O and C–O vibrational intensities was observed. SS NMR and zeta potential measurements showed changes characteristic of the cationic and anionic species, confirming the respective charge modification of the PVA/PVPi particles. The cationic and anionic charged PVA/PVPi particles are assigned the sample codes **C** (cationic) and **D** (anionic) for ease of reference.

4.5 Fluorescent labelling

The aim of this section of the work was to label (or tag) the surface of the particles and thereby extend analysis to fluorescence imaging techniques. With a fluorescent labelled (tagged) surface, these particles can be imaged in an aqueous suspension, as opposed to (or in addition to) immobile, dry sample imaging with SEM. Furthermore, with solution samples, the material properties and interaction with its surrounding solution environment can be investigated, as the particles are free to move wherever their charge and environment permit.

Fluorescent labelling has proven to be a very unique and novel method in polymer analysis. It serves great purpose and shows the direct interaction between, for example, the particles and the fibres. In this study, two complimentary coloured fluorescent labels were used to investigate the interaction of the charged particles with cellulose fibres and, in some cases, precipitated calcium carbonate (PCC) filler.

Rhodamine B isothiocyanate (RBITC) and fluorescein isothiocyanate (FITC) dyes were attached via the isothiocyanate and hydroxyl functional groups of the respective components (i.e. dye and alcohol), represented in Scheme 4.5. Described in Section 3.5.2, the cationic (sample **C**, Section 4.4) and anionic (sample **D**, Section 4.4) modified PVA/PVPi particles were labelled with the RBITC (red) and FITC (green) dyes, respectively. A control set of unmodified particles, i.e. PVPi (sample **A**, Section 4.2) and PVA/PVPi (sample $\mathbf{B_5}$, Section 4.3), were tagged with the red RBITC dye.

Scheme 4.5 **General labelling reaction; the isothiocyanate functional group of the dye undergoes a rearrangement addition reaction with the hydroxyl group on the polymer chain.**

4.5.1 Fluorescence imaging

Fluorescence images of the control samples and of the RBITC tagged cationic PVA/PVPi and FITC tagged anionic PVA/PVPi particles, reveal that they were successfully labelled (or tagged) with the respective fluorescent tag. As anticipated, the PVPi control sample (**A**), labelled with RBITC, showed no significant fluorescence, as seen in Figure 4.32. This is because there are no hydroxyl groups present in the pivalate polymer, hence, there would be no reaction with the isothiocyanate functional group, as the hydroxyl group is the key component needed for this type of reaction to occur. In

accordance with this, the hydrolysed PVA/PVPi sample does show fluorescence after the tagging reaction, (seen in Appendix J.1, $\mathbf{B_5}$), proving that fluorescent attachment is successful when hydroxyl functional groups are present.

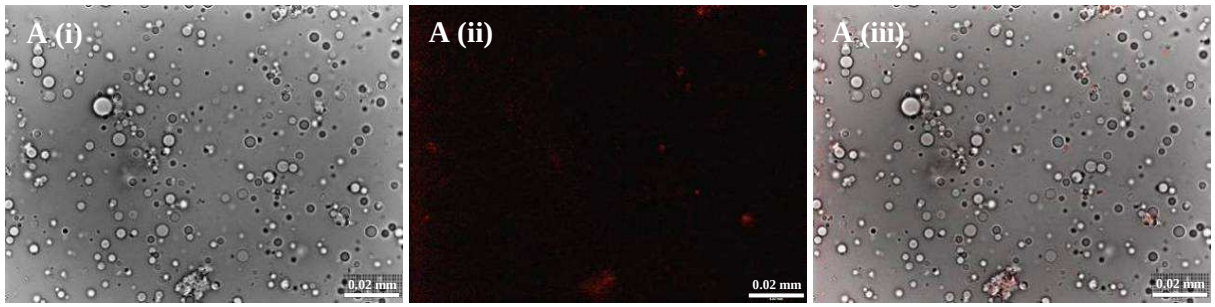

Figure 4.32 Fluorescence images of RBITC tagged PVPi particles (A): (i) transmission mode, (ii) fluorescence mode, and (iii) an overlay of (i) and (ii).

The cationic and anionic PVA/PVPi particles were successfully labelled with the rhodamine B and fluorescein tags, respectively. The fluorescence images of the RBITC cationic PVA/PVPi (red) and FITC anionic PVA/PVPi (green) particles are shown in Figure 4.33 and Figure 4.34, respectively.

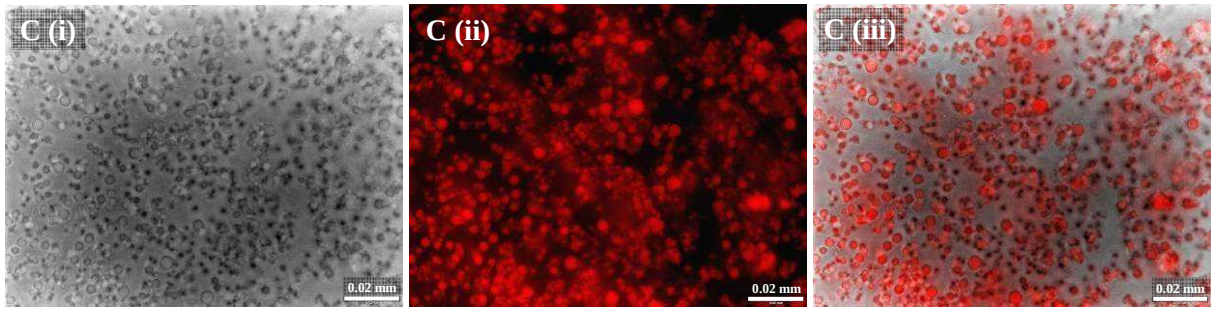

Figure 4.33 Fluorescence images of RBITC tagged cationic PVA/PVPi particles (C): (i) transmission mode, (ii) fluorescence mode, and (iii) an overlay of (i) and (ii).

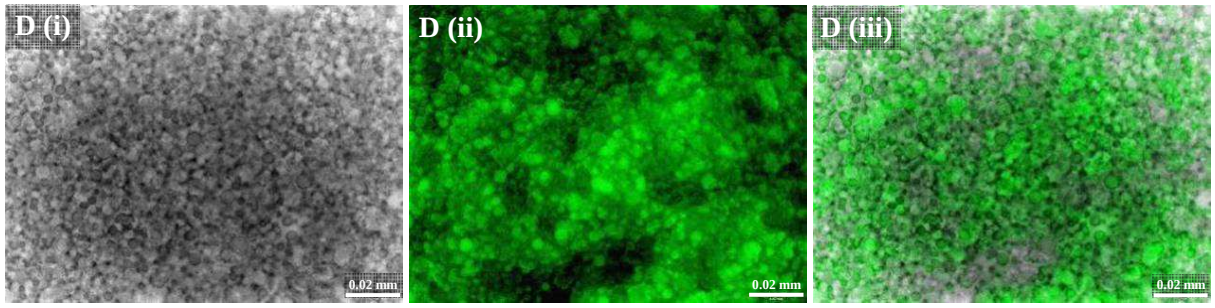

Figure 4.34 Fluorescence images of FITC tagged anionic PVA/PVPi particles (D): (i) transmission mode, (ii) fluorescence mode, and (iii) an overlay of (i) and (ii).

Additional information regarding particle size relative to chromophore distribution was obtained through statistical fluorescence analysis, i.e. flow cytometry.

4.5.2 Fluorescence statistical analysis

Fluorescence statistical analysis provides size versus fluorescence scatter plots (Figure 4.35), and fluorescence distribution curves (Figure 4.36) of the respective samples. In the scatter plots, the x and y axes represent the fluorescence intensity and particle size dimensions, respectively. The distribution curves correspondingly have x and y axes representative of fluorescence and count. It should be noted that both axes have arbitrary units of measurement and each dot in the scatter plots represents a single particle. Thus, the scatter plots provide a relative indication of the relationship between particle size and fluorescence. The scatter plots and distribution curves for the RBITC tagged (red) cationic PVA/PVPi (**C**) and FITC tagged (green) anionic PVA/PVPi (**D**) particles are shown in Figure 4.35 and Figure 4.36, respectively

Flow cytometry analysis of these particles indicates that particles of all sizes produce fluorescence, as seen in the size versus fluorescence scatter plots, Figure 4.35. Moreover, it is seen that the relationship between size and fluorescence is essentially proportional, i.e. as the size of the particles increase, so too does the intensity of fluorescence. Larger particles exhibit a higher intensity of fluorescence, and vice versa. This can be attributed to the fact that the larger particles have a larger surface area and higher number of easily accessible binding sights, hence a larger number of hydroxyl groups present on hydrolysis, and consequently a larger amount of fluorescent labelling sites. This observation is reinforced with the aid of the fluorescence distribution curves (Figure 4.36).

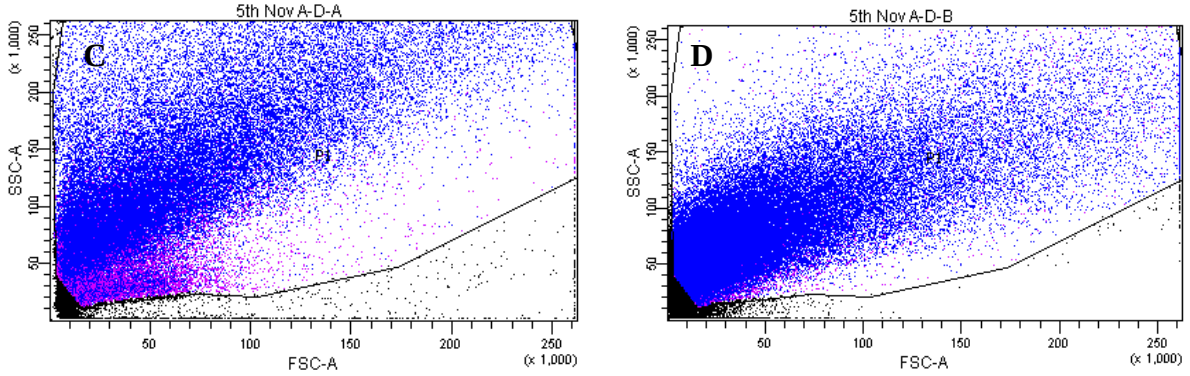

Figure 4.35 **Fluorescence scatter graphs for the RBITC tagged cationic (C) and FITC tagged anionic (D) modified PVA/PVPi particles, respectively. Graphs show the population size versus fluorescence plots for each sample.**

Figure 4.36 shows the distribution curves for the red- and green-fluorescence, labelled (i) and (ii), pink and blue plots respectively. Apart from providing information about the intensity of the sample, these distribution curves, along with the respective scatter plots, provides an indication as to which intensity (region) corresponds with which particle(s). When a specific intensity region of the distribution curve is selected, omitting the rest of the intensity range, the scatter plots reflect the same parameters, showing only the particles which fluoresce within the specified range. Experimentally, it was seen that when the higher intensity range of the distribution curve was selected, only particles in the larger size region of the scatter plots were visible. Hence, the larger particles have a higher intensity of fluorescence.

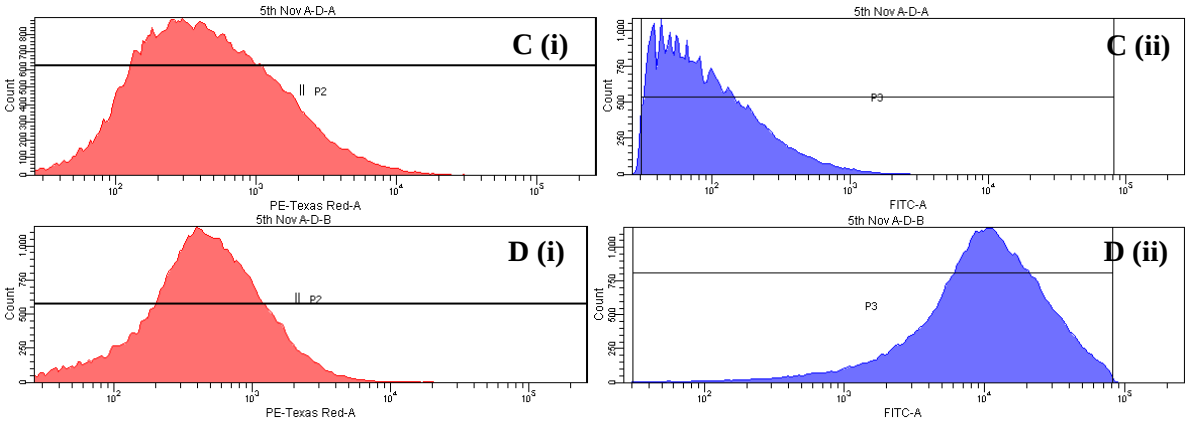

Figure 4.36 **Fluorescence distribution curves for the RBITC tagged cationic (C) and FITC tagged anionic (D) modified PVA/PVPi particles, respectively. The RBITC (i, pink) and the FITC (ii, blue) fluorescence distribution curves are shown, obtained at their respective excitation/emission wavelengths.**

What is also noticed from the distribution curves, Figure 4.36, is that all the samples show fluorescence in both colour regions (red and green light), even though each sample was only labelled with one chromophore. This is known as 'bleed through', and can also be attributed to the fact that the two fluorescent tags have overlapping excitation and emission wavelengths. Hence, when measuring or imaging in the green zone (FITC, λ_{max} ex/em = 490/520 nm), any red-tagged particles (RBITC, λ_{max} ex/em = 543/580 nm) will also show some green fluorescence, and vice versa. Thus, the red RBITC tagged cationic sample shows a distribution curve for the green-light fluorescence (ii) in addition to the red-light (**i**) distribution curves. The same applies for the green FITC tagged anionic sample, and evidently, this is dependent on the fluorescent dye concentration, and both chromophores show higher intensity fluorescence in its own characteristic light region. For example, the FITC tagged (green) anionic particles (**D**) show a higher intensity in the green-light distribution curve than in its

corresponding red-light curve. However, when imaging the particles with the respective fluorescence light (Section 4.5.3), only the RBITC tagged particles (red) show both colours in the fluorescence images. The different particles can therefore be combined but still distinguished from each other in that the FITC tagged particles (green anionic) will only fluoresce green, while the RBITC tagged particles (red cationic) will fluoresce both green and red, giving a yellowish-orange combined signal. This is seen in the following section.

Sufficient information has been obtained from the fluorescence images and the statistical data. The particles were now combined with cellulose fibres and the interaction therewith was investigated.

4.5.3 Particle–fibre study: fluorescence and SEM imaging

As described above, the red RBITC tagged particles fluoresces both red and green, and these two colours combined to yield a yellowish-orange tinge, while the FITC tagged particles (and FITC tagged/labelled cationic starch) fluoresce only green. This is convenient in aiding in identification of the particles, especially in cases where both cationic (red) and anionic (green) particles are combined. The particles are mixed with cellulose fibres in aqueous solution, and in some instances FITC labelled cationic starch and/or PCC. The samples, prepared by methods described in Section 3.7.10 and 3.7.4, were studied using fluorescence microscopy (in solution) and SEM of the respective (dried) samples.

4.5.3.1 Standard PVPi particles and PVA/PVPi particles with cellulose fibres

SEM was used to observe the interaction of the unhydrolysed PVPi standard (sample **A**) with the cellulose fibres, as well as that for the 15 min hydrolysed PVA/PVPi particles (sample $\mathbf{B_5}$) with cellulose fibres, Figure 4.37 (A and B_5, respectively). It was observed that there is some particle adhesion to the cellulose fibres, but only in sections and not on all fibres. Where there is good filtration (and microporosity plays little role), particles are left behind on the surface, but in general, there is little adhesion of the PVPi (A) to the cellulose fibres, and particles are mostly only evident where there are flat areas of microporosity (Appendix K.1). The PVA particles (B) adhere more frequently to the cellulose fibre surface but when compared to starch, adhesion it is infinitesimal; however, there is a definite sitting of the PVA particles on the fibres.

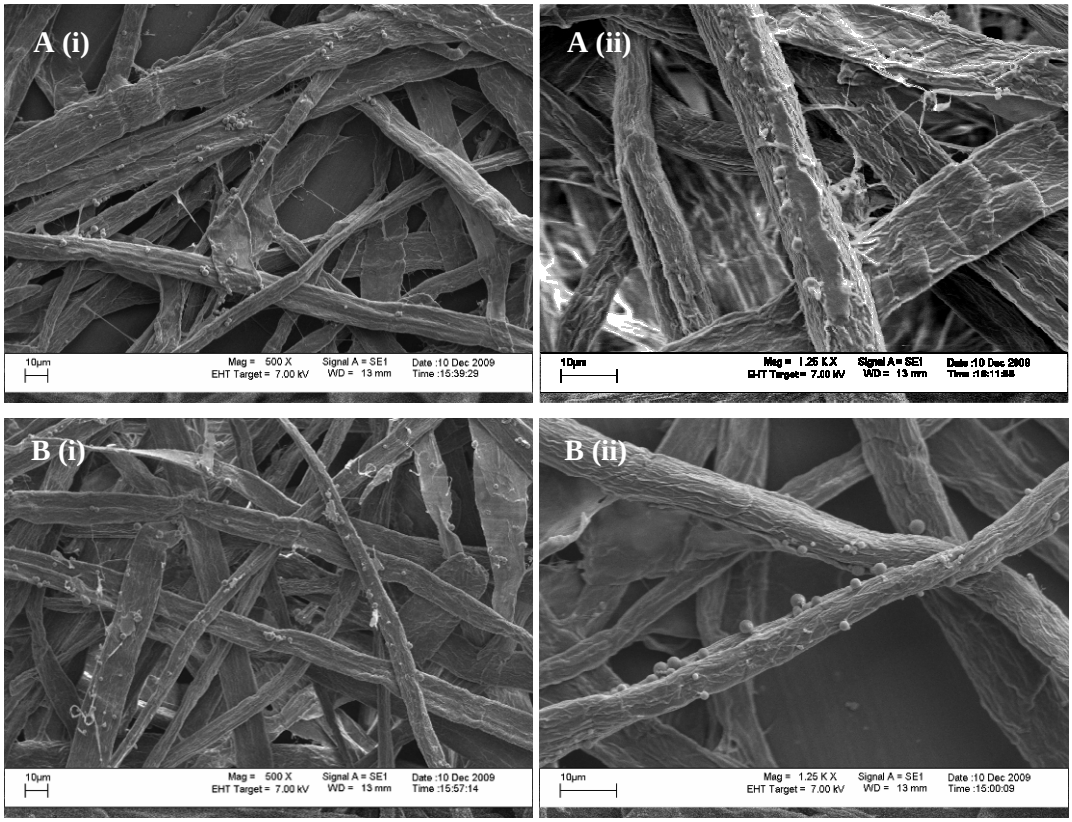

Figure 4.37 SEM images of (A) PVPi particles (unhydrolysed, A) and (B) PVA/PVPi particles (15 min hydrolysed, B_5) with cellulose fibres; (i) ×500, (ii) ×1250.

4.5.3.2 RBITC labelled cationic PVA/PVPi particles (red) with cellulose fibres

Fluorescence microscopy and SEM were used to study the RBITC labelled cationic particle (sample **C**) interaction with cellulose fibres; see Figure 4.38. RBITC labelled cationic PVA/PVPi particles were mixed with cellulose fibres and prepared for fluorescence and SEM imaging techniques, as described in Sections 3.7.10 and 3.7.4.

The red cationic PVA/PVPi particles (sample **C**) have a tendency to be closely situated around the cellulose fibres in solution (Figure 4.38 A–C), but very little actual surface contact is observed in the electron micrograph (Figure 4.38 D) after washing the excess loose particles away. The cationic particles sit infrequently on the fibre surface, which is in contradiction to previous work on cationic (and anionic) starch. In previous work by the author (unpublished) and colleagues on cationic starch (and the present work with cationic starch, next sections), it was shown that the floppy starch had better adhesion to the surface of the fibres. This is expected as the cationic particles (sample **C**) are rigid and cannot conform to fit onto (and around) the cellulose fibres, unlike the floppy starch material. The hard spherical form restricts contact area, thus, a limited number of ionic charged

groups adhere to the fibre surfaces, and the weight of the particles can force them to fall off during washing. It is proposed that the cellulose has intermittent carboxylic acid sites. Thus, a good adherence is achieved with the swollen floppy starch, as it can conform and adhere to as many of these sites as possible. Further fluorescence images are seen in Appendix L.1.

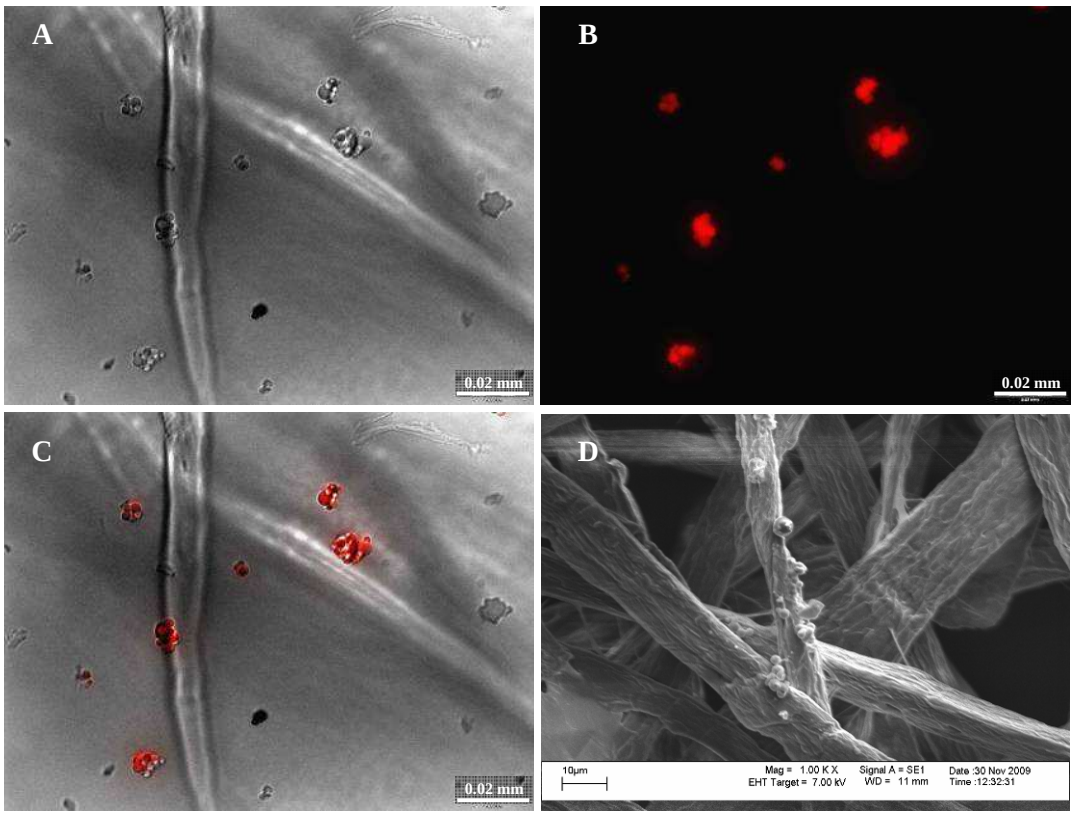

Figure 4.38 **RBITC tagged cationic PVA/PVPi particles with cellulose fibres, shown in fluorescence images: (A) transmission mode, (B) fluorescence mode and (C) transmission-fluorescence overlay; and (D) SEM image, ×1000.**

4.5.3.3 RBITC labelled cationic PVA/PVPi particles (red) with FITC labelled cationic starch (green) and cellulose fibres

In a follow up investigation, a fluorescein (FITC) labelled cationic starch (previously synthesised, Appendix M.1) was added in addition to the cationic particle–cellulose fibres study described above; see Figure 4.39.

The samples of cationic particles with cationic starch and cellulose fibres were prepared as described in Section 3.7.10. With fluorescence analysis of the RBITC labelled (red) cationic particles and FITC labelled (green) cationic starch, fluorescence images were measured in both red and green light zones, Figure 4.39 (B and C, respectively). As described above, the RBITC labelled species will

fluoresce mostly red but also green, and an overlay of the two fluorescence images will show these particles as yellowish in colour (Figure 4.39 D).

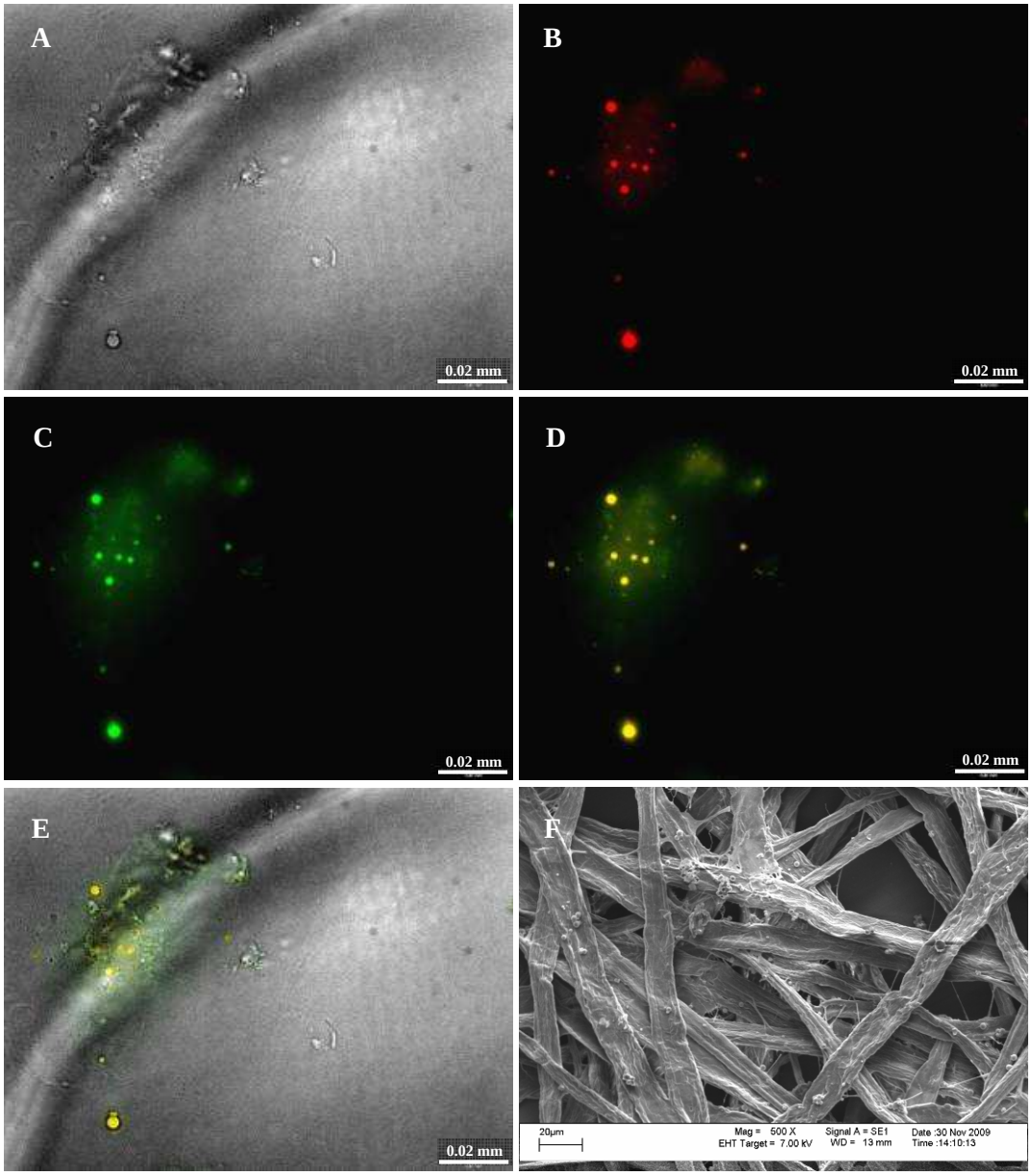

Figure 4.39 **RBITC tagged cationic PVA/PVPi particles with FITC tagged cationic starch and cellulose fibres, shown in fluorescence images: (A) transmission mode, (B and C) fluorescence mode, (D) fluorescence overlay and (E) transmission-fluorescence overlay; and (F) SEM image, ×500.**

With the cationic particles, there is less adhesion to the fibre in comparison (and in contrast) to cationic starch. This indicates that the negative charges on the fibre surface are few and far between

and not in clusters, which could attract a particle with little deformation. Instead, the rigid particles cannot adhere efficiently and a great deal of deformation (like that of the floppy starch) is required to create enough contact area (points) for adhesion. The starch has the ability to conform to the shape of the fibre and tends to spread out over the surface, whereas the cationic particles tend to adhere to the surface.

Although both the PVA/PVPi particles and starch were modified to possess positive cationic charges, the cationic starch does, in fact, aid in the adsorption of the cationic particles onto the cellulose fibre surface (Figure 4.39, E and F). The reason is that the cationic starch can conform to the round particles (and fibres), allowing multiple hydroxyl adhesives sites and greater particle–fibre surface area interaction. Thus, more cationic particles adhere to the fibre surface. Additional images (fluorescence and SEM) of the cationic particles with cationic starch and cellulose fibres are given in Appendices L.2 and L.3.

4.5.3.4 FITC labelled anionic PVA/PVPi particles (green) with cellulose fibres

Using methods identical to those used for cationic particles (Section 4.5.3.2), the anionic PVA/PVPi particles and their interaction with cellulose fibres were investigated. See Figure 4.40. FITC labelled anionic PVA/PVPi particles (sample **D**) were mixed with cellulose fibres and prepared for fluorescence and SEM imaging techniques as described in Section 3.7.10 and 3.7.4. From the fluorescence and SEM images, it is clear that there is very little interaction for the anionic particles with cellulose fibre. The anionic particles seem to be trapped between fibres, as seen in aqueous solution (fluorescence images Figure 4.40 A–C) and dry conditions (SEM, Figure 4.40 D), rather than there being any fibres attracting the anionic charged particles, which was expected from the anionic particles and negatively charged anionic cellulose fibre surface.

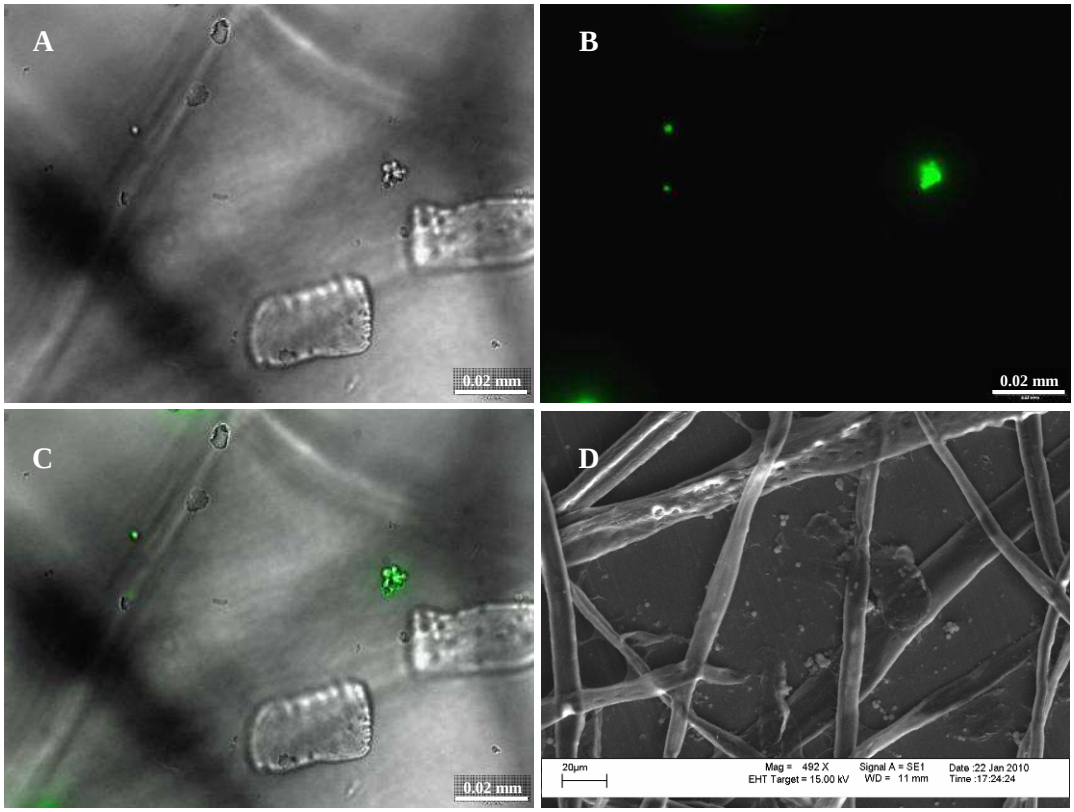

Figure 4.40 FITC tagged anionic PVA/PVPi particles with cellulose fibres, shown in fluorescence images: (A) transmission mode, (B) fluorescence mode and (C) transmission-fluorescence overlay; and (D) SEM image, ×492.

Additional fluorescence images are provided in Appendix L.4. As with the cationic particles, the use of cationic starch was used to assist and improve adsorption of the anionic particles onto the fibre surface.

4.5.3.5 FITC labelled anionic PVA/PVPi particles (green) with FITC labelled cationic starch (green) and cellulose fibres

As previously explained, as an additional investigation, a fluorescein (FITC) labelled cationic starch (previously synthesised, Appendix M.1) was added to the anionic particle–cellulose fibres study, described above. The samples of anionic particles with cationic starch and cellulose fibres were prepared as described in Section 3.7.10. As both the anionic particles and cationic starch are labelled with FITC, fluorescence will only occur and be observed in (and for) green light. The fluorescence and SEM images (Figure 4.41) show that the cationic starch markedly improves the interaction of the anionic particles with the cellulose fibre.

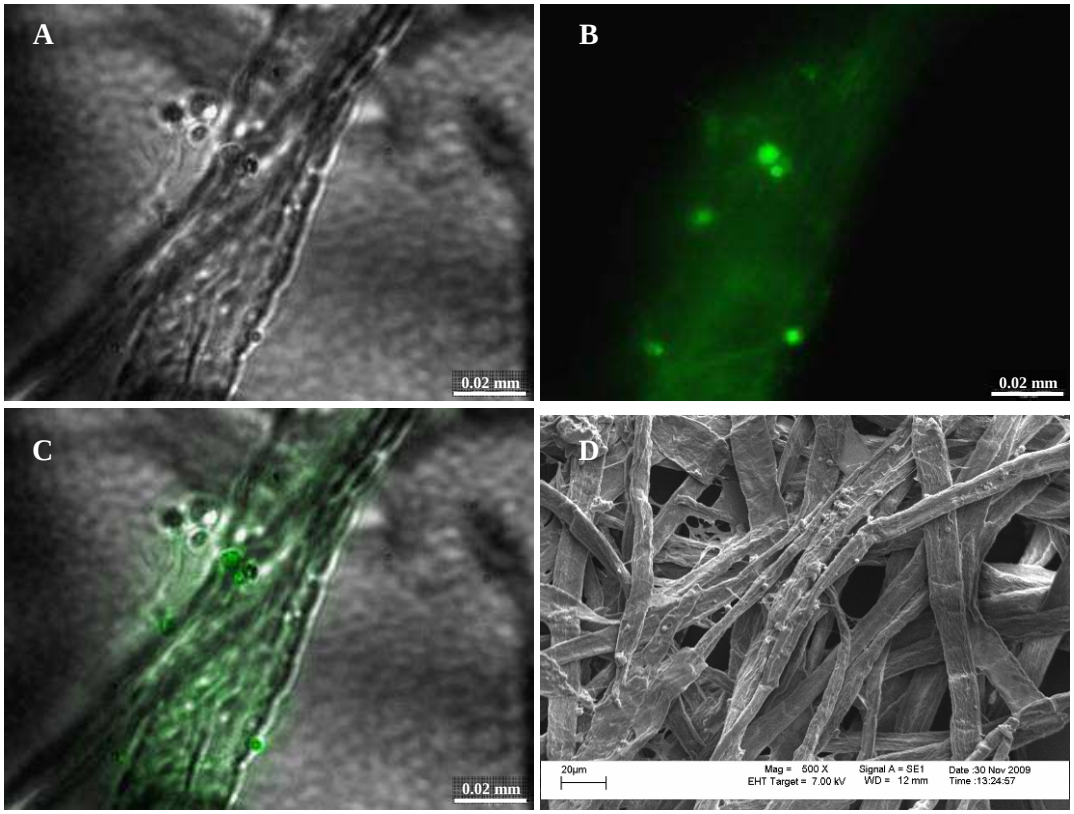

Figure 4.41 FITC tagged anionic PVA/PVPi particles with FITC tagged cationic starch and cellulose fibres, shown in fluorescence images: (A) transmission and (B) fluorescence mode, and (C) transmission-fluorescence overlay; and (D) SEM image, ×500.

The anionic rigid particles do not adhere well to the fibre surface, while the cationic starch can morph and conform to the shape of the fibre. The cationic starch adheres well to the negative fibre surface, and also shows good adhesion with the anionic particles. Hence, and as expected, the floppy cationic starch assists with and improves the adhesion of the anionic particles to the cellulose surface. Additional images (fluorescence and SEM) of the anionic particles with cationic starch and cellulose fibres are given in Appendix L.5, showing superb anionic particle-cationic starch interaction (fluorescence), but fewer particles are observed on the cellulose fibres (SEM).

4.5.3.6 Further studies of cationic (red) and anionic (green) PVA/PVPi particles with PCC and cellulose fibres

Additional investigations into the particles' nature show that when combined with each other (Figure 4.42 A), the RBITC labelled cationic (red) and FITC labelled anionic (green) PVA/PVPi particles interact well with each other, by flocculating together, as expected from the attraction of the oppositely charged particles. Figure 4.42 B shows the interaction of the cationic and anionic particles

with PCC paper filler; little interaction between the filler and the particles is observed. In these two images, the cationic particles fluoresces both red and green, together yielding the yellowish-orange colour observed.

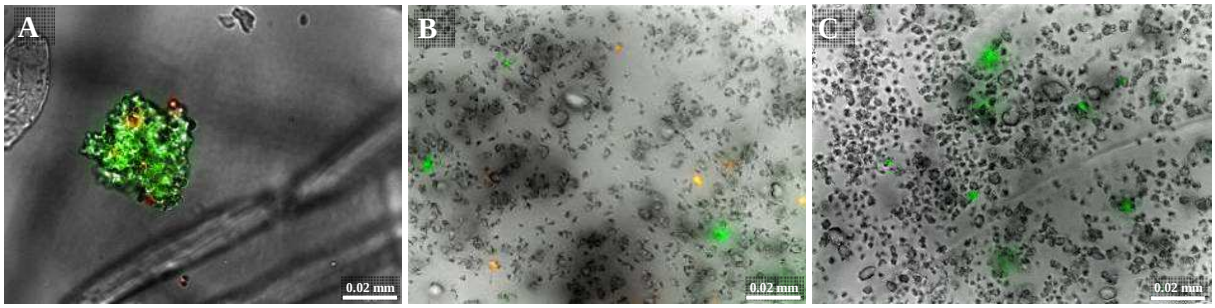

Figure 4.42 Fluorescence images (transmission-fluorescence overlays): both RBITC cationic (red) and FITC anionic (green) PVA/PVPi particles with (A) cellulose fibres and (B) PCC; (C) FITC anionic particles (green) with PCC and cellulose fibres.

The interaction of the anionic particles with PCC paper filler and cellulose fibres is seen in Figure 4.42 C, which illustrates how the PCC adsorbs onto the green anionic particles, though poorly in comparison to the floppy starch particles (see inlaid pictures B(ii) in Appendix M.1). This is to be expected as the two rounded surfaces don't provide sufficient binding or adhesion to each other.

4.5.4 Summary

The labelling with RBITC, for cationic particles and controls, and FITC, for anionic particles and starch, were successful, and fluorescence imaging proved valuable. The scatter plots indicate that there are a vast number of particles, all transmitting fluorescent signals, in both samples (cationic and anionic). The RBITC tag shows 'bleed through' into the green region of the fluorescence light spectra (distribution graphs), attributed to the strong RBITC signal. The imaging excitation wavelengths (at 472 nm and 572 nm) may also have affected the fluorescence of each chromophore species.

On analysis of flow cytometry data, when comparing the fluorescence scatter plots and distribution curves, if the larger emission portion (distribution curve) is selected, the larger particles are visible (in the scatter plots). The larger particles were therefore found to be in the higher emission range as these particles were highlighted when the higher emission range was selected. The same applies for smaller particles; remaining visible (while the others are shadowed out) when the lower emission range is selected. This explains the fact that the larger particles emit more fluorescence, as would be expected. This can be attributed to the fact that the larger particles have a larger (surface) area and more binding sights, and thus a larger number of fluorescent markers attached and ultimately

a higher strength emission. It is plausible to say that there is a relationship between the surface size of the particles and intensity of the fluorescence.

From fluorescence and SEM imaging, it was established that the cationic particles interact with the cellulose fibres more favourably than the anionic particles, but neither as efficiently or effectively as the floppy starch material. Appendix M.1 shows the results of the previously prepared FITC labelled cationic and anionic modified starches, and their interaction with cellulose fibres and PCC. This work showed that the cationic starch adhered well to both the cellulose fibres and PCC, while the anionic starch showed close interaction with the PCC particles, but not with the cellulose fibres. From this information, it was established, that for the study with fibre, the cationic starch would be most suitable for use in a follow up investigation with the cationic and anionic charged PVA/PVPi particles.

The spherical shape and rigidity of the particles limit contact area, and hence also adhesion to the cellulose fibres by hydrogen bonding and charge attraction. This is expected and proves that the floppy, soluble starch is more effective, in that it can mould and conform around the cellulose fibres, as well as PCC particles.

4.6 Particle size analysis by FFF

The size distribution properties of the prepared spherical PVPi (**A**) and PVA/PVPi (15 min hydrolysed, $\mathbf{B_5}$) particles were investigated using field-flow fractionation (FFF). Due to the relatively large size of these particles, the use of conventional chromatographic analysis (e.g. SEC) was not possible; as the particles would block the columns. Furthermore, there are no separation columns available for micron size separation. It is very difficult to obtain accurate measurements of particle size in the swollen state for large particles. This can be solved by using FFF, because it separates particles according to size and can separate over a broad molecular weight range, from about 5 nm to 100 μm.[57]

In this study, the asymmetric flow FFF (AsFl-FFF) coupled to particle size detector was used for particle fractionation and detection. Fractionation results of the PVPi (sample **A**) and PVA/PVPi (sample $\mathbf{B_5}$) are shown in Figure 4.43. Experimental conditions used were described in Chapter 3, Section 3.7.11.

Figure 4.43 A shows the particle elution curves of PVPi (sample **A**). The relative particle intensity versus elution time curves show little separation in the samples, but a slight shift in elution time is seen. Figure 4.43 B shows similar results for the fractionation of the PVA microspheres (15 min hydrolysed PVA/PVPi, sample $\mathbf{B_5}$). The curves show a slight shift in elution time, but separation is not large, in fact, all the particles effectively elute at similar times.

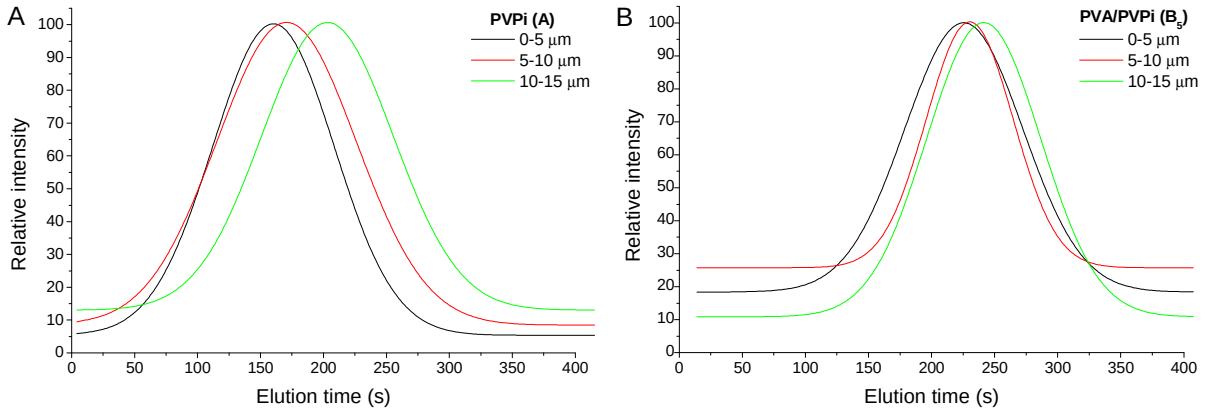

Figure 4.43 Relative number of particles versus elution time of (A) PVPi particles and (B) PVA/PVPi particles, fractionated by AsFl-FFF.

It was not possible to achieve better fractionation because fractionation is restricted by the particle size and a size exclusion effect. Normal mode separation occurs when particles have dimensions of < 1 μm, where the elution order is smallest to largest. When particle dimensions are

greater than 1 μm, a steric mode or "hyperlayer mode" separation will take place. In these cases, the elution order is from largest to smallest.[58] In this study, the dimensions of the prepared particles (A and B_5) are between 1 and 5 μm (see Section 4.2.3). Thus, with AsFl-FFF, using an asymmetric flow field force, hyperlayer mode separation will occur. The particles separated have a narrow size distribution, and fractionation of these narrowly dispersed particles was therefore difficult.

Figure 4.44 shows the particle size versus intensity plots of the unhydrolysed PVPi (A) and the hydrolysed PVA/PVPi (15 min, B_5) particles. The latter have narrow PVA shells (which may be swellable in THF to an unknown extent), but the distribution indicates that there is little difference in the sizes. In other words, the shells are very thin and do not swell very much, due to the crystalline behaviour of the PVA.

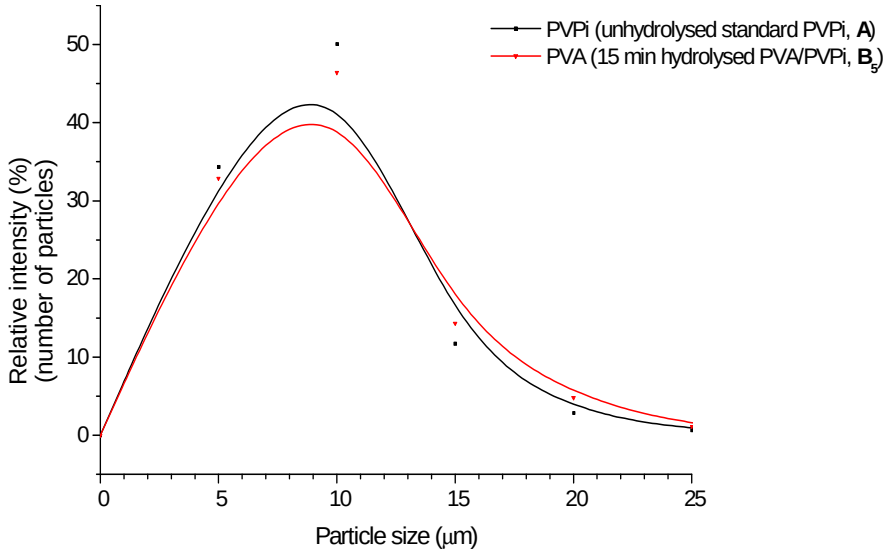

Figure 4.44 Particle size versus the intensity plots of the unhydrolysed PVPi (black, A) and 15 min hydrolysed PVA/PVPi (red, B_5) particles.

Currently, there are no means of measuring floppy particles of swollen cellulose. One of the useful aspects of this work was to have available particles of controlled shape and size with a surface similar to cellulose (with hydroxyl groups). Further research into and optimisation of analytical conditions is required in order to obtain better fractionation of these particles. Nonetheless, the potential exists for these modified PVA particles to be used as standards for sizing cellulose, cellulose derivates or other bio-macromolecule particles.

4.7 References

1. W.S. Lyoo, C.S. Park, K.H. Choi, J.W. Kwak, W.S. Yoon, and S.K. Noh, *Polym. Plast. Technol. Eng.*, **2005**, 44(3), 475-487.
2. W.S. Lyoo, J.W. Kwak, J.H. Yeum, B.C. Ji, C.J. Lee, and S.K. Noh, *J. Polym. Sci., Part A: Polym. Chem.*, **2005**, 43(4), 789-800.
3. S.G. Lee, J.P. Kim, W.S. Lyoo, J.W. Kwak, S.K. Noh, C.S. Park, and J.H. Kim, *J. Appl. Polym. Sci.*, **2005**, 95(6), 1539-1548.
4. Q.T. Pham, R. Pétiaud, H. Waton, and M.-F. Llauro-Darricades eds., *Proton and Carbon NMR Spectra of Polymers*, 5th edn., Wiley: Chichester, 2003.
5. D.L. Pavia, G.M. Lampman, and G.S. Kritz, *Introduction to Spectroscopy*, 3rd edn., Brooks/Cole: Washington, 2001.
6. H.D. Ghim, J.P. Kim, and W.S. Lyoo, *Polymer*, **2003**, 44, 895-900.
7. R. Arshady, *Colloid Polym. Sci.*, **1992**, 270(8), 717-732.
8. H.N. Cheng and A.D. English eds., *NMR Spectroscopy of Polymers in Solution and in the Solid State*, ACS Symposium Series, 834, American Chemical Society: Washington DC, 2003.
9. L.J. Mathias ed. *Solid State NMR of Polymers*, Plenum Press: New York, 1991.
10. P.A. Mirau, *A Practical Guide to Understanding the NMR of Polymers*, John Wiley & Sons, Inc.: New Jersey, 2005.
11. D.O. Hummel, H.F. Ebel ed. *Atlas of Polymer and Plastics Analysis*, 3rd edn., Vol. 1, Carl Hanser: Munich, 1991.
12. T.L. Uyen Nguyen, B. Farrugia, T.P. Davis, C. Barner-Kowollik, and M.H. Stenzel, *J. Polym. Sci., Part A: Polym. Chem.*, **2007**, 45(15), 3256-3272.
13. S.G. Lee, J.P. Kim, I.C. Kwon, D.S. Shin, S.S. Han, and W.S. Lyoo, *J. Appl. Polym. Sci.*, **2006**, 101(6), 4064-4070.
14. A.M. Atta and R.A.M. El-Ghazawy, *Int. J. Polym. Mater.*, **2003**, 52(7), 623-636.
15. M. Krumova, D. López, R. Benavente, C. Mijangos, and J.M. Pereña, *Polymer*, **2000**, 41(26), 9265-9272.
16. M.A. Gauthier, J. Luo, D. Calvet, C. Ni, X.X. Zhu, M. Garon, and M.D. Buschmann, *Polymer*, **2004**, 45(24), 8201-8210.
17. T. Chen and E.L. Burch. Use and Preparation of Crosslinked Polymer Particles for Inkjet Recording Materials. United States Patent: US007507439B2, 2009.

18. H. Warson and C.A. Finch, *Fundamentals of Polymer Chemistry*, in *Fundamental Chemistry of Latices and Applications in Adhesives*, ed. H. Warson, Vol. 1, John Wiley & Sons: Chichester, 2001.
19. Aldrich Chemical Co. Inc., *Aldrich Polymer Products Applicaton & Reference Information*, 1999 [cited 25/08/2010]; Available from: http://www.sigmaaldrich.com/etc/medialib/docs/Aldrich/General_Information/thermal_transitions_of_homopolymers.Par.0001.File.tmp/thermal_transitions_of_homopolymers.pdf.
20. J. Brandrup, E.H. Immergut, E.A. Grulke, A. Abe, and D.R. Bloch eds., *Polymer Handbook*, 4th edn., Wiley-Interscience: New Jersey, 1999.
21. E. Vivaldo-Lima, P.E. Wood, A.E. Hamielec, and A. Penlidis, *Ind. Eng. Chem. Res.*, **1997**, 36(4), 939-965.
22. B.V. Kichatov, A.M. Korshunov, and P.V. Assorova, *Theor. Found. Chem. Eng.*, **2003**, 37(3), 306-309.
23. W.S. Lyoo, C.S. Park, J.H. Yeum, B.C. Ji, C.J. Lee, S.S. Lee, and J.Y. Lee, *Colloid Polym. Sci.*, **2002**, 280(12), 1075-1083.
24. W.S. Lyoo, S.G. Lee, J.P. Kim, S.S. Han, and C.J. Lee, *Colloid Polym. Sci.*, **1998**, 276(11), 951-959.
25. W.S. Lyoo and H.W. Lee, *Colloid Polym. Sci.*, **2002**, 280, 835-840.
26. W.S. Lyoo, S.S. Han, J.H. Kim, W.S. Yoon, C.J. Lee, I.C. Kwon, J. Lee, B.C. Ji, and M.H. Han, *Angew. Makromol. Chem.*, **1999**, 271(1), 46-52.
27. I. Sakurada and T. Okaya, *Vinyl Fibres*, in *Handbook of Fibre Chemistry*, ed. M. Lewin, 3rd edn., CCR Press: New York, 2007, pp. 261-329.
28. C.A. Finch ed. *Polyvinyl Alcohol: Developments*, John Wiley & Sons Ltd: Chichester, 1992.
29. M. Kobayashi, I. Ando, T. Ishii, and S. Amiya, *J. Mol. Struct.*, **1998**, 440(1-3), 155-164.
30. H. Ohgi, T. Sato, S. Hu, and F. Horii, *Polymer*, **2006**, 47(4), 1324-1332.
31. K. Katsuraya, K. Hatanaka, K. Matsuzaki, and S. Amiya, *Polymer*, **2001**, 42(24), 9855-9858.
32. H.F. Mark, *Encyclopedia of Polymer Science and Technology*, ed. J.I. Kroschwitz, 3rd edn., Vol. 12, John Wiley & Sons, Inc.: Hoboken, 2003, pp. 168-169.
33. Y. Nagara, T. Nakano, Y. Okamoto, Y. Gotoh, and M. Nagura, *Polymer*, **2001**, 42(24), 9679-9686.
34. H.F. Mark, *Encyclopedia of Polymer Science and Technology*, ed. J.I. Kroschwitz, 3rd edn., Vol. 8, John Wiley & Sons, Inc.: Hoboken, 2003, pp. 339-437.
35. J.-L. Shie, Y.-H. Chen, C.-Y. Chang, J.-P. Lin, D.-J. Lee, and C.-H. Wu, *Energ. Fuel.*, **2002**, 16(1), 109-118.

36. W.S. Lyoo and W.S. Ha, *J. Polym. Sci., Part A: Polym. Chem.*, **1997**, 35(1), 55-67.
37. R. Ricciardi, F. Auriemma, C.D. Rosa, and F. Lauprêtre, *Macromolecules*, **2004**, 37(5), 1921-1927.
38. J.-T. Yeh, P. Xu, and F.-C. Tsai, *J. Mater. Sci.*, **2007**, 42(16), 6590-6599.
39. K. Pal, A.K. Banthia, and D.K. Majumdar, *AAPS PharmSciTech*, **2007**, 8(1), 1-5.
40. Y. Wang and Y.L. Hsieh, *J. Appl. Polym. Sci.*, **2010**, 116(6), 3249-3255.
41. W.S. Lyoo, S. Chvalun, H.D. Ghim, J.P. Kim, and J. Blackwell, *Macromolecules*, **2001**, 34(8), 2615-2623.
42. E.M. Cloete, *Crystal Characterisation Unit*, Central Analytical Facility of Stellenbosch University; Personal communications. 2010.
43. W.S. Lyoo and W.S. Ha, *Polymer*, **1999**, 40(2), 497-505.
44. J.H. Yeum, B.C. Ji, S.K. Noh, H.Y. Jeon, J.W. Kwak, and W.S. Lyoo, *Polymer*, **2004**, 45(12), 4037-4043.
45. W.S. Lyoo, J. Blackwell, and H.D. Ghim, *Macromolecules*, **1998**, 31(13), 4253-4259.
46. J. McMurry, *Organic Chemistry*, 6th edn., Brooks/Cole: Belmont, 2004.
47. J.M. Bailey and W.J. Whelan, *J. Biol. Chem.*, **1961**, 236(4), 969-973.
48. S. Santacruz, R. Andersson, and P. Aman, *Carbohydr. Polym.*, **2005**, 59(3), 397-400.
49. J.F. Pedersen, S.R. Bean, D.L. Funnell, and R.A. Graybosch, *Crop Sci.*, **2004**, 44(3), 764-767.
50. V. Haack, T. Heinze, G. Oelmeyer, and W.-M. Kulicke, *Macromol. Mater. Eng.*, **2002**, 287(8), 495-502.
51. R. Auzély-Velty and M. Rinaudo, *Int. J. Biol. Macromol.*, **2003**, 31(4-5), 123-129.
52. T. Moritani and J. Yamauchi, *Polymer*, **1998**, 39(3), 559-572.
53. B. Volkert, F. Loth, W. Lazik, and J. Engelhardt, *Starch-Stärke*, **2004**, 56(7), 307-314.
54. G.S. Mukherjee, N. Shukla, R.K. Singh, and G.N. Mathur, *J. Sci. Ind. Res.*, **2004**, 63(7), 596-602.
55. C. Aguir and M.F. M'Henni, *J. Appl. Polym. Sci.*, **2006**, 99(4), 1808-1816.
56. S.Y. Nam, H.J. Chun, and Y.M. Lee, *J. Appl. Polym. Sci.*, **1999**, 72(2), 241-249.
57. R.J. White, *Polym. Int.*, **1997**, 43(4), 373-379.
58. F.A. Messaud, R.D. Sanderson, J.R. Runyon, T. Otte, H. Pasch, and S.K.R. Williams, *Prog. Polym. Sci.*, **2009**, 34(4), 351-368.

Chapter 5: Summary, Conclusions and Recommendations

5.1 Summary

The poly(vinyl alcohol) (PVA) precursor, poly(vinyl pivalate) (PVPi), was successfully prepared by thermally initiated free radical polymerisation of vinyl pivalate (VPi) in water, as confirmed by nuclear magnetic resonance spectroscopy (NMR). Reactions at higher polymerisation temperatures (65 °C and 75 °C) were most suitable because they resulted in higher conversions at faster rates. Furthermore, scanning electron microscopy (SEM) analysis showed that the particles polymerised at these high temperatures were more stabile in terms of maintaining their spherical form. Suspension polymerisation was successfully carried out and reactions carried out under 'standard' suspension conditions afforded relatively uniformly distributed spherical PVPi particles, with diameters 0.5–10 μm and polydispesity index (PD) of 1.4.

An investigation into the effects of various polymerisation conditions on the particle sizes and distributions was carried out. Selected reaction conditions were altered and the resulting suspension polymerised PVPi samples studied using laser diffraction spectrometry (LDS) and SEM. The particle distribution curves obtained were compared and interpreted with the aim of determining the most suitable reaction conditions for obtaining uniform particle size distributions from the suspension polymerisation of VPi. It was subsequently found that several factors influence the distribution of the particles. Although further research into the effects of different reaction conditions is required, for the purpose of this study, the reaction conditions used for the preparation of the so-called 'standard' PVPi sample were considered suitable for preparing the desired particle size, with reasonably good distribution.

Cross-linking of the 'standard' PVPi particles (reaction temperature 65 °C, sample **A**) was necessary to preserve the particles' spherical shape in the subsequent experimental procedures, i.e. surface saponification and modification. This cross-linking was achieved during suspension polymerisation, in a copolymerisation reaction, using tri(ethylene glycol) divinyl ether (TEGDE) as cross-linking comonomer. Although low concentrations were used, cross-linking of the PVPi particles significantly restricted the types of analyses that could be carried, e.g. solution NMR and size exclusion chromatography (SEC), the introduction of cross-linking was considered essential to maintain the spherical morphology in the succeeding experimental steps. The cross-linked PVPi particles prepared by standard suspension polymerisation conditions was assigned sample A.

The PVPi particles were then saponified in tetrahydrofuran (THF) as swelling solvent to PVA with various degrees of saponification, as confirmed by solid state (SS) ^{13}C NMR. The spherical shape was lost and fibrous material was obtained when uncross-linked PVPi particles were saponified. Cross-linking the spherical PVPi particles (PVA precursor) proved to be valuable in maintaining the spherical structure during saponification to PVA, as confirmed by SEM. Various degrees of saponification were obtained by varying the time periods of saponification. The cross-linked PVA/PVPi particles were analysed using thermogravimetric analysis (TGA) and differential scanning calorimetry (DSC). With increasing saponification time and degree of saponification (DS), there were obvious changes in thermal properties: onset temperature of thermal decomposition (T_{onset}) decreased but glass transition temperature (T_g) and crystallinity (or crystalline segment melting temperature (T_m^*)[†]) increased, until fully hydrolysed. The fully hydrolysed samples, with extended saponification time, seemed to deviate from the normal behavioural sequences in terms of DSC and TGA data. Nonetheless, saponification was successfully achieved and the PVA/PVPi (B_5) prepared using 15 min hydrolysis time (DS 9%), where the cross-linked particle morphology was preserved, was selected for use in the subsequent research steps. This PVA/PVPi sample, with 15 min hydrolysis and DS 9%, is referred to as sample B_5. Sample code assignments for the full hydrolysis series are tabulated in Chapter 3, Table 3.3.

Analysis of sample B_5 revealed the following. DSC analysis showed that sample B_5 gave a T_g of 78 °C, close to that of sample A (75 °C). Thereafter, from the 15 min (B_5) to the 60 min totally hydrolysed PVA/PVPi sample (B_{10}), the DSC showed an increase in T_g with increasing DS. It was also seen that the T_m^* increased with increasing DS, i.e. 157 °C for the 15 min sample and 198 °C for the 30 and 45 min samples (B_7 and B_9, respectively). The latter B_7 and B_9 samples show slightly less perfection and indicates that residual PVPi units restrict crystallinity to small crystals (i.e. short segments that are crystallising), in comparison with the 60 min sample (DS ≥ 98%) which showed crystalline melting (T_m^*) at 210 °C.

It is therefore imperative to compare the DSC results with the X-ray diffraction (XRD) patterns, which show the perfect crystalline structure already present in the samples of lower saponification times (i.e. 2.5 min, B_1, and 7.5 min, B_3). Although XRD does not show crystalline size, it does indicate that no PVPi units are accepted into the crystal structure (which is predictable when considering the size of the pivalate groups). Significant visual depictions of the DS was provided by iodine staining of the samples: where with longer saponification times and a higher DS, a darker blue colour was seen, indicating longer PVA units and less PVPi disruptions.

[†] T_m^* refers to the melting (seen as a DSC endotherm) of the crystalline segments within cross-linked sections.

Surface modification of the B_5 particles was successfully carried out with cationic and anionic groups via the Williamson ether synthesis. The TGA data of the cationic and anionic PVA/PVPi particles (C and D, respectively) showed an increase in thermal stability (T_{onset}) and T_g, but a loss of crystallinity, compared to the unmodified PVA/PVPi (B_5). This is attributed to the attached cationic and anionic groups, respectively, and their disruption of the PVA crystalline structure. This cationic and anionic modifications of the rigid spherical PVA/PVPi particles were carried out in order to study their adherence to cellulose fibres, and compare that to the adherence of the floppy modified starches used in previous work and earlier studies by other workers.[1,2]

Fluorescence labelling of each type of particle (i.e. PVPi (A), 15 min PVA/PVPi (B_5) and cationic (C) and anionic (D) modified PVA/PVPi) was then carried out with two complimentary coloured fluorescent markers. Fluorescence imaging and SEM allowed for the observation of particle–particle, and particle–fibre interactions. Previous studies of floppy modified starches had shown that the cationic and anionic starch would conform and adhere to the cellulose fibres and precipitated calcium carbonate (PCC), respectively. In the present study, however, fluorescence and SEM imaging showed that there were no strong associations with the cationic and anionic modified PVA/PVPi particles and the fibres or PCC, as the rigid shape restricts surface contact area. This was considered significant, as a better adhesion was obtained with floppy material as apposed to rigid spheres, as was expected. This fluorescence technique is valuable in allowing for aqueous solution based imaging, in contrast to SEM imaging. To the best of the author's knowledge, this type of suspension PVPi microspheres, saponified to PVA and modified, while still maintaining their shape, has not yet been reported.

Simple studies using the field-flow fractionation (FFF) separation technique was carried out on these relatively large cross-linked particles (immeasurable by SEC), with the objective of separating the particles according to size. Separation of these particles by FFF is potentially a unique procedure, in that (firstly) these particles are cross-linked and (secondly) they would have fixed diameters, as the extent of particle swelling is restricted depending on (and possibly proportionally to) the degree of cross-linking and DS. Preliminary FFF separation of the A and B_5 samples (PVPi and 15 min PVA/PVPi, respectively) showed very slight separation. Separation was restricted by particles size and the hyperlayer operation mode. An in-depth investigation is required to achieve better particle fractionation of these particles.

5.2 Conclusions

1. Using a suspension polymerisation technique, VPi was successfully polymerised to create spherical PVPi particles, with controlled particle size and particle size distributions.
   - PVPi particles with size distribution 1–5 μm were prepared using higher AIBN initiator concentrations than normally used in literature (where lower concentrations are used, but particle sizes are larger, $D_{vad} \geq 100$ μm).[3-5]
   - Cross-linked particles were achieved by using a divinyl comonomer (TEGDE) as cross-linking agent during polymerisation. Cross-linking affords high molecular weights as the particles are composed of a cross-linked single molecule. Cross-linking (and a large number of chain ends due to the high initiator concentration) resulted in the PVPi having a T_g lower than the literature reported value of 86 °C. Nonetheless, cross-linking was achieved and ensured that particles maintained their spherical form during subsequent saponification steps.
2. These PVPi particles were hydrolysed for short to long periods, i.e. from 2.5 min to 24 hr. (Where times are included, they refer to hydrolysis/saponification times, unless otherwise stated.) Observable amounts of hydrolysis only occurred when THF was used as swelling solvent, and not when water was used as saponification medium.
   - SS ^{13}C NMR was successfully used to obtain an indication of the DS. For this purpose, the sharp methyl peak from the three identical methyl carbons (of the pivaloyl group) on the pivalate was used. Considering the decrease in signal intensity with increasing saponification time (i.e. loss of methyl carbons of the pivaloyl group with increasing saponification), the DS was determined to be about 4% for 2.5 min (B_1), 9% for 15 min (B_5) and ≥ 98% for 60 min (B_{10}) saponification times, respectively.
   - SEM and transmission electron microscopy (TEM) imaging techniques were used to confirm the spherical shape of the particles before and after saponification. The particles retained their spherical form, even at 60 min hydrolysis (B_{10}), after which the particles began to lose their round shape. Deformation of structures was observed after 5 hr (B_{14}) saponification time and longer. This indicated either chain scission or a loss of cross-linking after longer saponification times (reaction conditions: 60 °C, 20% KOH/MeOH/H_2O in a 0.20 v/v ratio with the PVPi solution).
   - Thermal analysis (DSC) of the samples showed that there was an increase in T_g and degree of crystallinity (and T_m^*) with increasing DS. Crystallinity of the cross-linked samples was confirmed by XRD analysis.

3. The PVA/PVPi particles (15 min, DS 9%, B_5) were modified by adding either carboxylic functionality (using sodium monochloroacetate, for anionic groups) or quaternary functional nitrogen (using 3-chloro-2-hydroxy-propyltrimethylammonium chloride, for cationic groups) to the surface via the Williamson etherification reaction. These then mimic the flexible anionic and cationic polysaccharide/starch gel particles recently patented by fellow researchers,[1,2] yet they are spherical particles that maintain their shape and are unable to morph or deform. Modification was confirmed using SS ^{13}C NMR, Fourier transform infrared spectroscopy (FTIR) and zeta potential measurements. TGA and DSC measurements indicate a disruption of the crystalline structure and inter-chain hydrogen bond interactions (between adjacent chains).

4. In continuation, fluorescence dyes were added to these charged particles, with the anionic and cationic particles labelled with green fluorescein isothiocyanate (FITC) and red rhodamine B isothiocyanate (RBITC) dyes, respectively.

   - These were then tested on cellulose paper fibre. We expected a random 'spotty-type' adhesion rather than overall adhesion as the round particle cannot conform to the surface. SEM and fluorescence imaging showed that there was no marked adhesion of large numbers of particles; the expected spotty adhesion was seen. This suggests that there is not widespread functionality evenly distributed throughout on the surface of the cellulose, although it does possess anionic functionality and attract cationic starches (which can conform and adhere to the fibre surface).
   - There was also no significant interaction between the anionic particles and PCC filler particles, as observed to be a very weak interaction in fluorescence images. Again, this was anticipated, as the rigid anionic particles could not morph to fit the surface of the PCC.

5. The PVPi (A) and 15 min PVA/PVPi (B_5) particles were characterised in an asymmetric flow FFF apparatus, and results showed very slight separation. These round particles have the potential to be used as possible FFF standards because they mirror the chemistry of functionalised starch and cellulose particles, yet maintain their shape and have a fixed size, measurable by SEM and TEM.

5.3 Recommendations for future work

It would be interesting to study the various particles with different degrees of saponification, different cross-linking densities (solubilities and swelling abilities) and different ionic charges (cationic and anionic) using different FFF techniques. This would open doors for further research on these modified particles (microspheres) for advanced applications, such as standards to the industry for FFF calibration in asymmetric flow, thermal and electrical techniques.

Should I continue with this work in a PhD study, I would choose to make these particles thermally expandable (foaming) at around 80 °C, in which case they would be trapped in paper fibres by combining them with the adherent functional starch (which would morph onto both the particles and fibres, aiding in adherence). During drying, a blowing agent added to the PVPi core would vapourise at the softening temperature of the PVPi, thereby causing the particles to expand and sealing all the paper fibres into a barrier for papers and boxes. The aim of incorporating these particles into the paper making process (and paper materials), would be to add a filler that expands to fill the voids between fibres, acting as a barrier and reinforcing agent, strengthening the material by a strong bond with the fibre, while simultaneously reducing costs. In order to reduce costs, the use of poly(vinyl acetate) (PVAc) homopolymer or copolymers of PVAc/PVPi should be considered. It is envisaged that these would be more cost effective than the PVPi homopolymer, and offer even lower blowing temperatures.

Finally, to make these particles commercially useful, studies could be carried out on their possible use in inkjet printing materials, which might be in competition with the patent by Chen[6] that appeared recently, during the course of this study.

5.4 References

1. A. Kornherr, F. Eder, B. Janse, R. Sanderson, J. Terblanche, and M. Zou. Process for Preparing Polysaccharide Gel Particles and Pulp Furnish for Use in Paper Making. European Patent Application: 09450061.8 – 2115, 2009.
2. A. Kornherr, F. Eder, B. Janse, R. Sanderson, J. Terblanche, and M. Zou. Process and Device for Preparing Starch Microgel Particles for the Paper Industry. European Patent Application: 09450062.6 – 2115, 2009.
3. W.S. Lyoo, J.W. Kwak, J.H. Yeum, B.C. Ji, C.J. Lee, and S.K. Noh, *J. Polym. Sci., Part A: Polym. Chem.*, **2005**, 43(4), 789-800.
4. W.S. Lyoo, C.S. Park, K.H. Choi, J.W. Kwak, W.S. Yoon, and S.K. Noh, *Polym. Plast. Technol. Eng.*, **2005**, 44(3), 475-487.
5. S.G. Lee, J.P. Kim, W.S. Lyoo, J.W. Kwak, S.K. Noh, C.S. Park, and J.H. Kim, *J. Appl. Polym. Sci.*, **2005**, 95(6), 1539-1548.
6. T. Chen and E.L. Burch. Use and Preparation of Crosslinked Polymer Particles for Inkjet Recording Materials. United States Patent: US007507439B2, 2009.

Appendix A: SS NMR data

A.1 Solid state ^{13}C NMR spectra of PVPi particles (uncross-linked and cross-linked)

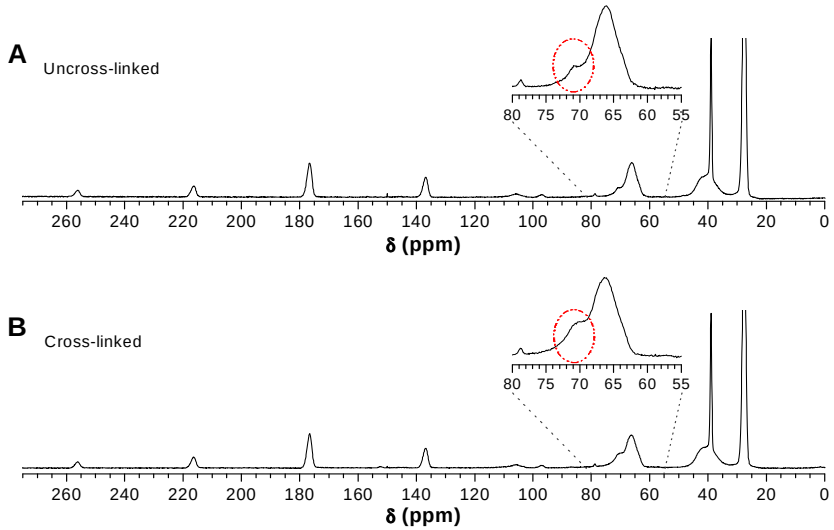

Figure A.1 **Comparison of the uncross-linked (A) and cross-linked (B) PVPi samples, showing an increase in intensity of the 'shoulder' at ca. 70 ppm.**

A.2 SPE/MAS and CP/MAS SS ^{13}C NMR spectra of cross-linked PVPi

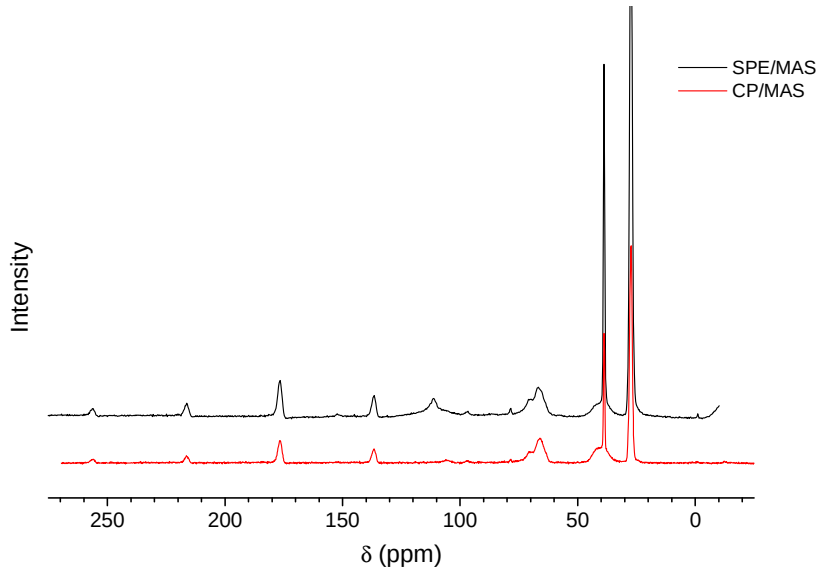

Figure A.2 **SPE/MAS versus CP/MAS spectrum for a standard cross-linked PVPi, sample A.**

Appendix B: FTIR of PVPi

B.1 Infrared spectra of uncross-linked and cross-linked PVPi particles

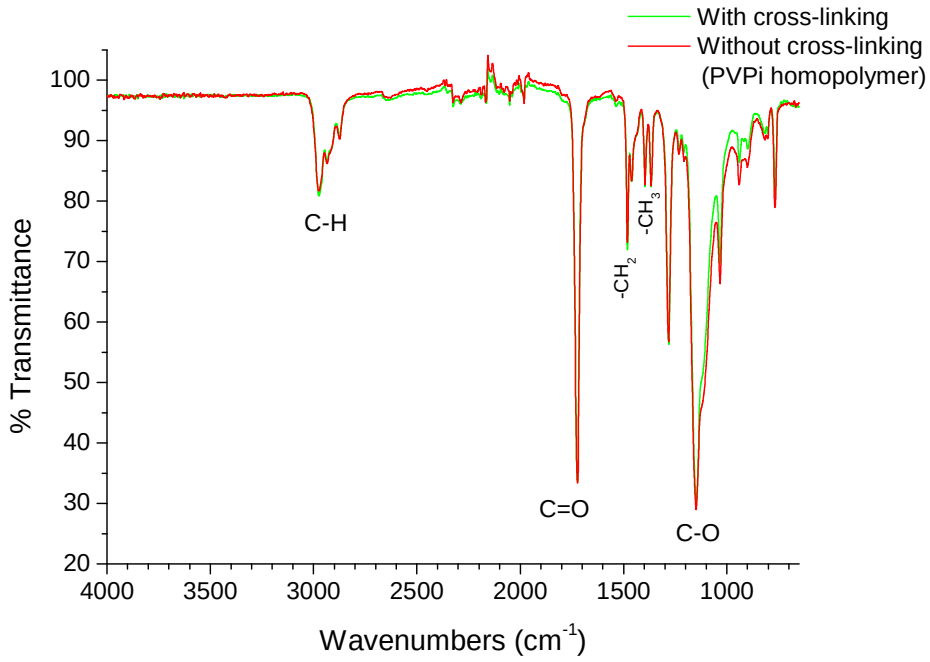

Figure B.1 ATR-FTIR spectra of cross-linked and uncross-linked PVPi samples.

Appendix C: PVPi T_g

C.1 T_g data plot of PVPi samples with different degrees of cross-linking

A plot of T_g versus the degree of cross-linking shows the decrease in T_g with increasing cross-linker concentration: Figure C.1.

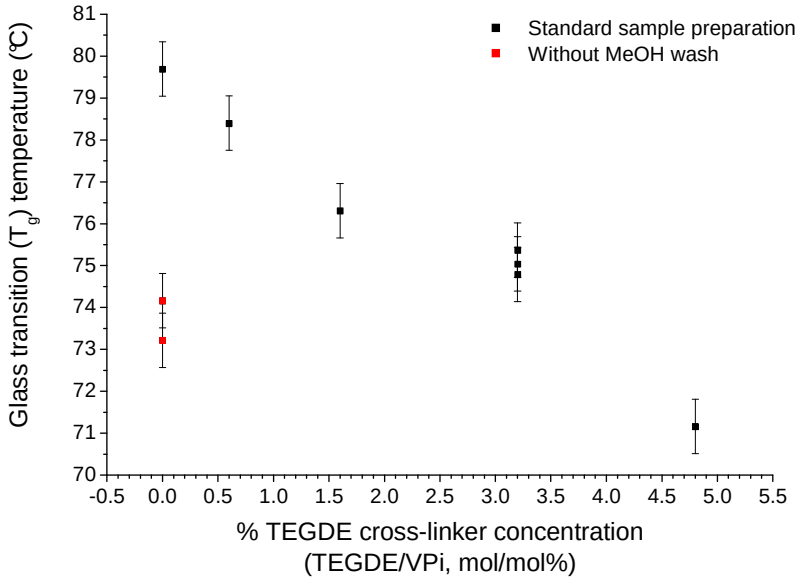

Figure C.1 T_g values of PVPi samples prepared using different cross-linker concentrations.

In a comparison between samples of the uncross-linked PVPi particles, the particles washed and purified only with water (indicated red) maintained their spherical shape but had a lower T_g (ca. 74 °C) than the uncross-linked PVPi samples washed and purified with both water and MeOH. The latter, having lost their spherical morphology, had a T_g of 80 °C. It is interesting to note the difference in thermal properties, and this again reinforces the idea that although the uncross-linked PVPi loses its spherical shape, the MeOH washing is necessary for efficient sample purification.

Appendix D: Particle distribution graphs

D.1 Particle size distribution graphs of uncross-linked PVPi

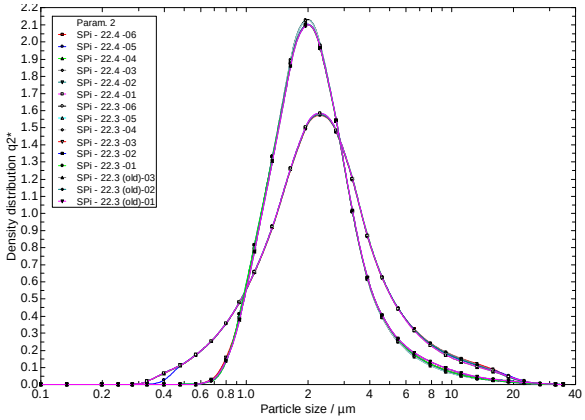

Figure D.1 Comparison between two uncross-linked PVPi samples, prepared using the same procedure.

Two uncross-linked samples were analysed and their particle distributions compared. Figure D.1 shows that there are variations in the broadness of the distribution curves of the two samples.

D.2 Particle size distribution graphs of cross-linked PVPi

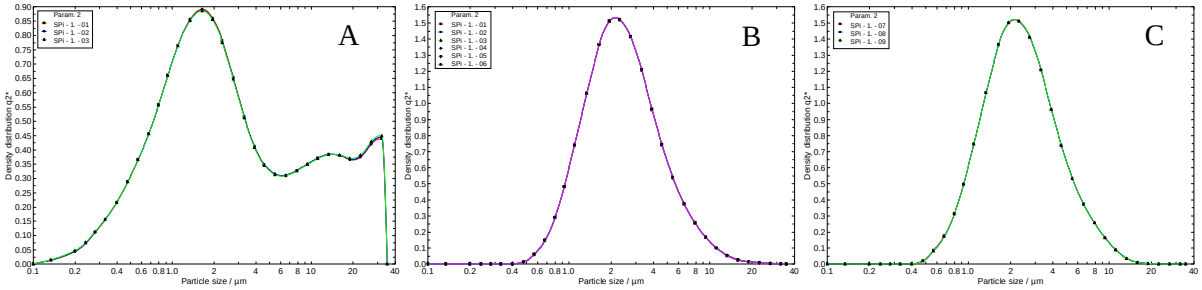

Figure D.2 Preliminary standard (cross-linked) PVPi sample distribution curves obtained with increasing amounts of sonication (A<B<C). The sample was subjected to (A) ≤ 3, (B) ≤ 5 and (C) > 6 half hour sonication cycles.

A preliminary PVPi sample was prepared in the developmental stages of the polymerization process and sample preparation procedure. During polymerization, the reaction temperature was elevated from 65 °C to 75 °C. Changing the temperature during a polymerisation run from 65 °C to 75 °C resulted in increased conversion but the sample showed an undesirable particle distribution.

The particle size distribution of this preliminary PVPi sample was tested and it showed that agglomerates were present in the sample after standard preparation and sonication. The sample was then subjected to longer sonication times, and the results showed that agglomerations were removed and particles were efficiently broken up and dispersed Figure D.2 (B and C). Thus, it was determined that when large agglomerates are still present after standard preparation procedures and sonication, extended periods of sonication was needed to effectively separate agglomerated particles.

Appendix E: TGA data

E.1 TGA and DTGA thermograms for the PVA/PVPi particles of different saponification times

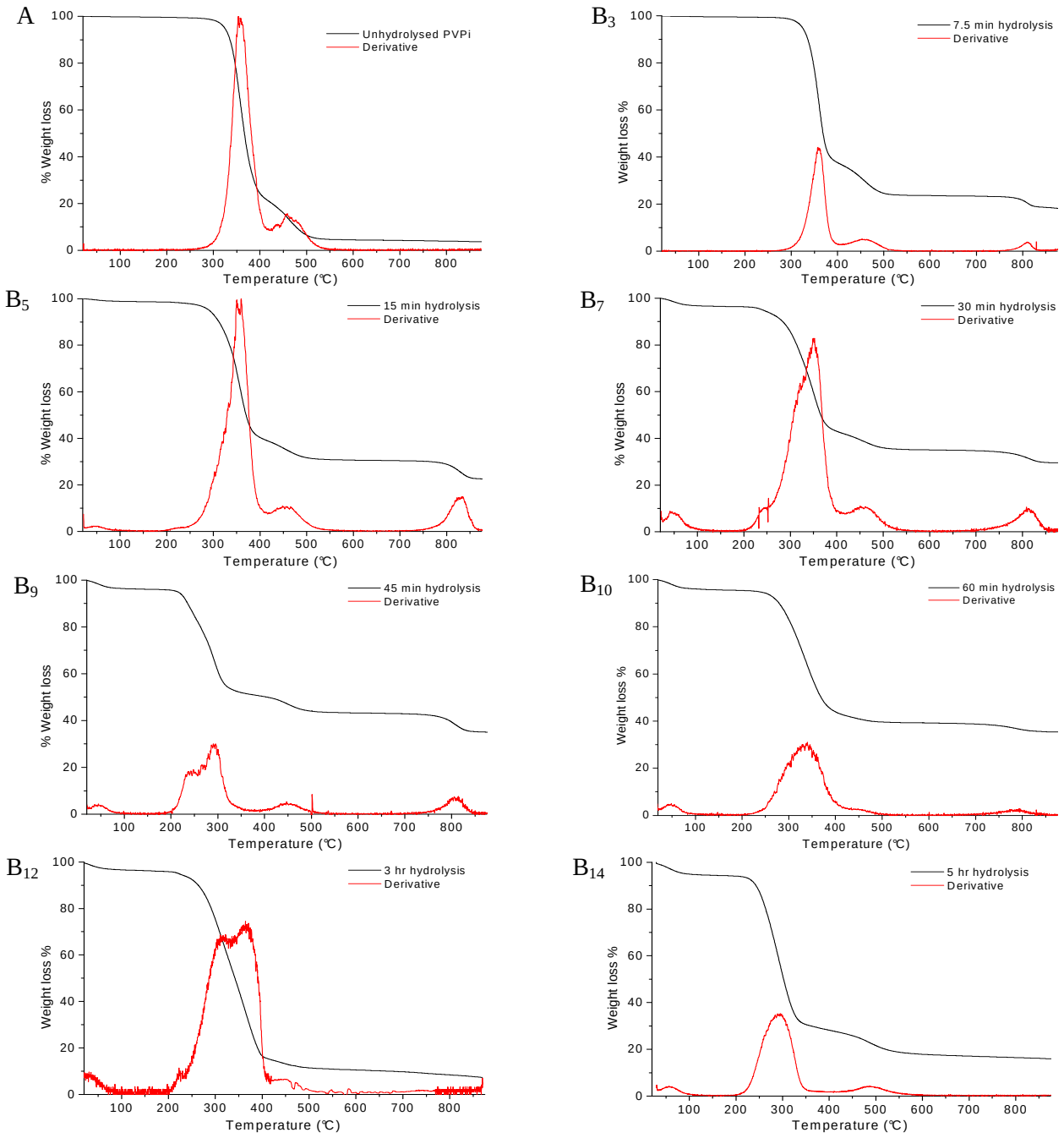

Figure E.1 **DTGA thermograms (red) for the standard PVPi (A), partially hydrolysed PVA/PVPi (B_3, B_5, B_7, B_9) and fully hydrolysed PVA/PVPi (B_{10}, B_{12}, B_{14}).**

Appendix F: XRD

F.1 XRD comparison between repeated 15 min PVA/PVPi samples

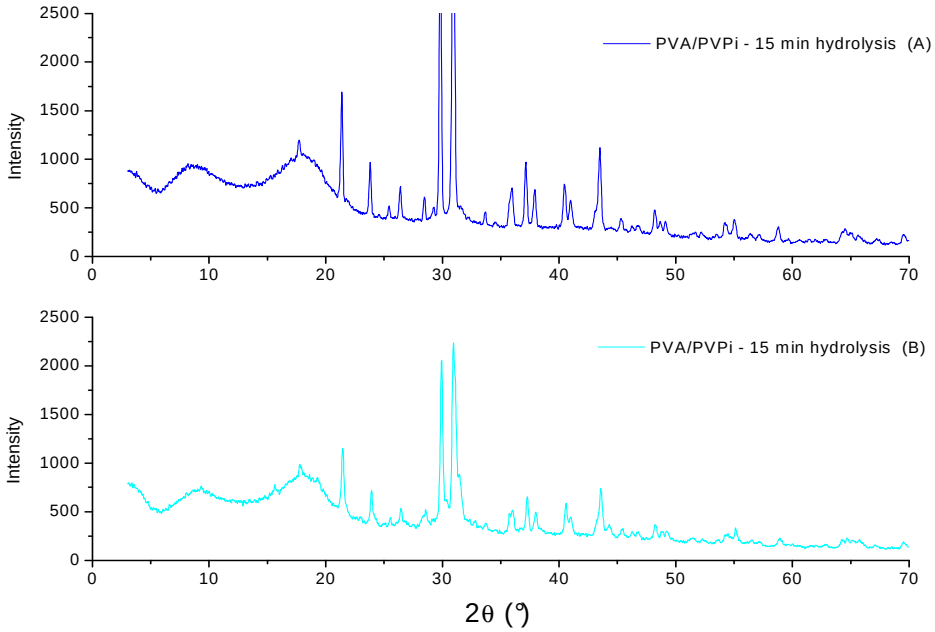

Figure F.1 **XRD pattern comparison between two different samples of PVA/PVPi (B_5) prepared in separate experiments under identical conditions.**

Figure F.1 shows two different samples of 15 min hydrolysed PVA/PVPi (B_5). The samples show that the crystalline peaks are equal, except for slight intensity deviations, and samples are reproducible.

Appendix G: SEM images of particles

G.1 SEM images of uncross-linked PVPi before and after saponification

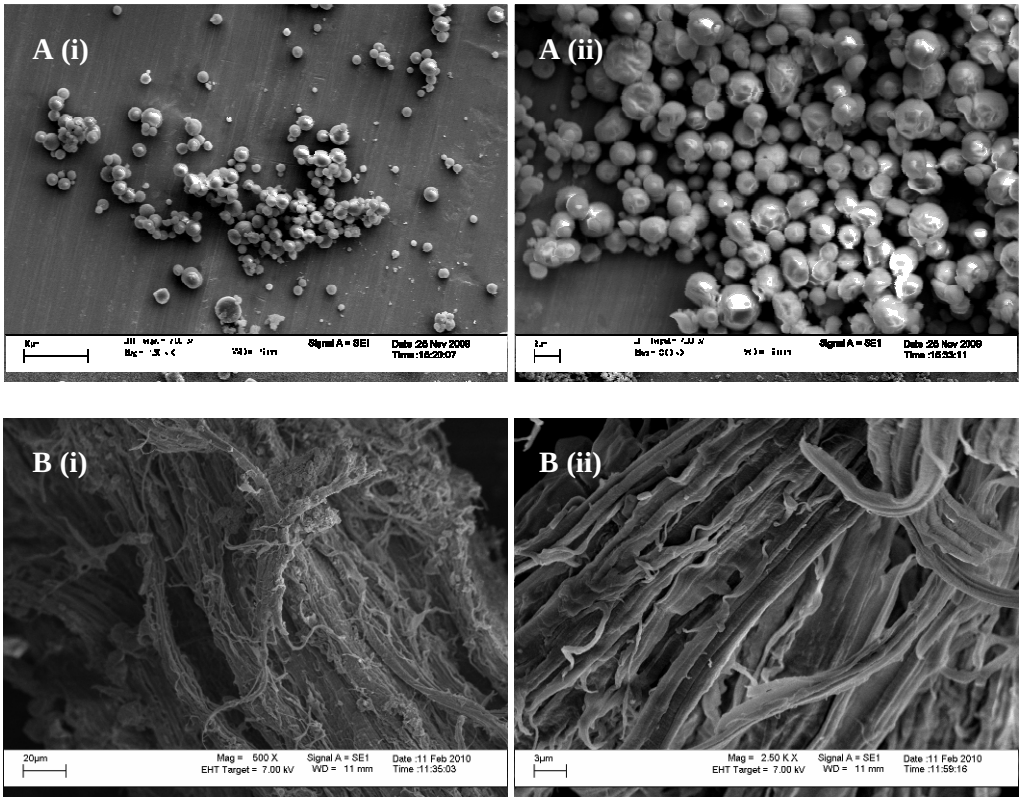

Figure G.1 **SEM images of (A) PVPi uncross-linked particles (i) ×1500 and (ii) ×3000; (B) PVA/PVPi 15 min hydrolysed, uncross-linked fibrous material (i) ×500 and (ii) ×2500.**

The electron micrographs (SEM images, Figure G.1) show the hydrolysis effect on the uncross-linked PVPi sample, where the spherical morphology (A, PVPi before) is lost in the saponification reaction and fibrous PVA material results (B, after 15 min saponficiation).

G.2 SEM images of fully hydrolysed, cross-linked PVA/PVPi

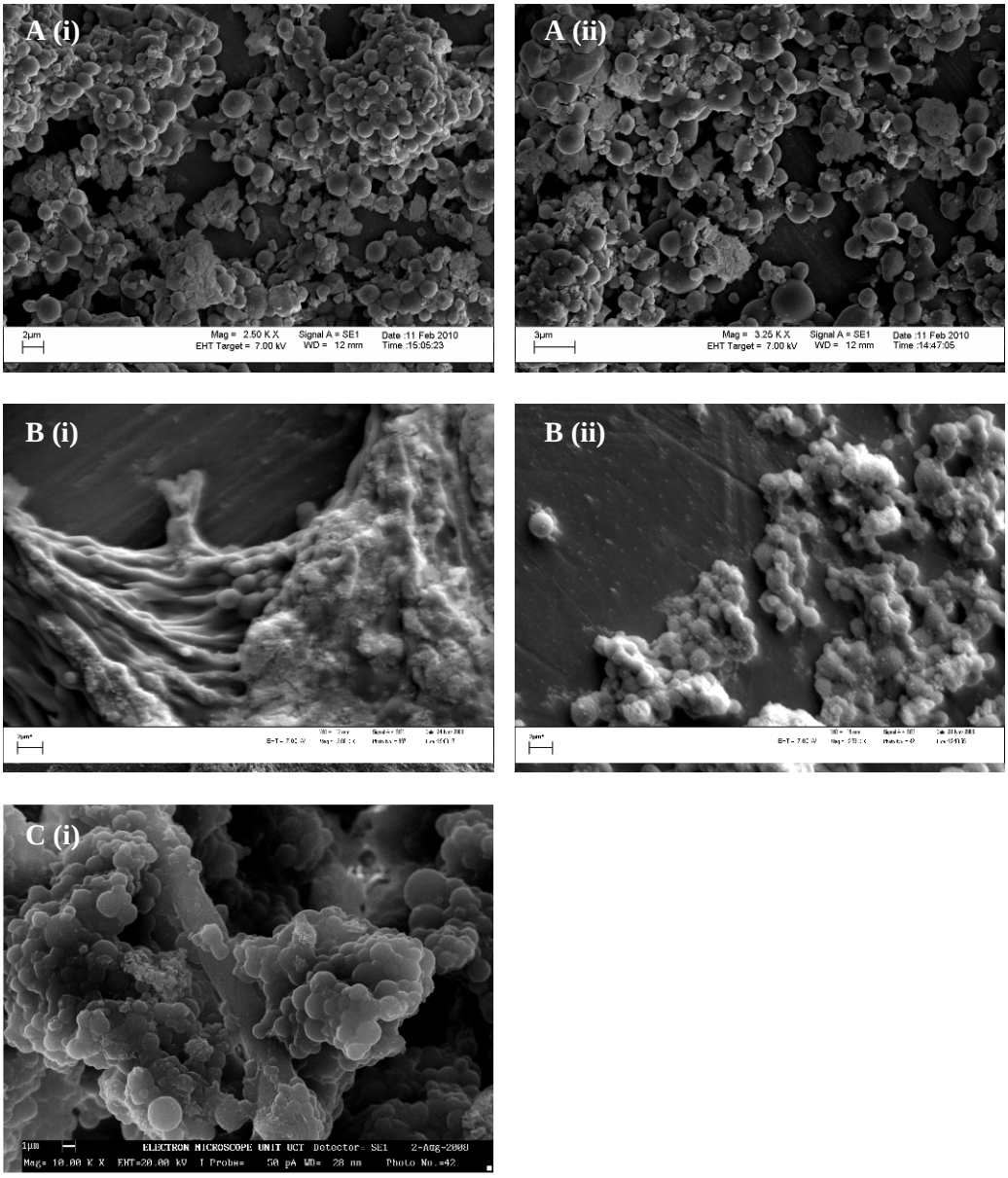

Figure G.2 **SEM images showing the flattening and deforming of the fully hydrolysed samples of cross-linked, hydrolysed PVA/PVPi, after: (A) 60 min, DS ≥ 98% (i) ×2500 and (ii) ×3250; (B) 5 hr, DS ≥ 99% (i) ×3000 and (ii) ×2730; and (C) 24 hr, DS > 99% (i) ×10000.**

Appendix H: FTIR of modified PVA/PVPi

H.1 Infrared spectra of PVA/PVPi and cationic modified PVA/PVPi particles

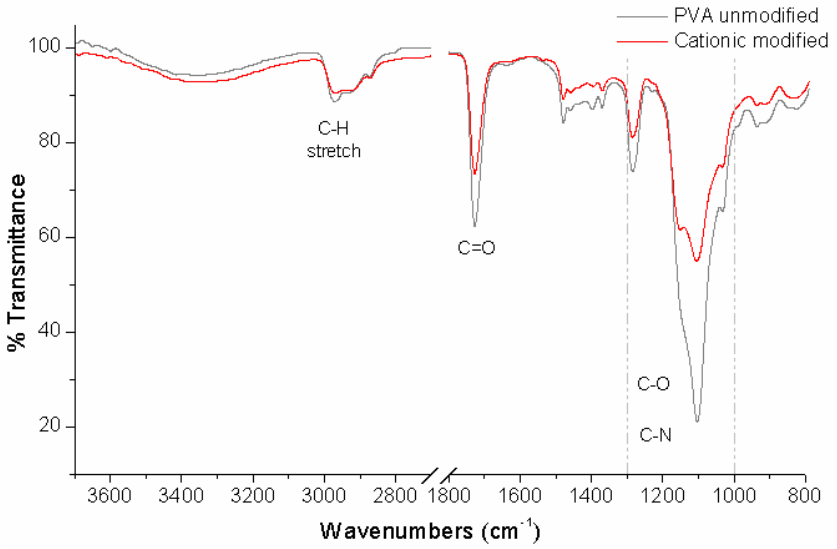

Figure H.1 **ATR-FTIR spectra of the 15 min hydrolysed PVA/PVPi particles (grey) and the cationic modified PVA/PVPi particles (red).**

Appendix I: Thermal data

I.1 DSC thermograms for a full sample series comparison: PVPi, PVA/PVPi, cationic and anionic modified PVA/PVPi

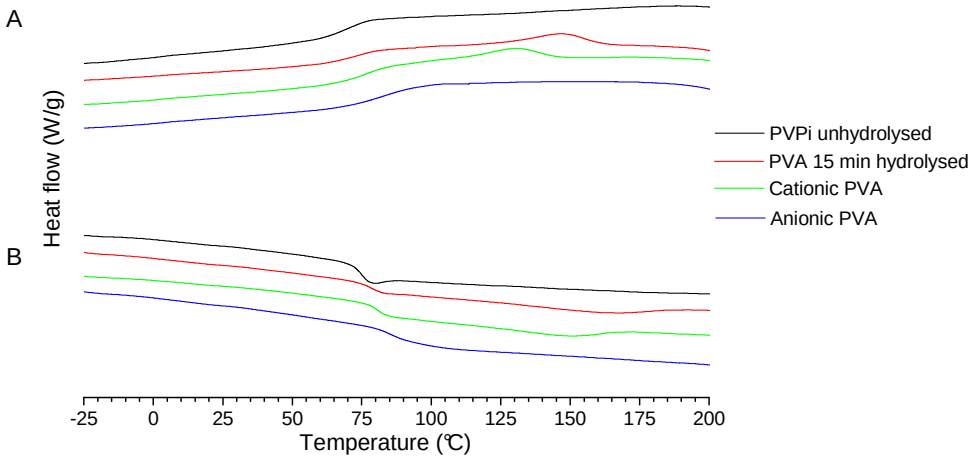

Figure I.1 **Total series comparison: DSC thermograms for a complete synthesis series i.e. standard PVPi (black), 15 min PVA/PVPi (red), cationic PVA/PVPi (green) and anionic PVA/PVPi (blue); DSC cycle 2 (A) and cycle 3 (B).**

I.2 TGA thermograms for a full sample series comparison: PVPi, PVA/PVPi, cationic and anionic modified PVA/PVPi

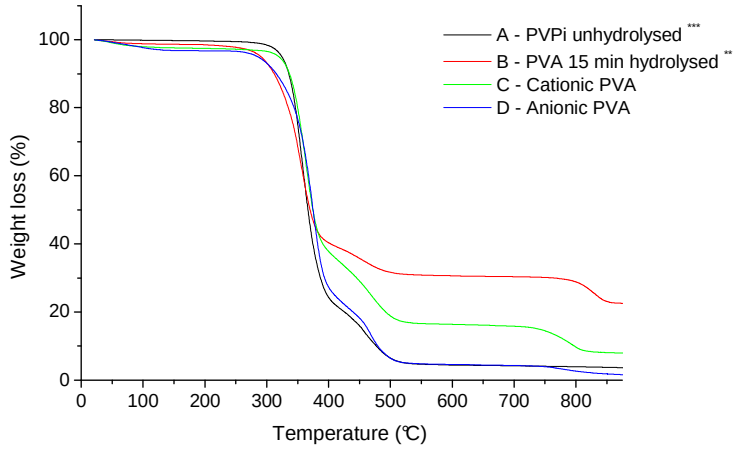

Figure I.2 **TGA thermograms of total sample series (Sample A, B, C and D), illustrating the changes in thermal stability with ionic modification: (A) PVPi (black), (B) 15 min PVA/PVPi (red), (C) cationic PVA/PVPi (green) and (D) anionic PVA/PVPi (blue).**

*** The number of stars (*) indicates the number of curves per sample used to produce the averaged curve shown.**

Appendix J: Labelled PVA/PVPi control

J.1 Fluorescence images of RBITC labelled PVA/PVPi particles

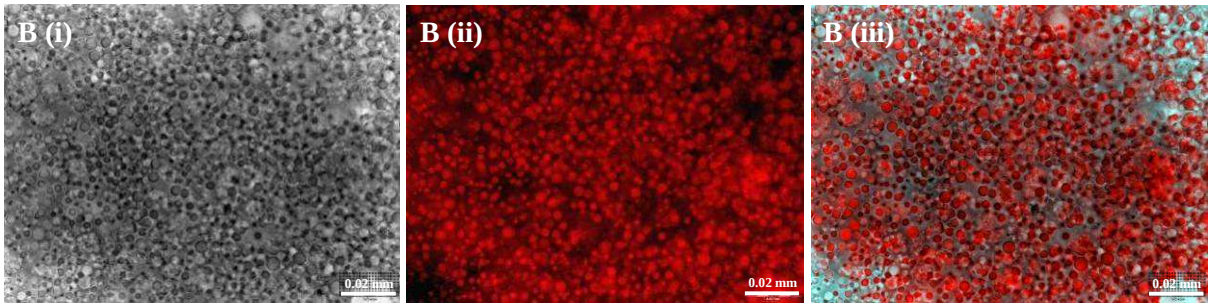

Figure J.1 **Fluorescence images of RBITC tagged PVA/PVPi particles (B): (i) transmission mode, (ii) fluorescence mode, and (iii) an overlay of (i) and (ii).**

Appendix K: SEM images of particles with cellulose fibres

K.1 SEM images showing excess flocculation of particles in certain areas on cellulose fibres

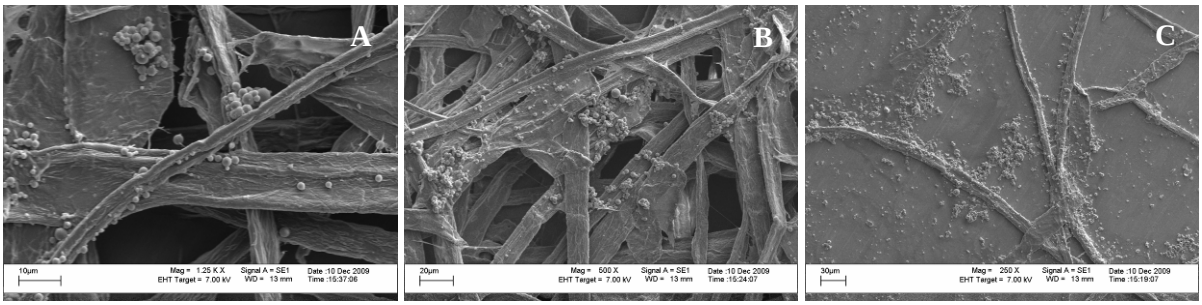

Figure K.1 Electron micrographs (SEM) of standard PVPi particles with cellulose fibres, showing flat areas of micro-porosity; (A) ×1250, (B) ×500 and (C) ×250.

The above SEM images show the excess PVPi particle flocculation in certain areas on the cellulose fibres, but not throughout; the rest of the fibre material is relatively bare of any particle adhesion. This may be an artefact of the sample preparation procedure, where excess particles are filtered (by the cellulose fibres) during the drying process and have come to settle on the cellulose fibres in agglomerated piles, especially in the flat regions, like the flat surface below (drying platform). These particles coincidently sit on the cellulose fibres, not because of any real interaction with the cellulose fibres, but rather because of being trapped by filtration and settling together in agglomerates.

Appendix L: Fluorescence images

L.1 Additional fluorescence images of RBITC labelled cationic PVA/PVPi particles with cellulose fibres

Figure L.1 **Fluorescence images of RBITC tagged cationic PVA/PVPi particles with cellulose fibres: (A) transmission mode, (B) red-green fluorescence overlay and (C) transmission-fluorescence overlay.**

L.2 Fluorescence images of RBITC labelled cationic PVA/PVPi particles with FITC labelled cationic starch and cellulose fibres

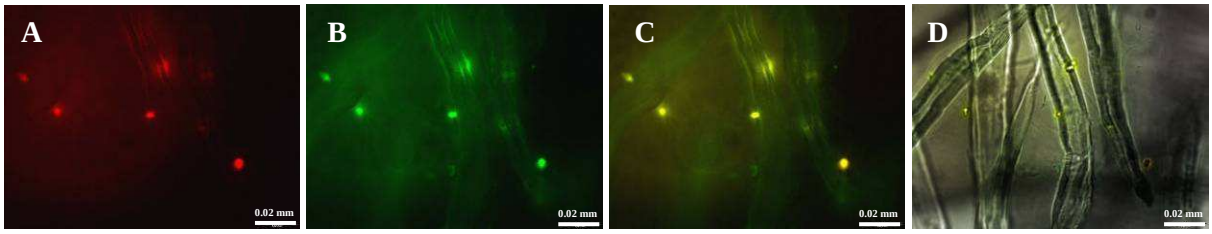

Figure L.2 **Fluorescence images of RBITC tagged cationic PVA/PVPi particles with FITC labelled cationic starch and cellulose fibres: in (A) red and (B) green fluorescence mode, (C) fluorescence overlay and (D) transmission-fluorescence overlay.**

L.3 Fluorescence and SEM images of RBITC labelled cationic PVA/PVPi particles with FITC labelled cationic starch and cellulose fibres

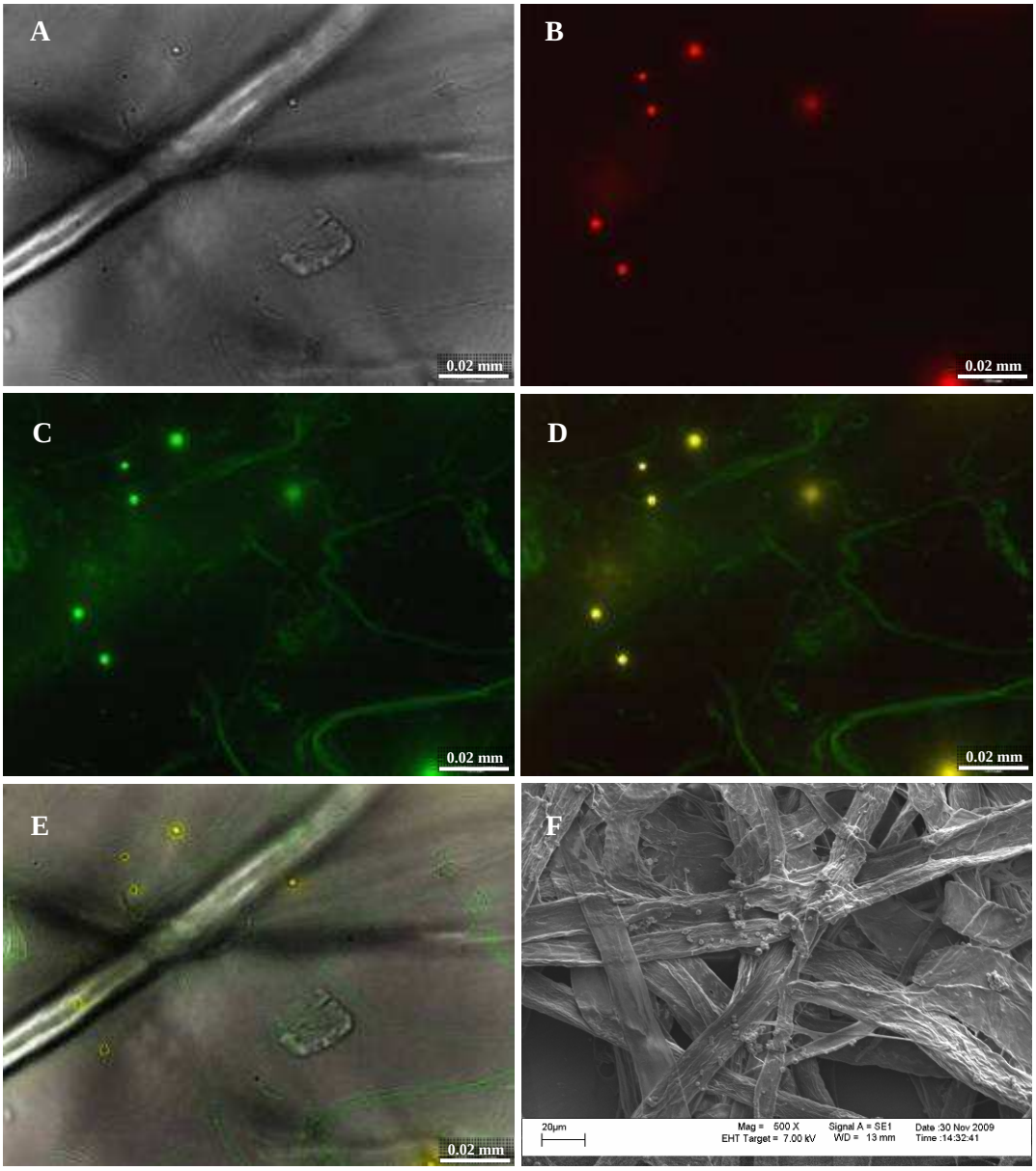

Figure L.3 **RBITC tagged cationic PVA/PVPi particles with FITC tagged cationic starch and cellulose fibres, shown in fluorescence images in (A) transmission mode, (B) red fluorescence mode, (C) green fluorescence mode, (D) fluorescence overlay and (E) transmission-fluorescence overlay; and (F) SEM image, ×500.**

L.4 Additional fluorescence images of FITC labelled anionic PVA/PVPi particles with cellulose fibres

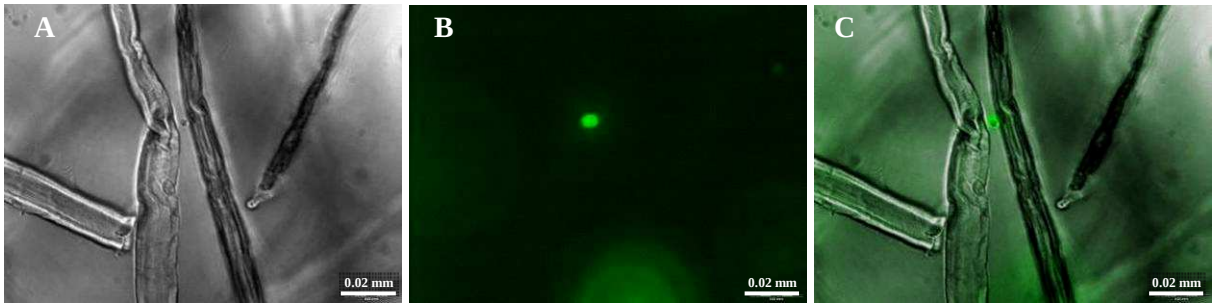

Figure L.4 **Fluorescence images of FITC tagged anionic PVA/PVPi particles with cellulose fibres: (A) transmission, (B) fluorescence mode and (C) transmission-fluorescence overlay.**

L.5 Fluorescence images of FITC labelled anionic PVA/PVPi particles with FITC labelled cationic starch and cellulose fibres

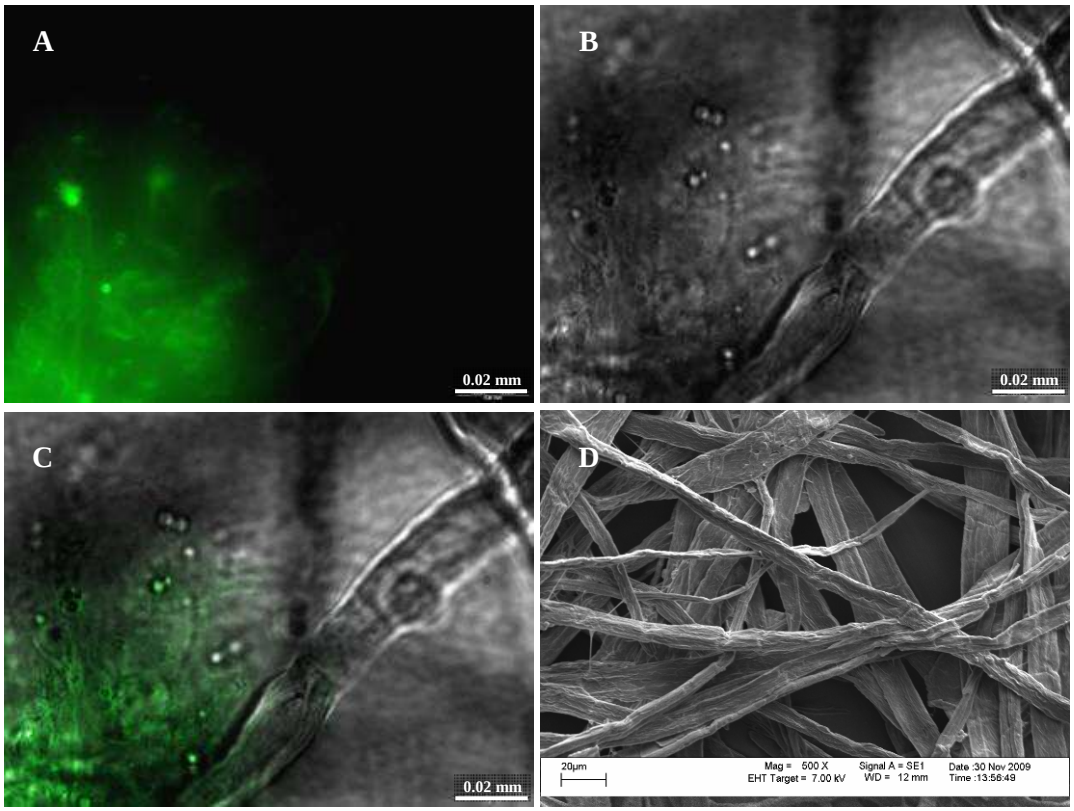

Figure L.5 **FITC tagged anionic PVA/PVPi particles with FITC tagged cationic starch and cellulose fibres, shown in fluorescence images in (A) transmission and (B) fluorescence mode, and (C) transmission-fluorescence overlay; and (D) SEM image, ×500.**

Appendix M: Modified starch

M.1 FITC labelled cationic starch compared with FITC labelled anionic starch (previous work) and the interaction with cellulose fibres and PCC

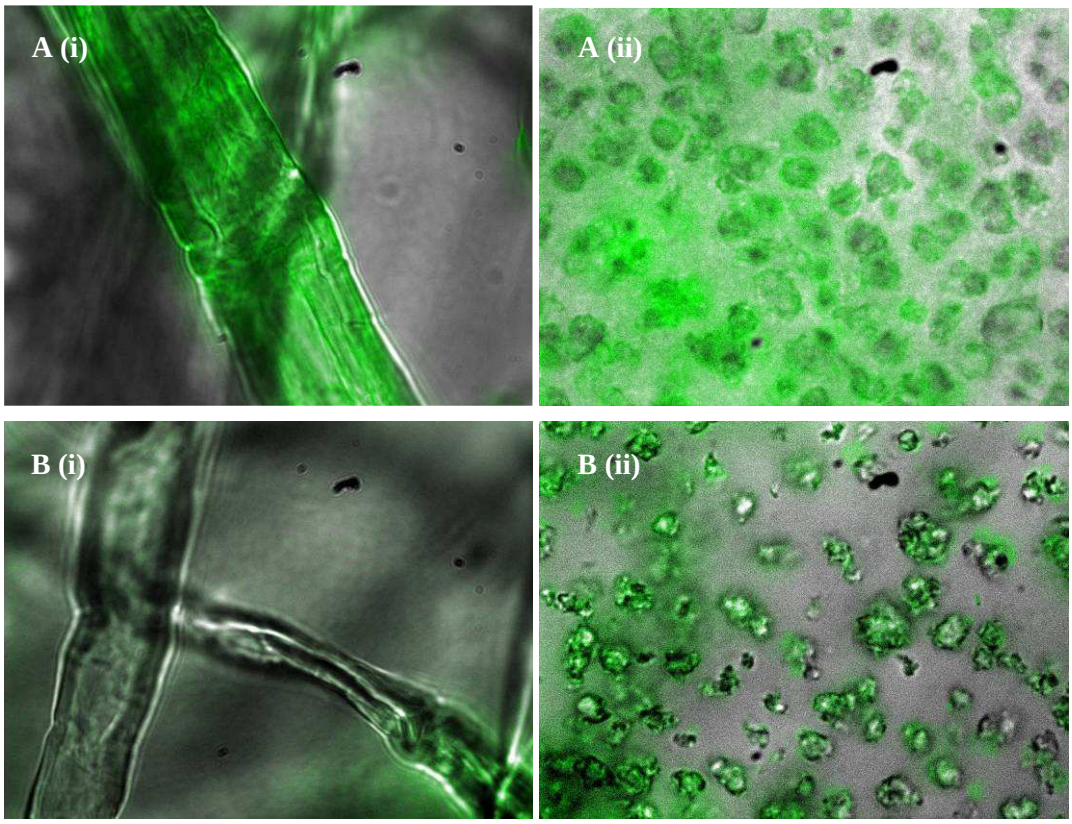

Figure M.1 **Fluorescence images (transmission-fluorescence overlay) illustrating the interaction of green FITC labelled (A) cationic starch and (B) anionic starch with (i) cellulose fibres and (ii) PCC, respectively.**

From the fluorescence images in Figure M.1, it is clearly seen that the (green) fluorescein labelled cationic starch (A) interacts well with both the cellulose fibres (i) and PCC particles (ii), whilst the (green) fluorescein labelled anionic starch (B) shows little interaction with the cellulose fibres (i), but strong adsorption onto the PCC particles (ii).